# Host Cell Proteins and Cell Cycle Phase Affect Adeno-Associated Virus DNA Replication / Gene Expression

---

**Dissertation**

**zur**

**Erlangung der naturwissenschaftlichen Doktorwürde**
**(Dr. sc. nat.)**

**vorgelegt der**

**Mathematisch-naturwissenschaftlichen Fakultät**

**der**

**Universität Zürich**

**von**

Francesca Daniela Franzoso

**Promotionskommission**

Prof. Dr. Cornel Fraefel (Vorsitz und Leitung der Dissertation)

Prof. Dr. Urs Greber

Prof. Dr. Michael Linden

**Zürich,** 2017

Content

# 1. Summary

The study of adeno-associated virus (AAV) has a dual importance for research and therapeutic applications: as a nonpathogenic virus that can interact in a co-infection with its helper virus in order to replicate and as a widely used viral vector for gene therapy. Although both sides have been extensively studied, many questions still remain to be answered.

The two aims of my PhD study tackled this dual facet by investigating (i) the performance of single-stranded (ss) and double-stranded (ds), self-complementary (sc) AAV vectors in transducing cells and (ii) the replication of wild type (wt) AAV2 in co-infection with HSV-1.

Concerning the first Specific Aim, we showed that HSV-1 provided helper functions do not allow AAV2 to replicate in different phases of the cell cycle. AAV2 and HSV-1 replicate in different sets of cells. In particular, AAV2 replication as well as gene expression from both single-stranded (ss) and self-complementary (sc) AAV2 vectors preferentially occurs in S/G2 cell cycle phase cells. Moreover, the ss and scAAV vectors can differentially affect the cell cycle progression. In a multifluorescence live cell microscopy assay we observed that the vast majority of transduced cells were in S/G2 phases of the cell cycle independent of the genome structure ss or sc or the presence or absence of HSV-1. We therefore hypothesized that second-strand synthesis is likely not responsible for the cell cycle preference of AAV2 replication/gene expression.

In the second Specific Aim, we performed a high-throughput image-based siRNA screening of 62 cellular factors previously identified as components of AAV2 replication compartments in human cervical carcinoma cell line (HeLa ATCC cells) to identify their roles in ss and sc AAV vector transduction. Some cellular proteins were found to inhibit (e.g. Mre11, NBN, Rad50, MSH3, PCNA) or enhance (e.g. EEF1A1) transduction by both ss and ds AAV vectors. Other proteins appeared to enhance or inhibit transduction by one vector but did not have an effect on the other vector; for example, the knockdown of replication factor 2 (RFC2) inhibited the infection rate of the ss AAV vector but had no effect on that of the sc AAV2 vector. An interesting group of proteins includes replication protein A 1 (RPA1) and mismatch repair proteins MSH2 and MSH6, where siRNA knockdown led to opposite effects for ss and sc AAV vectors. The role of RPA1 and RPA2, which together with RPA3 form the heterotrimeric RPA complex, was

further investigated by posttranscriptional knockdown of endogenous and complementation with exogenous genes. These assays revealed that RPA1 and RPA2 both had a differential effect on the transduction efficiencies of the ss and ds AAV vectors and that only RPA2 enhanced HSV-1 supported AAV2 replication, while RPA1 had no significant effect on AAV2 DNA replication.

# 2. Zusammenfassung

Das Adeno-asoziierte Virus (AAV), ein *Dependoparvovirus* innerhalb der Familie der *Parvoviridae*, hat eine doppelte Signifikanz, einerseits für die Virusforschung und andererseits für therapeutische Anwendungen. AAV ist ein replikations-defektes, nichtpathogenes Virus, das nur in Anwesenheit eines Helfervirus replizieren kann. Gleichzeitig ist AAV ein weit verbreiteter Virusvektor für die Gentherapie. Obwohl beide Aspekte eingehend untersucht wurden, gibt es noch viele Fragen zu beantworten.

Die Ziele meiner Doktorarbeit waren (i) die Effizienz von einzelsträngigen (ss) und doppelsträngigen (ds), selbst-komplementären (sc) AAV-Vektoren bei der Transduktion von Wirtszellen und (ii) die Replikation von Wildtyp (wt) AAV2 in Co-Infektion mit HSV-1 zu untersuchen.

Im ersten Teil haben wir gezeigt, dass AAV2 Replikation und Genexpression Zellzyklus abhängig ist und in der S/G2 Phase stattfindet. Dies wiederum führt dazu, dass das Helfervirus nun hauptsächlich in G1 Zellen repliziert. In ko-infizierten Kulturen replizieren AAV2 und HSV-1 also in verschiedenen Zellen, die sich in ihrem Zellzyklus unterscheiden. Interessanterweise ist nicht nur die Genexpression von ss rekombinanten (r) AAV Vektoren Zellzyklus abhängig, sondern auch jene de sc AAV Vektoren. Erstaunlicherweise können die ss- und scAAV-Vektoren den Zellzyklusverlauf unterschiedlich beeinflussen: ssAAV Vektoren induzieren einen Zellzyklus-Stop während scAAV Vektoren die Progression des Zellzyklus erlauben.

Im zweiten Teil haben wir ein siRNA-Screening von 62 zellulären Faktoren durchgeführt, die zuvor als Komponenten von AAV2-Replikations Kompartimenten identifiziert wurden, um deren Effekt auf die Transduktion von ss- und sc-AAV-Vektoren zu untersuchen. Dabei haben wir Proteine identifiziert, welche die Transduktioneffizienz sowohl von ss als auch von sc-AAV-Vektoren verkleinern (z. B. Mre11, NBN, Rad50, MSH3, PCNA) oder erhöhen (z. B. EEF1A1). Andere Proteine schienen die Transduktionseffizienz eines Vektors zu verstärken oder zu inhibieren, hatten aber keinen Effekt auf den anderen Vektor. So hemmte zum Beispiel der Knockdown von RFC2 die Transduktionsrate des ss-AAV-Vektors, hatte aber keine Auswirkung auf die des sc AAV2-Vektors. Eine interessante Gruppe von Proteinen wie RPA1, MSH2 und MSH6, hatte einen entgegengesetzten Einfluss auf die Transduktionseffizienz von ss- und sc-AAV-Vektoren. Die Rolle von RPA1 und RPA2, die zusammen mit RPA3 den

heterotrimeren RPA-Komplex bilden, wurde durch den posttranskriptionellen Knockdown von endogenen und Komplementierung mit exogenen RPA Genen weiter untersucht. Diese Experimente zeigten, dass RPA1 und RPA2 beide einen differentiellen Effekt auf die Transduktionseffizienzen der ss- und ds-AAV-Vektoren hatten, dass aber nur RPA2 die HSV-1-unterstützte AAV2-Replikation verstärkte, während RPA1 keine signifikante Wirkung auf die AAV2-DNA-Replikation hatte.

Insgesamt ermöglicht diese Arbeit ein besseres Verständnis der komplexen und faszinierenden AAV-Biologie und erlaubt die Entwicklung verbesserter viraler Gentherapievektoren.

# 3. Introduction

## 3.1. Adeno-associated virus type-2 (AAV2) and its helper virus herpes simplex virus type-1 (HSV-1)

### 3.1.1. AAV biology, structure and genome organization

Adeno-associated virus (AAV) belongs to the genus *Dependoparvovirus* within the family of the *Parvoviridae.* It is a non-enveloped, non-pathogenic, helper-dependent virus with a single-stranded (ss) DNA genome of approximately 4.68 kb and a size of 25 nm in diameter. It was initially found as a contaminant of human adenovirus (Ad) isolates in cell cultures (1). AAV induces low immune responses in comparison to other viruses (2). There are more than twelve human serotypes described, 100 from nonhuman primates (3) with different tissue tropism (4–6) and several others from avian, bovine, avian canine and equine species. Endogenous AAV sequences were predominantly found in liver, bone marrow and spleen (7), as well as in tonsils and adenoids in children (8). It is believed that most probably AAV enters via oropharynx together with adenovirus that acts as a helpervirus in the replication process. After several rounds of replication and dissemination to different tissues, the host immune system will finally inhibit the infectious process (8).

The AAV serotype 2 (AAV2) was the first discovered infectious clone (9) with high ability to transduce common cell lines such as HeLa or HEK-293T (10), and it has continuously been the most extensively studied virus of all AAV serotypes.

The AAV2 genome is a linear single-stranded DNA and encodes two clusters of genes, *rep* and *cap*, that are flanked by inverted terminal repeats (ITRs) of 145 nucleotides (11–13). The *rep* gene cluster encodes four Rep proteins: two large required for DNA replication, Rep68 and Rep78, and two small Rep proteins, Rep40 and Rep52, involved in gene expression and packaging (14, 15). The *cap* gene is controlled by the p40 promoter and encodes three capsid proteins VP1, VP2, VP3 which, due to alternative start codons, differ in their N-termini (16, 17). The assembly-activating protein (AAP) that is required for AAV2 capsid assembly in the nucleolus, is encoded in a nested open reading frame within the *cap* gene (18). The crystal and genomic structure of AAV2 are shown in Fig. 1.

### 3.1.2. AAV2 intracellular transport

*AAV2 attachment and entry*

AAV2 requires a primary glycan receptor, first identified as heparin sulfate proteoglycan (HSPG) for AAV2 (19), together with a co-receptor for optimal attachment and internalization such as fibroblast growth factor receptor 1 (FGFR1) (20), hepatocyte growth factor receptor (MET) (21), laminin receptor (22), integrin αVβ5 (23), integrin α5β1 (23). Nevertheless, some of these receptors failed to be confirmed in other studies (24, 25). Recently it was discovered, via a genetic screening in human haploid cells, a new key host receptor for AAV infection both *in vitro* and *in vivo*, AAV receptor (AAVR), previously known as the type I transmembrane protein, KIAA0319L, that presented strong capabilities of endocytosis from the plasma membrane and trafficking to the *trans*-Golgi network (25).

AAV2 internalization can take about 30 minutes and occurs via endocytosis (26). Several pathways have been reported to be involved in AAV2 endocytosis, such as clathrin-mediated uptake (26, 27), Rac1-mediated and PI3 kinase activation cascade (28), or the recently characterized clathrin-independent carriers/GPI-enriched endocytic compartment (CLIC/GEEC) pathway (29). Di Pasquale and colleagues, showed that only intact AAV4, AAV5 or BAAV viral particles applied on the apical side of polarized cells can cross by transcytosis process (30, 31).

*AAV2 intracellular trafficking and nuclear import*

The majority of AAV2 particles will accumulate in the perinuclear region, whereas only few will access the nucleus, as demonstrated in an *in vitro* assay (26). Transport steps were found to be involving Golgi apparatus for AAV2 and AAV5 virions or late endosomes enriched in Rab7 and Rab11 for fractions of AAV2 particles (32–34). Endosomal processing exposes the VP1 and VP2 N-terminal domains outside of the capsid which allows an efficient viral transduction (18, 35).

Intact virions can be apparently detected inside the nucleus (26, 28, 36), and they can be as well recovered as fully infectious particles (37, 38). However, Sonntag and colleagues reported an inefficient and rate-limiting AAV2 nuclear import, based on poor

infectivity of virions with exposed VP1/2 N-termini following cytoplasmic injection (18). To have more insight into the mechanisms of the transport to the nucleolus, some studies reported that AAV2 capsids can interact with nucleolin or B23/nucleophosmin (38–40). The kinetics of DNA release showed a cell-type dependency, as in HeLa cells it was less efficient for AAV6 than for AAV2 with AAV6 more efficient in cardiac cells (41, 42). Duan et al. (42) and Yan et al. (43) showed that proteasome inhibitors can increase AAV trafficking to the nucleus, suggesting that capsid ubiquitination may play a role in AAV transduction.

#### 3.1.3. AAV2 DNA replication

For productive replication, AAV2 depends not only on a cell but on a helper virus, such as herpes simplex virus type 1 (ref), adenovirus 2 (AdV2), or human papillomavirus (HPV) 16 (44–46). Not only alphaherpesviruses, such as HSV-1 and HSV-2 (44), but also betaherpesviruses, including human cytomegalovirus (HCMV) (47) and human herpes virus 6 (HHV6) (48), can act as helper viruses for AAV2 replication. However, of all herpes viruses that can act as helper viruses for AAV2 replication, HSV-1 is the best characterized.

The unique replication strategy of AAV2 is based on a rolling-hairpin mechanism in which the 3'-ITR acts as essential primer for second-strand synthesis (49). Replication of AAV2 was also demonstrated in several cell lines upon genotoxic stress (50, 51). AAV2 can also replicate autonomously in cultured differentiating keratinocytes (52). The helper functions have been well studied and are well characterized for both Ad and HSV-1. The following Ad genes provide helper functions for AAV2 replication: E1a, E1b, E2a, E4 and the VA RNA (53); The HSV-1 proteins required for AAV2 replication include: UL30/42, UL9, UL5/8/52 (helicase-primase) and UL29 (ssDBP also known as ICP8) (reviewed in (54)). Alazard-Dany et al. (55) showed that the herpesvirus regulatory proteins ICP0, ICP4 and ICP22, although not essential, can also enhance AAV2 DNA replication. Moreover, ssDNA-binding protein ssDBPs of Ad (Ad-DBP), HSV-1 (ICP8) and the cell (RPA) enhance binding and nicking of Rep proteins at the origin of DNA replication (56), which consist of Rep binding elements (RBE and RBE') and a terminal resolution site (TRS) and are located within the ITRs (3).

AAV2 DNA replication occurs in intranuclear replication compartments (RCs) that colocalize with Rep protein (56–58). The RCs were found associated with promyelocytic

leukemia (PML) nuclear bodies (NBs) in the case of AAV2 and AdV coinfection but not when HSV-1 was used as helper virus (57).

*Cellular factors and AAV2 DNA replication*

There are two important proteomics studies that revealed the complexity of AAV2 replication and interactions with the host cell machinery. In the first study, Nash and colleagues (59) used a tandem affinity purification approach in cells coinfected with AAV2 and AdV5 to identify 188 cellular proteins from 16 functional categories involved in DNA repair and replication, transcription, translation, protein degradation and RNA splicing. In the second proteomic study, Nicolas and colleagues (60) elucidated which cellular and HSV-1 factors are recruited within RCs and associated with Rep protein. The proteins identified were functionally classified into the main categories of DNA and RNA metabolism or associated to cytoskeleton and mitochondrial structures. Thus, components of the DNA replication machinery such as RPA, RFC, MCM or PCNA were shown to be recruited into HSV-1-induced AAV RCs and to colocalize with Rep protein. Moreover, some of the proteins and functional categories were found to be similar to the ones discovered in the AdV-dependent AAV2 replication compartments reported in the first proteomics screen. As shown in Fig. 2 different interactions and networks between the discovered Rep-associated proteins were suggested (60). The viral and cellular proteins found in AAV2 RCs were further reviewed and discussed in Vogel et al (61). Importantly, the results of these studies constituted the base of Specific Aim 2 of this PhD project and will be described in more detail in chapters 5.1 and 5.2.
Further reports showed that purified cellular factors RPA, PCNA and RFC and a partially purified cellular DNA polymerase fraction were necessary for AAV2 DNA replication (62).

*Viral factors and AAV2 DNA replication*

AAV2 relies primarily on cellular replication proteins when coinfected with AdV, as Ad DNA replication proteins such as Ad DNA polymerase, Ad terminal protein and Ad DBP did not show a significant effect on AAV2 replication (63, 64). In contrast, in the case of coinfection with HSV-1, the expression of single-stranded DBP, UL9 and the helicase-primase complex, UL5/UL8/UL22, is required for AAV2 DNA replication (65, 66).

The ss DBPs Ad DBP, UL29 and RPA2 were found to colocalize in infected cell nuclei with AAV Rep protein and AAV DNA (57, 67). Moreover, the interaction between these DBPs and Rep protein enhanced AAV DNA replication up to five-fold through enhanced processivity (49, 68) and site-specific endonuclease activity at the trs (56).

### 3.1.4. AAV2 integration

In absence of a helper virus, AAV2 enters latency. Its gene expression program is auto-repressed and the genome is integrated into the host cell genome, preferentially into a region on the long arm of human chromosome 19 (19q13.3-qter) designated *AAVS1* (69–71). This very well characterized locus was found in the vicinity of the muscle-specific genes *p85*, *TNNT1* and *TNNI* (69, 72, 73), in a transcription-competent chromosomal region (74). The AAV components required for its integration are the ITRs in *cis*, Rep78 or Rep68 in trans and an integration efficiency element (IEE) located within the p5 promoter in *cis* (75). The AAV2 genome can also persist as an episome in the cell nucleus (71).

### 3.1.5. Recombinant AAV vectors, limitations of their cellular transduction and gene therapy applications

AAV is one of the most frequently used viral vectors in gene therapy due to its absence of pathogenicity, ability to express transgenes for long time periods, low immunogenicity, efficient transduction of postmitotic cells and general lack of toxicity (3, 76, 77). The most widely used recombinant AAV vectors belong to the serotype 2 and include ss and ds, sc vectors. The scAAV vectors have a smaller transgene capacity and a higher transduction efficiency both *in vitro* and *in vivo*, due to bypassing the second-strand synthesis step that has been identified as a rate-limiting element in AAV gene expression (15, 78, 79), as shown in Fig. 3. The DNA hairpin structures of ss recombinant (r)AAV vectors can attract Mre11 and ATM proteins involved in ds break repair (80, 81). However, Fragkos and colleagues (82) demonstrated that rAAV2 vectors without p5 promoter do not provoke a DNA damage response of a stalled replication fork.

The mechanisms of AAV transduction in cells and tissues still remain unclear. However, in several publications it was shown that transduction of cells with recombinant AAV

vectors could be increased by genotoxic agents and DNA damaging treatment (83, 84), and negatively influenced by ATM kinase (85) and proteins of the MRN complex (86, 87).

Target diseases for AAV vector mediated gene therapy include monogenic disorders such as cystic fibrosis (88), hemophilia (89), or others such as rheumatoid arthritis (90), spinal muscular atrophy (91) and Parkinson's disease (92). The first AAV gene therapy-based vector product that has received marketing authorization under exceptional circumstances in Europe in 2012 is alipogene tiparvovec (Glybera®), which is used for the treatment of patients with lipoprotein lipase deficiency (LPLD) (93–95). This was a significant step forward for numerous AAV gene therapy applications and gave further hope and great perspectives for using this virus as an effective therapeutic agent.

### 3.1.6. HSV-1 biology: structure, life cycle and DNA replication

*HSV-1 pathogenesis and genome structure*

Herpesviruses, belonging to the family of the *Herpesviridae*, are large double-stranded DNA viruses. There are eight different human herpesviruses known to date. All herpesviruses can establish both lytic infections at the site of entry and latent infections. HSV-1 for example can establish latency in sensory ganglia. Studies of latently infected mouse ganglia have revealed HSV-1 DNA in 1–30% of neurons (96–99).

HSV-1 and HSV-2 are human pathogens that can cause vesicular to ulcerative lesions on mucosal epithelium, skin or cornea. In some cases encephalitis can rarely occur in children or adults, whereas newborn infants can suffer from severe disseminated disease (100).

The pleomorphic herpesvirus particle is approximately 300nm in diameter and is composed of the DNA core, an icosahedral capsid, a tegument and an envelope consisting of a lipid bilayer containing viral membrane proteins and glycoproteins (Fig. 4A). The viral envelope contains 11 viral glycoproteins which play a role in viral entry (101, 102). Virus-encoded proteins form the tegument with primary role in initial steps of infection such as trafficking to the nucleus, inhibition of cellular gene expression and initiation of viral gene expression (103). HSV-1 proteins expressed from the genes UL18, UL19, UL26, UL26.5, UL35, UL38 and UL6 (104) constitute the capsid.

The 152-kb linear double-stranded HSV-1 genome encodes more than 90 proteins and is divided into unique long ($U_L$) and unique short ($U_S$) regions which are both flanked by inverted repeats (100, 105). Seven virus proteins are important for viral DNA replication including the components of helicase-primase complex, the origin-specific DNA-binding protein (OBP), the ssDBP (ICP8), the DNA polymerase and accessory factor (106, 107). The origins of DNA replication are present within the unique longue region (*oriL*) and within the c repeats bounding the unique short region (*oriS*) (94). oriL and oriS contain regions rich in A/T flanked by recognition sites for origin-binding proteins OBPI, OBPII and UL9 (108). DNA packaging signals (*pac*) are found at the ends of the genome and at the junction between the long and the short segment (109). (Fig. 4B)

*HSV-1 entry*

Binding of HSV-1 to cells is mediated principally by viral envelope glycoprotein gC protein, secondarily by gB and gD proteins that could as well substitute for gC. Virus entry requires fusion of the virion envelope with the cell membrane and depends on the action of gB, gD, gH, and gL (99, 100). gC and gB can bind to heparan sulfate proteoglycans (HSPGs) which can further promote the attachment of HSV-1 to the cell (103).

The first HSV entry receptor identified was originally named herpesvirus entry mediator (HVEM) (110), later renamed as herpesvirus entry protein A (HveA) (111) and then catalogued as TNFRSF14. Additional human entry receptors HveC and HveB were then described (112) and proved to be related members of the immunoglobulin superfamily (111, 113).

The entry process occurs via direct fusion of the plasma membrane either with the viral envelope or with the intracellular vesicle after endosomal or phagosomal uptake of the virus (114, 115, 116). Nicola et al (117) showed that the predominant entry pathway of HSV into the chinese hamster ovary cells CHO-K1 and HeLa cells can be strongly affected by a low pH and endocytosis, suggesting that, following to one or multiple receptor binding, HSV can use two different entry pathways depending of the cell type. The fusion process requires the glycoprotein complex including gB, gD and gH/gL (103) and cellular receptors such as nectin-1 or nectin-2 in epithelial cells and neurons, HVEM

in fibroblasts and retinocytes or 3-O sulfated heparan sulfate in corneal fibroblasts (118).

*HSV-1 transcription and DNA replication*

After fusion of the virion envelope and the cell membrane and the transport of the viral nucleocapsid along microtubules, the viral genome is released into the nucleus through the nuclear pores. The linear HSV-1 DNA is then circularized and transcribed in three kinetic phases including immediate-early (IE), early (E) and late (L) genes (117). IE and E genes encode for proteins necessary for the gene expression and DNA replication, whereas proteins encoded by L genes are required for virus assembly and egress (119). L genes can be divided in leaky late, that become upregulated at later times of infection, and true late expressed only after viral DNA replication started (101). The HSV-1 genes are transcribed by the host RNA polymerase II (101). Initiation of gene expression depends on histone demethylation associated with viral DNA after nuclear entry, mediated by lysine-specific demethylase 1 (LSD1) (120).

HSV-1 DNA replication and gene expression occurs in nuclear compartments that form in the proximity of promyelocytic leukemia nuclear bodies (PML NBs) (121). IE gene products expressed 2-4 hours after infection include ICP0, ICP4, ICP22, ICP27 and ICP47. VP16, an HSV-1 tegument protein contains an acidic activator domain and activates the transcription of IE genes in concert with cellular transcription factors (122). VP16 and host cell factor (HCF) form a complex within the nucleus that binds to the host transcription factor octamer-binding protein 1 (OCT1) (122). IE gene products in turn transactivate the transcription of the E genes. For example, ICP4 has the ability to regulate gene expression by forming a tripartite complex with TATA-binding protein and TFIIB (123). The E gene products constitute proteins involved in DNA metabolism which signal the onset of viral DNA replication. DNA replication is followed by the synthesis of the L proteins which include the structural components of the virus.

VP16, ICP0 and $U_s3$ (unique S component open reading frame 3) have been involved in the control of chromatin structure of HSV lytic genes (reviewed in (124, 125)). From this, ICP0 is a viral gene that is responsible not only for the lytic replication but also for reactivation from latency. ICP0 as a transactivator of all three kinetic phases of HSV-1 genes and contains several key domains: the N-terminal RING-finger domain, the C-

terminal ND10 localization signal (126, 127), a dimer/multimer motif (128) and a binding site for ubiquitin-specific protease 7 (USP7) (129).

HSV-1 DNA replication requires either oriS or oriL and the initiator protein UL9. It initiates as a origin-dependent *theta* replication, followed by a predominant origin-independent rolling-circle mechanism (130, 131). The essential HSV-1 replication genes are located within UL and include: UL5, UL8, UL9, UL29 (its product is ICP8, the single-strand DNA-binding protein), UL30 (DNA polymerase), UL42 and UL52 (131–133). The rolling circle replication model was reconstituted in vitro by extracts of HSV-1 infected cells (134).

*HSV-1 egress*

In both epithelial cells and neurons the directed spread of the virus is highly dependent on the transmembrane glycoprotein gE (reviewed in (135)). Virus lacking gE presented a limited and less efficient spread in vivo.

The nuclear egress complex (NEC) of herpesviruses is essential for nuclear budding and is composed of viral proteins UL31 and UL34 (136, 137). Formation of the NEC is required for the localization of both UL31 and UL34 in the inner nuclear membrane (INM), for the recruitment of viral and cellular kinases with role in modification of host cell chromatin and nuclear lamina and for efficient nuclear egress of nucleocapsids (reviewed in (135, 136, )). Modifications of the INM shape around the capsid have been described (138). Importantly, Hagen et al (139) used a multimodal imaging approach to visualize the NEC in situ forming coated vesicles and reported the identification via cellular electron cryo-tomography of a protein layer with two hexagonal lattices at the proximal and distant membrane faces. However, it was shown that the NEC is sufficient to induce vesiculation of the nuclear envelope in transfected cells (140). A recent report suggested that NEC can function as minimal virus-encoded membrane-budding machinery during nuclear egress and does not require additional cellular factors (141).

3.1.7. Figures and Figure Legends

A

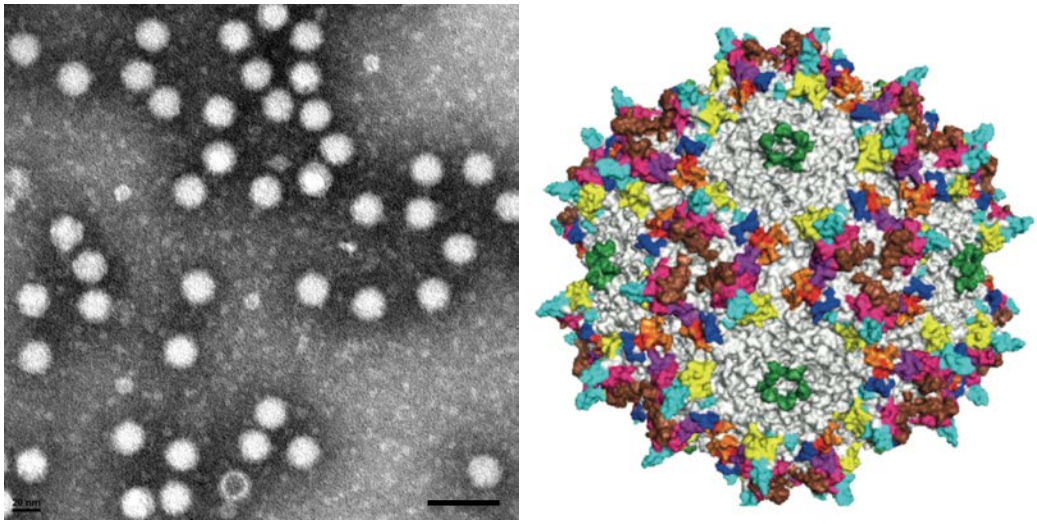

B

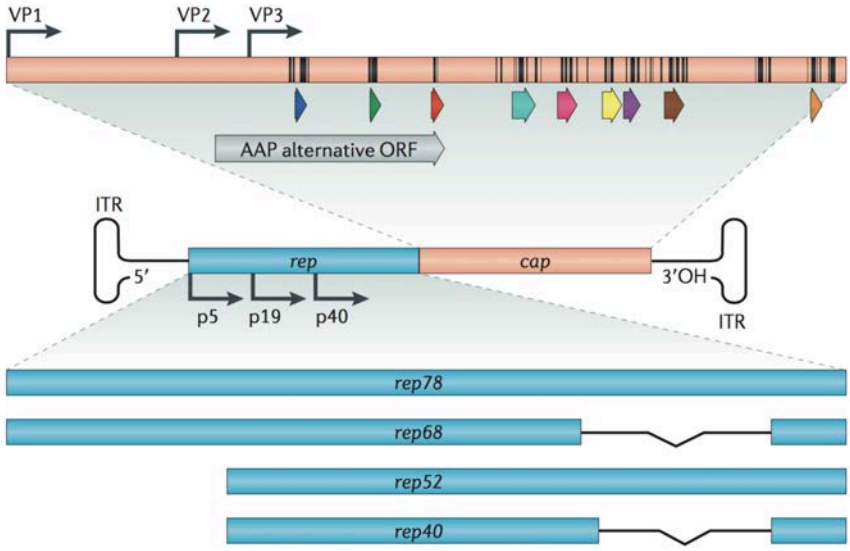


**Figure 1. AAV2 virion and genome structure.**
(A) Electronmicrograph (approximately 20 nm virions) and crystal structure of the AAV capsid with VP3 hypervariable regions coloured to the matching genetic regions. The electronmicrograph is courtesy of E. Schraner, Institute of Virology, University of Zurich. Bar: 100nm.
(B) The AAV2 genome contains two clusters of genes flanked by T-shaped hairpins at each end forming the inverted terminal repeats (ITRs). The four non-structural proteins (Rep40, Rep52, Rep68 and Rep78) are encoded by the *rep* genes, whereas the structural proteins (VP1, VP2, and VP3) that form the viral capsid are encoded by the *cap* genes. The assembly-activating protein (AAP) is encoded by an alternative ORF within *cap*. Coloured arrows: hypervariable regions.
Figure from *Kotterman MA and Schaffer DV, 2014, Nature Reviews Genetics 15:445-451 (with permission).*

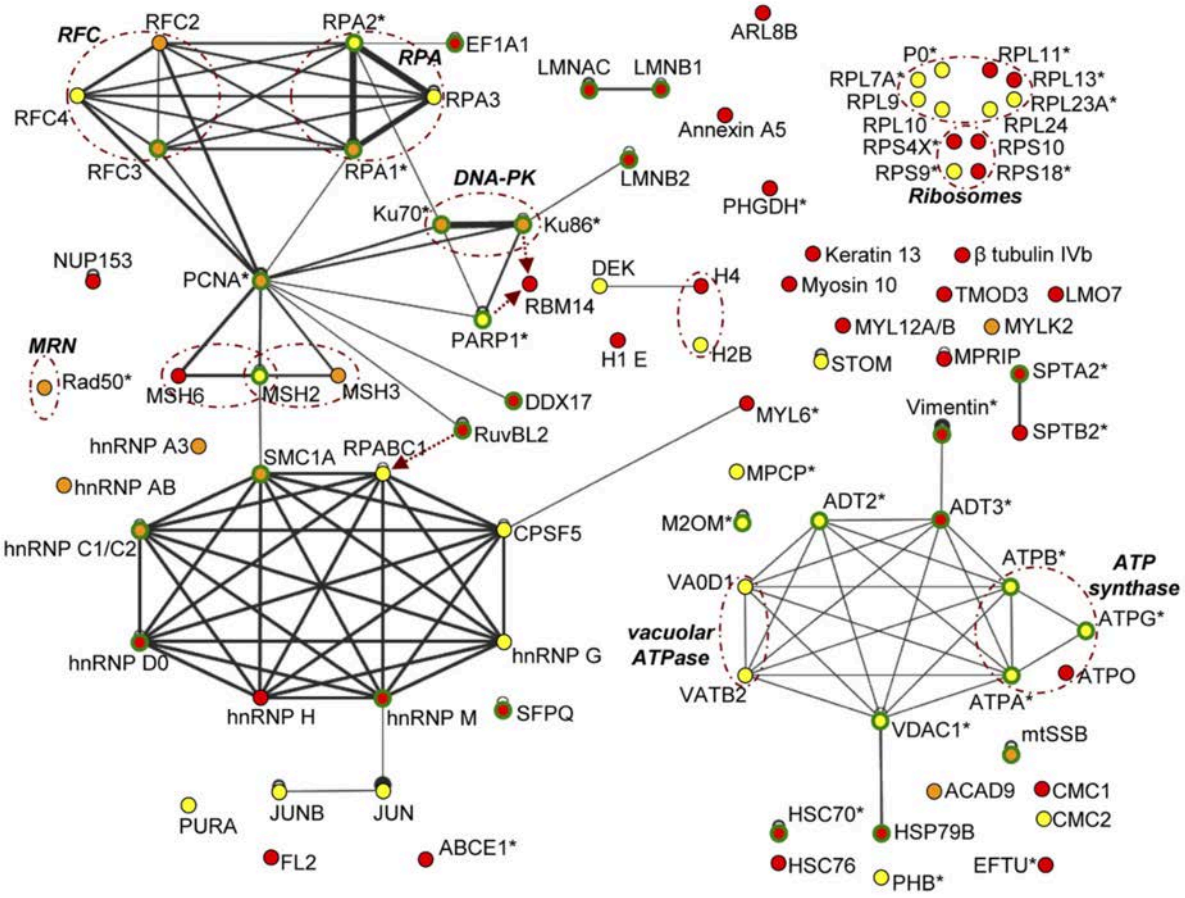


**Figure 2. Schematic map of interaction networks of Rep-associated proteins found in AAV and either HSV-1 or AdV co-infected cells.**

The color codes refer to the protein specific interactions identified from HeLaAAVtCR cells infected with wt HSV-1 (red), HSV1UL30 (yellow), or both helper viruses (orange); proteins for which a physical or functional interaction with a protein from another virus has already been reported (green); self-interacting proteins (black); proteins identified in Rep-containing complexes purified from adenovirus- and AAV-coinfected cells (asterisks); proteins constituting a known functional complex (dashed brown circles).

Figure taken from *Nicolas A et al, 2010, Journal of Virology 84: 8871-8887 (with permission)*

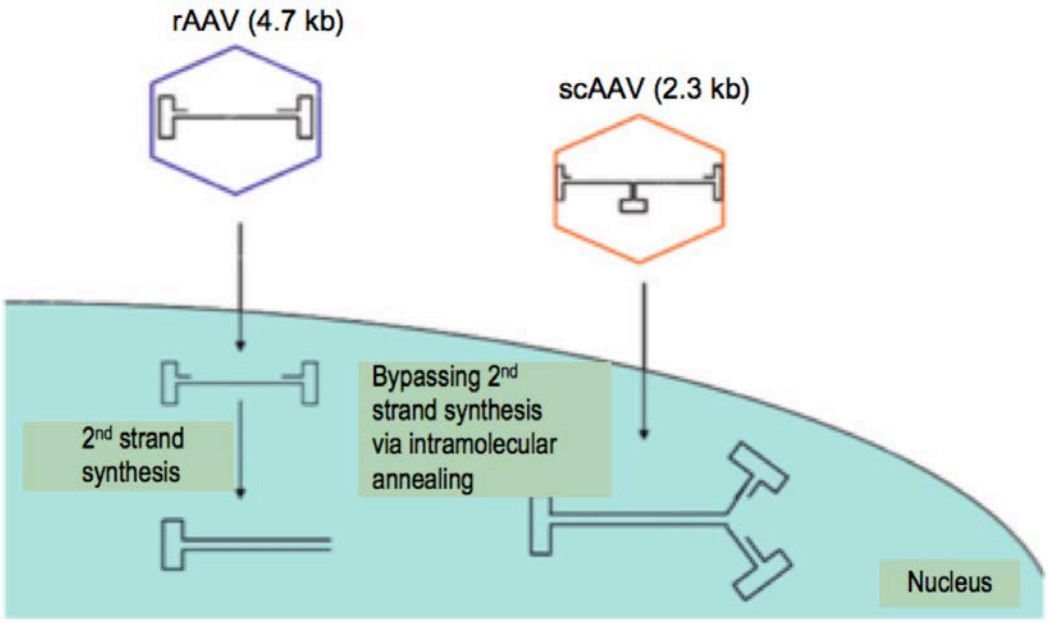


**Figure 3. Comparison between recombinant ss (rAAV) and ds (scAAV) vectors.**

Figure adapted from: *Daya S and Berns KI, 2008, Clinical Microbiology Reviews 21: 583-593.*

A

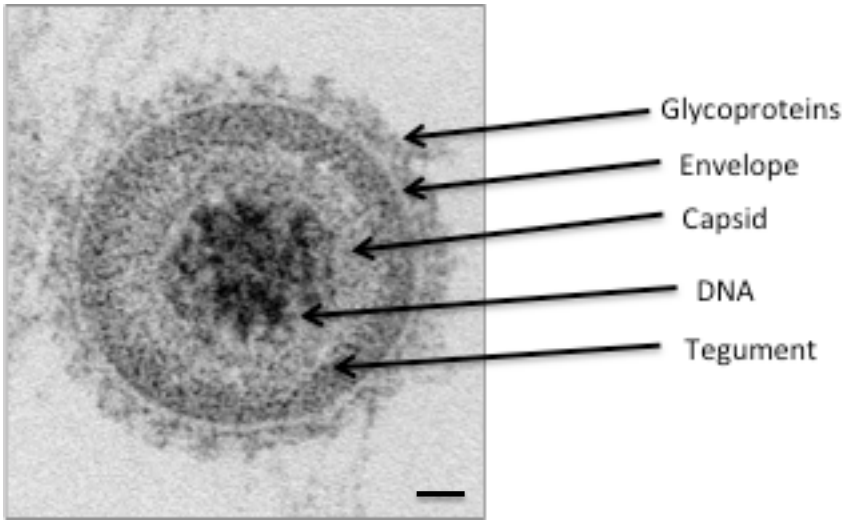


B

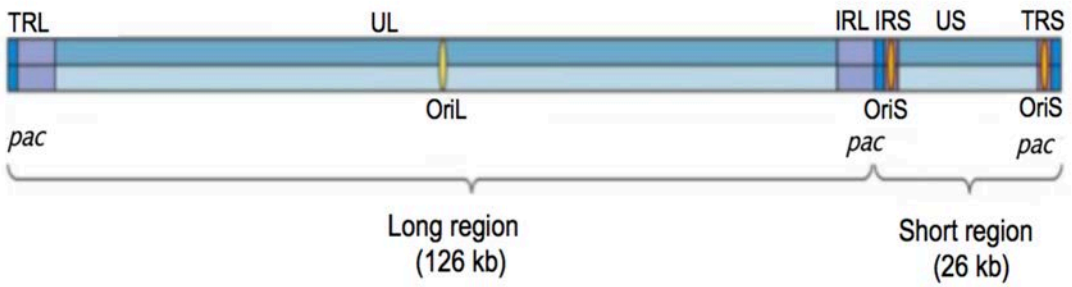


Figure 4. HSV-1 structure and genome organization
(A) Electronmicrograph and schematic representation of the HSV-1 particle.
The diameter of the whole particle varies between 200 and 300 nm. The electronmicrograph is courtesy of E. Schraner, Institute of Virology, University of Zurich. Bar: 100 nm.
(B) The HSV-1 genome is composed of two distinct segments, unique long (UL) and unique short (US) and terminal and internal inverted repeats of the long (L) and short (S) segments (TRL, IRL, IRS, TRS). The origins of DNA replication (oriL and oriS) and the DNA packaging/cleavage signals (pac) are the sole *cis* elements required for DNA replication and packaging.

Figure adapted from *Flint Principles of Virology, 4th Edition, 2015*

## 3.2. Viruses and the cell cycle

The cell cycle is driven through the four stages G1, S, G2 and mitosis by kinase complexes formed by cyclins bound to cyclin-dependent kinases (Cdk). The levels of regulation are achieved by Cdc25 family of protein phosphatases (142) and the small inhibitory proteins CDK-inhibitors (CKIs). During G2, cyclin B1 forms a kinase complex with Cdk1 that remains inactive and can be further catalyzed by a nuclear protein Wee1 (143). In late G2, the kinase complex is activated by Cdc25C that is regulated through phosphorylation of Cdk1. Importantly, Cdk1/cyclin B1 complex can be inactivated by the anaphase-promoting complex (APC) possibly by degrading cyclin B1 (144).

During S phase, cyclin A functions with Cdk2 to phosphorylate pre-replication complexes to ensure that only one single round of DNA replication occurs. G2/M transition and exit from mitosis are regulated by various kinases and phosphatases (145, 146) whereas the activation of checkpoints is controlled mainly by ATM and ATR kinases. ATM and ATR initiates the phosphorylation cascade from Chk2 to Wee1 to Cdk1 leading to their activation and phosphorylation of Cdc25C (147–149).The checkpoint pathways can maintain Cdk1/cyclin B1 complexes inactive and prevent their nuclear accumulation. Moreover, the induction of G2 arrest is regulated by p53 that, by controlling p21, can lead to the inhibition of the kinases' activity (145).

Viruses can manipulate the cell cycle progression and alter checkpoint signaling in order to provide a proper environment for their replication (150, 151).

One of the common strategies used by viruses such as retroviruses, DNA and RNA viruses, is to induce cell cycle arrest at G2/M (reviewed in (152)). Other viruses, like oncogenic viruses, manipulate the cell cycle transition in G1/S via p53 inactivation (reviewed in (153)). However, many viruses can interplay with all phases of the cell cycle. Here an overview of possible molecular mechanisms underlying these strategies of interaction with viral proteins and cell cycle factors is described.

G2/M arrest is achieved by either inactivation of Cdk1 at the G2/M checkpoint and/or interference with mitotic progression. Human papillomavirus (HPV) type 1 E4 protein can induce G2 arrest by maintaining the Cdk1 phosphorylation that will finally result in a delay of Cdk1/cyclin B1 kinase activation (154, 155). The parvovirus B19 NS1 protein mediates G2 arrest in the presence of an active Cdk1/cyclin B1 complex inducing activation of checkpoint pathways that can regulate cyclin B nuclear export (156, 157).

An alternative strategy used by E4 protein of HPV16 is to prevent the nuclear entry of the Cdk1/cyclin B complex by sequestering the Cdk1/cyclin B kinase complex within the cytoplasm (158). Other viral proteins are suggested to induce G2/M arrest and inhibit the mitotic exit by interference with kinetochores, such as ICP0 protein of HSV-1 (159) or EC27 protein of the baculovirus that can act as a non-degradable Cdk1/cyclinB analog (160). EBV-EBNA3C inhibits the G2/M checkpoint (161), which may be realized via manipulation of Chk2 signaling (162). E1B-55K and E4orf3 genes of adenovirus type 5 are sufficient to prevent mitotic arrest in the infected cell (163). However, one of the most studied viral G2 arrest is that induced by Vpr protein of HIV showing ability to manipulate key cellular pathways to ensure efficient replication. In the arrested cells the Cdk1/cyclin B1 complex remains inactive by binding of Vpr to chromatin or to specific splicing factors that activate ATR and promote the activity of the Wee1 kinase while inhibiting Cdc25 phosphatase (164–166). The results of this activation are changing the levels of Wee1 protein and downregulate the expression of genes in the MAPK pathway (167).

By contrast, the AAV-induced G2 arrest is likely induced by the viral genome – a ssDNA molecule with terminal hairpin loops, prone to activate DNA damage responses, cell cycle arrest and/or, in cells lacking p53, apoptosis (168).

The cell cycle could play an important role also in the expression of HSV-1 late proteins by the activation of Cdk1 (169). In papillomaviruses (PV), an increased synthesis of capsid proteins in the G2 phase may involve mechanisms of transcription and translation during G2/M (170).

Manipulation of cell cycle progression for more efficient viral replication is accomplished in the case of some viruses by creating a pseudo-S phase at the stage when the cellular DNA replication is complete. Thus, for the baculovirus both the viral EC27 protein and PCNA contribute to S phase entry following infection (160), whereas for HPV the involvement of the viral proteins E6 and E7 were demonstrated (171).

Furthermore, the cell cycle phase can influence virion assembly and release as in the case of baculovirus. Specifically the viral EC27 protein is involved in the maturation of the viral particle and is required for the inter-insect transmission by the so-called occlusion-derived (ODV) viral form (172).

Influenza A virus strains A/WSN/33 (H1N1), H3N2, H9N2 and PR8H1N1 can induce a cell cycle arrest in G0/G1 phase in infected cells associated to a decreased amount of hyperphosphorylated retinoblastoma (Rb) protein. DNA viruses such as SV40 (173,

174), HPV (154) or adenovirus (175–177) can promote entry into S phase of the infected cells for an optimal synthesis of viral DNA. Other large DNA viruses like herpesviruses can promote G0/G1 phase arrest to avoid competition for cellular DNA replication resources (178).

DDR pathways may also be involve in the viral G1/S arrest. Damage sensed via ATM/ATR pathways results in phosphorylation and activation of Chk2 and/or Chk1, two checkpoint kinases that can also phosphorylate downstream targets to initiate G1/S arrest (162, 179). Chk1/Chk2-mediated phosphorylation of p53 results in upregulation of p21, which functions as a Cdk2 inhibitor (180). In addition to upstream activators, Chk1 and Chk2 are direct targets for viral inactivation of damage responses. HBV-HBx can have inhibitory effects on Chk1 activity while preventing ATR-mediated phosphorylation of Chk1 and intra-S phase checkpoint activation (181–183).

The oncogenic viruses group can control G1/S transition via p53 inactivation to prevent apoptosis in infected cells. For example, HPV-E6 (184), KSHV-LANA (185), Ad-E1B55K/E4orf6 (186) mediate the ubiquitination and proteasome-mediated degradation of p53 via recruitment of cellular factors. SV40-LTag association with p53 leads to p53 inhibition (187). HBV-Hbx inhibits transcription from the p53 promoter, resulting in reduced p53 levels (188).

Some viruses promote CDk2 activity via manipulation of its regulators. EBV-infected cells fail to accumulate p21 in response to DNA damaging agents even if p53 expression and damage-induced phosphorylation remains unaffected (189). HBV, while activating ATR and downstream Chk1 phosphorylation, inhibits downstream signaling via degradation of p21, promoting viral replication (190).

Understanding these complex interactions between viruses, cellular DNA damage and checkpoint responses can provide further tools for possible applications. For example, cellular repair proteins could represent potential targets for antiviral drugs. Another possibility is to use viruses as tools to study the role of cellular proteins in repair processes.

Overall, the strategies used by viruses to manipulate the cell cycle are complex and involve a multitude of pathways with not yet completely understood consequences.

*Parvoviruses and the cell cycle*

Parvoviruses are able to block entry into the S phase using a mechanism of cell cycle regulation involving nuclear capsid assembly (191). The reaction of ssDNA convertion requires DNA polymerase delta, PCNA (192) as well as other S phase-induced factors. Interestingly, the S phase activation of the minute virus of mice (MVM) promoter P4, which directs the transcription unit encoding the NS proteins, is dependent on an E2F motif located in its proximal region (193).

As the infection progresses, most parvoviruses destabilize the cell cycle eliciting a DDR as a strategy to support viral replication (179, 194, 195) and arresting cells at the S or G2/M phases. It is still unknown whether the cell cycle regulatory machinery or the S-phase induced molecular interactions, could regulate parvovirus assembly and maturation. However, Riolobos et al (196) showed that the phosphorylation of Raf-1 kinase of MAPK signaling pathway can play an important role in the nuclear entry of minute virus of mice (MVM) capsid assembly intermediates, being as well required for viral maturation.

AAV2, a helpervirus dependent human parvovirus, exerts oncosuppressive activities on cells mainly by manipulating the cell cycle through a Rep78-dependend S-phase arrest (197). Furthermore, Rep78 can activate pRb and induce a S-phase arrest depending on a functional zinc finger motif within the C-terminus (197, 198). Interestingly, adenovirus E1A protein can rescue the Rep78-mediated cell cycle arrest during a productive infection. Importantly, Hermanns et al (199) reported a cell cycle arrest of AAV2 infected primary human fibroblasts particularly by lowering the levels of cell cycle regulatory proteins the cyclins A and B1, hypophosphorylated pRb and p107 and increasing levels of CKI p21.

## 3.3. RPA and DNA replication

Replication protein A (RPA) was initially identified as an essential protein for SV40 DNA replication (200–202). RPA constitutes a heterotrimeric complex that is the main ss DNA binding protein (DBP) involved and equally required in many DNA processes such as repair, recombination, replication (203) or activation of cell cycle checkpoints (204) (shown in Figure 5).

The main subunits are RPA1 (70 kDa), RPA2 (32 kDa), RPA3 (14 kDa). Additionally, Wold and colleagues (205) characterized a naturally occurring homologous form of the RPA2 subunit, named RPA4, that can substitute for RPA2 in complex formation but cannot however support chromosomal DNA replication and cell proliferation. In another study of Wold et al (206) described an alternative RPA complex (aRPA) containing RPA1, RPA3 and RPA4 that, although it interacts with ssDNA in a similar fashion to the canonical RPA complex, it did not support DNA replication *in vitro*.

The central elements of the biochemical composition of RPA are the six oligosaccharide/oligonucleotide binding folds (OB-folds) composed of five ß-strands arranged in a ß-barrel structure (207). RPA1 contains four OB-folds (DNA binding domain- A, DBD-B, DBD-C, and DBD-F), RPA2 and 3 contain only one each (DBD-D and DBD-E, respectively) (Figure 5A). DBD-F presents a lower affinity for ssDNA compared to DBD-A and DBD-B that constitute the major ssDNA binding affinity initiated at the 5'-side of ssDNA of 8-10 nucleotides (208). RPA3 is required for the stability of the heterotrimer (209). Importantly, RPA2 can interact with other proteins by its two domains, the N terminal phosphorylation and C-terminal alpha-helix domain (210).

In the DNA repair process, RPA plays an important role in nucleotide excision repair interacting in the gap-filling reaction with RFC and PCNA (211), or with Rad51 and Rad52 in the homologous recombination repair of DSBs (212, 213).

Moreover, RPA can interact and co-localize with the MRN complex. RPA is also involved in ATM signaling by stimulating ATM downstream activity to p53 and Chk2 (214).

During DNA replication, RPA participates in the initiation and elongation process by promoting the recruitment of DNA polymerases, in the switch of polymerase on the lagging strand as well as in coordinating the processing of Okazaki fragments (215).

Although it was first described more than 30 years ago, the stress-dependent and –independent phosphorylation of the RPA32 N-terminus still remains the most studied post-translational modification of the RPA complex (216). This process is demonstrated to be depended on the cell cycle (217) mainly at the G1/S phase transition being followed by a dephosphorylation phase after mitosis. At this stage, the activity of DNA-PK, ATM and ATR appear to play an important role (218). ATR activation on RPA binding ssDNA activates cell cycle checkpoints, stabilizes stalled forks, supports DNA repair and the genome integrity (219).

Vassin et al (220) found that RPA2 phosphorylation mutants which mimic the hyperphosphorylated form could not localize to DNA replication centers. The same study showed that RPA phosphorylation following DNA damage inhibited RPA from activating DNA replication and the recruitment of repair factors to sites of DNA damage.

Knockdown studies showed the role of RPA on the cell cycle, DNA damage signaling and replication. Thus, RPA1 depleted cells appear to have a slower S phase progression followed by an G2/M arrest and formation of gamma-H2AX foci (221). Moreover, RPA1 depletion leads to phosphorylation of Chk2, ATM and activation of p21 expression (222) but does not affect RPA2 or RPA3 levels in the cell (223). While some RPA1 mutants of ssDNA binding domains do not appear to affect RPA1 cellular functions, a deletion of DBD-C was unable to support DNA replication (223).

*RPA and viral DNA replication*

Although the two main RPA subunits RPA1 and RPA2 are known to be recruited to viral replication compartments of some DNA viruses, such as HSV-1, AdV, HPV, SV40, the exact role of each subunit in viral DNA replication is still unclear. Wilkinson and Weller (224) showed, by using a polymerase null virus, that the HSV-1 DNA synthesis did not induce RPA2 hyperphosphorylation and that endogenous hyperphosphorylated forms of RPA were not colocalized with the replication compartments of HSV-1.

By knocking down RPA1 and other ATR pathway proteins such as ATRIP, CINP, Claspin, TopBP1 and HCLK2 it was shown that HSV-1 DNA replication significantly decreased (225). Loo and Melendy (226) reported that the interaction of RPA1 with the viral protein E1 of HPV was strongly inhibited by ssDNA, suggesting a possible role in HPV DNA viral replication.

However, most extensive studies on the involvement of specific RPA subunits in viral DNA replication used SV40 as a well-established model to study the molecular mechanisms involved in eukaryotic DNA replication (216, 227). Erdile and colleagues (228) expressed the 70-kDa human RPA subunit in *E.coli* and demonstrated that this subunit was unable to replace the RPA complex in SV40 DNA replication, suggesting that the other subunits are required for DNA replication. This conclusion was further supported by other results of the same group showing that monoclonal antibodies against the RPA2 subunit could inhibit the DNA replication (202). Furthermore, antiserum raised against purified recombinant RPA3 could inhibit the DNA replication to a certain extend indicating that this subunit may be involved in some steps of DNA replication (229). Importantly, the alternative RPA complex (aRPA) containing RPA1, RPA3 and RPA4 can interact with ssDNA and can inhibit the “canonical” RPA complex (RPA1, RPA2 and RPA3) from functioning in DNA replication due to two regions identified on RPA4 (206). By contrast, it was reported that a purified, recombinant subcomplex form composed of the 32- and 14-kDa subunits of RPA did not bind to the ss DNA, was unable to substitute the complete RPA complex and did not inhibit DNA replication, possibly by not interacting with proteins required for replication (201).

Importantly, these studies indicate that the RPA2 and not the RPA1 subunit plays an essential role in the SV40 DNA replication (201, 228).

Our present results support this concept of differential effects of the RPA subunits in viral DNA replication with RPA2 as the required gene for HSV-1 supported AAV2 DNA replication.

Other studies on RPA implication in AAV DNA replication showed rather mixed results. In cells co-infected with AAV2 and either Ad or HSV-1, RPA2 was shown to be localized in the AAV RCs, even in absence of a viral ssDBP (230). The cellular RPA2 and the HSV-1 UL29 (ICP8) protein or the ss DNA binding protein (DBP) of adenovirus colocalize and interact with AAV Rep proteins and AAV DNA (57, 230, 231). Interestingly and in line with our results, Ni et al (12) showed that AAV DNA replication was significantly inhibited up to 90% upon treating the cells with monoclonal antibodies against either RPA2 or RFC and concluded that, together with PCNA and RFC, RPA2 is an essential component for AAV DNA replication. Of note, RPA2, PCNA and RFC were demonstrated to be required for SV40 DNA replication as well (200).

Moreover, the addition of RPA2 or Ad-DBP to uninfected cell extracts enhanced AAV DNA replication (232), suggesting an important role of RPA2 in AAV DNA replication.

Taken together, these results show the duality and the complex role of the two main RPA subunits in DNA replication and repair: RPA2, a well-known DNA damage marker, with implications mainly in viral DNA replication and RPA1, containing the main ssDNA-binding core that is necessary and sufficient for high affinity DNA binding.

**A**

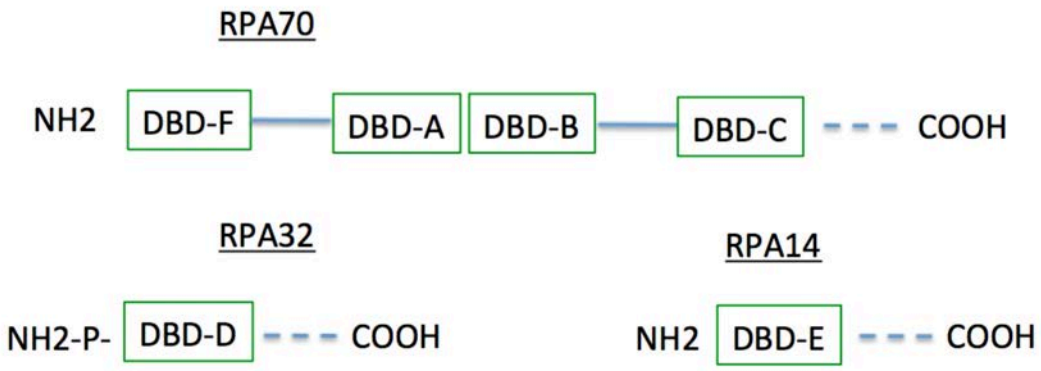


**B**

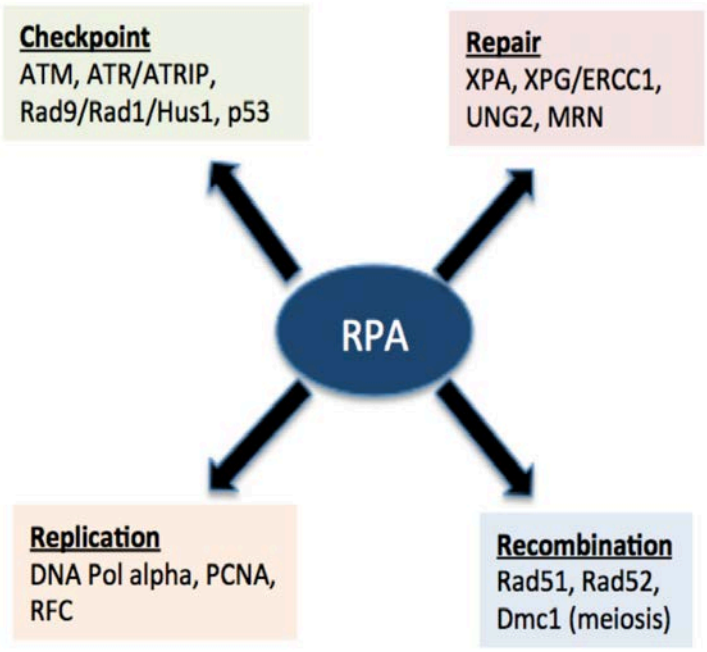


**Figure 5.** A: Schematic representation of RPA1 (RPA70), RPA2 (RPA32) and RPA3 (RPA14) protein DNA binding domains (DBD). RPA70: DBD-A, DBD-B, DBD-C, and DBD-F.; RPA2: DBD-D; RPA3 (DBD-E). The N-terminal domain of RPA32 exists as an extended unstructured domain and contains most of the phosphorylation sites for the trimer. B: RPA protein as required for all four major DNA metabolism pathways and proteins involved as listed.

Figure adapted from: Zou Y, Liu Y, Wu X, Shell SM, 2006, Functions of Human Replication Protein A (RPA): From DNA Replication to DNA Damage and Stress Responses, *J Cell Physiol* 208: 267-273.

# 4. Specific aims of PhD thesis

The first aim of this thesis was to establish an assay that allowed visualizing and investigating AAV2 gene expression/DNA replication and cell cycle progression by live cell microscopy. This work was recently published in the Journal of Virology (doi 10.1128/JVI.00357-17).

In this study, our specific question was how AAV2 and HSV-1 can co-exist in a cell population. We showed that in co-infected cultures, AAV2 DNA replication takes place almost exclusively in S/G2 cells, while HSV-1 DNA replication is restricted to G1. We observed that AAV2 *rep* gene expression is cell cycle dependent, and gives rise to distinct time controlled windows for HSV-1 replication. High Rep protein levels in S/G2 phases support AAV2 replication and inhibit HSV-1 replication. Conversely, low Rep protein levels in G1 permit HSV-1 replication, but are insufficient for AAV2 replication. Live microscopy revealed that not only wtAAV2 replication but also reporter gene expression from both single-stranded and double-stranded (self-complementary) recombinant AAV2 vectors preferentially occurs in S/G2 cells, suggesting that the S/G2 preference is independent of the nature of the viral genome. Interestingly, however, a substantial proportion of the S/G2 cells transduced by the double-stranded but not the single-stranded recombinant AAV2 vectors progressed through mitosis in absence of the helper virus. We concluded that cell cycle-dependent AAV2 *rep* expression facilitates cell cycle-dependent AAV2 DNA replication, and inhibits HSV-1 DNA replication. This may limit competition for cellular and viral helper factors, and hence, creates a biological niche for both viruses to productively replicate in distinct sets of dividing cells.

The second aim was to investigate the effect of cellular proteins that are known to interact with AAV2 DNA either directly or via the AAV2 Rep proteins on the transduction efficiencies of single-stranded and double-stranded AAV2 vectors.

Thus, we performed an image-based RNAi screen to investigate the effects of a functional group of cellular proteins known to interact with AAV2 DNA directly or via the AAV2 Rep proteins in AAV2 replication compartments, on the transduction efficiencies of ss and ds AAV vectors on a single cell level. We identified cellular proteins that

positively or negatively affected the transduction efficiency of both ss and ds AAV2 vectors as well as proteins that presented differential effects on the two different vector types. In particular, the posttranscriptional knockdown of the single-stranded DNA binding protein RPA1 resulted in the most differential transduction efficiencies of ss and ds AAV vectors of all proteins tested, and these effects were reversed when the knockdown of endogenous RPA1 was complemented with exogenous RPA1 in our validation assay. The RPA2 subunit of the RPA heterotrimer had a similar effect as RPA1 on the transduction efficiencies of the two vector types. Interestingly however, RPA2 appeared to enhance HSV-1 supported AAV2 replication while RPA1 had no significant positive or negative effect on virus replication. In conclusion, this RNAi-based study provides novel insights into the roles of host factors, such as the subunits of the main cellular ss DNA binding protein RPA, in AAV vector transduction and AAV2 DNA replication.

# 5. Results

## 5.1. Cell cycle-dependent expression of AAV2 Rep in HSV-1 co-infections gives rise to a mosaic of cells replicating either AAV2 or HSV-1

Francesca D. Franzoso, Michael Seyffert, Rebecca Vogel, Artur Yakimovich, Bruna de Andrade Pereira, Anita F. Meier, Sereina O. Sutter, Kurt Tobler, Bernd Vogt, Urs F. Greber, Hildegard Büning, Mathias Ackermann, and Cornel Fraefel

*Journal of Virology*, in press

**Own contributions:**

I have established a live cell fluorescence microscopy assay to assess the cell cycle phase-dependent gene expression and replication of AAV2. This work is shown here as part of the manuscript that was recently published in *Journal of Virology*.

Designed and performed live imaging experiments (Figures 5 and 7; Tables 2 and 3; Supplementary files 1, 2, 3, 4)
Designed and performed qPCR experiments (Figure 3)
Minor contribution to the fluorescence in situ hybridization (FISH) assay development (Figures 2 and 4)
Contributed to the preparation of the manuscript and figures.

AMERICAN SOCIETY FOR MICROBIOLOGY | Journal of Virology®





# Cell Cycle-Dependent Expression of Adeno-Associated Virus 2 (AAV2) Rep in Coinfections with Herpes Simplex Virus 1 (HSV-1) Gives Rise to a Mosaic of Cells Replicating either AAV2 or HSV-1

**Francesca D. Franzoso,[a] Michael Seyffert,[a,b] Rebecca Vogel,[a] Artur Yakimovich,[c*] Bruna de Andrade Pereira,[a*] Anita F. Meier,[a] Sereina O. Sutter,[a] Kurt Tobler,[a] Bernd Vogt,[a] Urs F. Greber,[c] Hildegard Büning,[d,e] Mathias Ackermann,[a] Cornel Fraefel[a]**

Institute of Virology, University of Zurich, Zurich, Switzerland[a]; Whitehead Institute for Biomedical Research, Cambridge, Massachusetts, USA[b]; Institute of Molecular Life Sciences, University of Zurich, Zurich, Switzerland[c]; Center for Molecular Medicine Cologne, University of Cologne, Cologne, Germany[d]; Institute for Experimental Hematology, Hannover Medical School, Hannover, Germany[e]

**ABSTRACT** Adeno-associated virus 2 (AAV2) depends on the simultaneous presence of a helper virus such as herpes simplex virus 1 (HSV-1) for productive replication. At the same time, AAV2 efficiently blocks the replication of HSV-1, which would eventually limit its own replication by diminishing the helper virus reservoir. This discrepancy begs the question of how AAV2 and HSV-1 can coexist in a cell population. Here we show that in coinfected cultures, AAV2 DNA replication takes place almost exclusively in S/$G_2$-phase cells, while HSV-1 DNA replication is restricted to $G_1$ phase. Live microscopy revealed that not only wild-type AAV2 (wtAAV2) replication but also reporter gene expression from both single-stranded and double-stranded (self-complementary) recombinant AAV2 vectors preferentially occurs in S/$G_2$-phase cells, suggesting that the preference for S/$G_2$ phase is independent of the nature of the viral genome. Interestingly, however, a substantial proportion of S/$G_2$-phase cells transduced by the double-stranded but not the single-stranded recombinant AAV2 vectors progressed through mitosis in the absence of the helper virus. We conclude that cell cycle-dependent AAV2 *rep* expression facilitates cell cycle-dependent AAV2 DNA replication and inhibits HSV-1 DNA replication. This may limit competition for cellular and viral helper factors and, hence, creates a biological niche for either virus to replicate.

**IMPORTANCE** Adeno-associated virus 2 (AAV2) differs from most other viruses, as it requires not only a host cell for replication but also a helper virus such as an adenovirus or a herpesvirus. This situation inevitably leads to competition for cellular resources. AAV2 has been shown to efficiently inhibit the replication of helper viruses. Here we present a new facet of the interaction between AAV2 and one of its helper viruses, herpes simplex virus 1 (HSV-1). We observed that AAV2 *rep* gene expression is cell cycle dependent and gives rise to distinct time-controlled windows for HSV-1 replication. High Rep protein levels in S/$G_2$ phase support AAV2 replication and inhibit HSV-1 replication. Conversely, low Rep protein levels in $G_1$ phase permit HSV-1 replication but are insufficient for AAV2 replication. This allows both viruses to productively replicate in distinct sets of dividing cells.

**KEYWORDS** AAV2, HSV-1, Rep protein, biological niche, cell cycle, helper virus

**Received** 2 March 2017 **Accepted** 5 May 2017

**Accepted manuscript posted online** 17 May 2017

**Citation** Franzoso FD, Seyffert M, Vogel R, Yakimovich A, de Andrade Pereira B, Meier AF, Sutter SO, Tobler K, Vogt B, Greber UF, Büning H, Ackermann M, Fraefel C. 2017. Cell cycle-dependent expression of adeno-associated virus 2 (AAV2) Rep in coinfections with herpes simplex virus 1 (HSV-1) gives rise to a mosaic of cells replicating either AAV2 or HSV-1. J Virol 91:e00357-17. https://doi.org/10.1128/JVI.00357-17.

**Editor** Richard M. Longnecker, Northwestern University



Address correspondence to Cornel Fraefel, cornel.fraefel@access.uzh.ch.

* Present address: Artur Yakimovich, MRC LMCB, University College London, London, United Kingdom; Bruna de Andrade Pereira, Boehringer Ingelheim Pharma GmbH & Co. KG, Biberach an der Riss, Germany.

F.D.F., M.S., and R.V. contributed equally to this work.

Viruses depend on host cell factors for the replication of their genome. As the nucleic acid metabolites accumulate during the S phase of the cell cycle, many DNA viruses, such as autonomous parvoviruses, adenoviruses, or herpesviruses, have evolved mechanisms to manipulate cell cycle progression and induce S- or $G_2$-phase arrest, which allows them to replicate their genomes in concert with cellular DNA (1–3). Herpes simplex virus 1 (HSV-1) is an enveloped human pathogen with a double-stranded DNA genome of 152 kbp encoding approximately 90 proteins (reviewed in reference 4). Among these proteins are 7 enzymes, which are essential and sufficient to support HSV-1 DNA replication in cells, and several accessory proteins, including uracil DNA glycosylase, alkaline exonuclease, thymidine kinase, or ribonucleotide reductase, which are homologous to important cellular S-phase proteins. HSV-1 may therefore be less dependent on cellular proteins and a specific phase of the cell cycle. Indeed, unlike many other DNA viruses, HSV-1 has been shown to replicate well outside the S phase and to possess mechanisms for actively arresting cells in $G_1$ and $G_2$ phases (5–9).

In contrast, adeno-associated virus 2 (AAV2) is a nonpathogenic human parvovirus with a small, single-stranded DNA genome of 4,680 nucleotides. As for herpesviruses, the AAV2 genome is packed in an icosahedral capsid; however, it lacks a lipid envelope and is smaller than the herpesvirus capsid. The AAV2 genome contains only two clusters of genes, *rep* and *cap*, flanked by inverted terminal repeats (ITRs), which contain the viral origin of DNA replication and a packaging signal. *cap* gene expression is controlled by the p40 promoter and gives rise to the capsid proteins VP1, VP2, and VP3, which, due to alternative start codons, differ in their N termini (reviewed in reference 10). In addition, a nested open reading frame within the *cap* gene encodes a protein designated assembly-activating protein, which is believed to be required for AAV2 capsid assembly in the nucleolus (11). The *rep* gene cluster encodes four Rep isoforms, Rep40, Rep52, Rep68, and Rep78, due to transcription from two different promoters, p5 and p19, and alternative splicing at an intron near the C terminus. The multifunctional Rep proteins are involved in diverse processes of the AAV2 life cycle, including DNA replication, the regulation of gene expression, genome packaging, and site-specific integration (12–17). The functions of the Rep proteins include site-specific DNA-binding and endonuclease activities (Rep68 and -78) as well as site-nonspecific ATPase/helicase activity (all Rep isoforms) (18–22). Likely because of its low genetic complexity, AAV2 depends not only on a cell for productive replication but also on the presence of a helper virus, such as HSV-1, adenovirus 2 (AdV2), or human papillomavirus 16 (HPV16) (23–25). In the absence of a helper virus, AAV2 enters cells and establishes latent infection by maintaining its DNA episomally or inserting it into the host cell genome, preferentially at a site termed AAVS1 on human chromosome 19 (14, 26–28). The dependence of AAV2 on a helper virus inevitably leads to competition for cellular resources and viral factors that are essential for both AAV2 and helper virus replication, such as the HSV-1 ICP8 protein and the helicase/primase complex (29–31). HSV-1 also provides accessory proteins, including the ICP0 protein and the viral DNA polymerase (31), and may condition the cellular environment to promote AAV2 replication, e.g., by interfering with cellular DNA damage signaling (32) or cell cycle progression (5–9, 33).

AAV2 has been demonstrated to efficiently inhibit the replication of its helper viruses human adenovirus 2 of species C (HAdV-C2) (34–36) and HSV-1 (37, 38). For example, the Rep-mediated inhibition of the protein kinases protein kinase A (PKA) and cAMP-dependent protein kinase catalytic subunit (PRKX), both members of the cyclic AMP (cAMP) signal transduction pathway, results in the decreased expression of cAMP-responsive genes and contributes to the Rep-mediated inhibition of AdV replication (39–42). Although the mechanism of how AAV2 inhibits HSV-1 replication is less well understood, it also involves the large Rep proteins, in particular the DNA-binding and ATPase/helicase activities of Rep68 and -78 (43). We have previously shown that Rep68 can bind to consensus Rep-binding sites located on the HSV-1 genome and that the Rep helicase domain is sufficient to inhibit DNA replication if binding is facilitated (44). Interestingly, however, while the formation of mature HSV-1 replication compartments (RCs) is almost entirely prevented in cells that support productive AAV2 repli-

cation (38), the yield of HSV-1 progeny from coinfected cultures is only approximately 10-fold lower than that in cultures infected with HSV-1 alone (our unpublished observations). Because of this observation and the fact that HSV-1 can replicate well in different phases of the cell cycle, we addressed the following two questions: (i) do HSV-1-provided helper functions allow AAV2 to replicate in different phases of the cell cycle, and (ii) do AAV2 and HSV-1 replicate in different sets of cells in coinfected cultures?

The results presented here imply that HSV-1 does not extend its ability to replicate in different phases of the cell cycle to AAV2. In fact, AAV2 gene expression in both the presence and absence of the helper virus and AAV2 replication occur almost exclusively in S/$G_2$-phase cells. HSV-1 lost its ability to replicate in S/$G_2$-phase cells in the presence of AAV2 *rep* gene expression/DNA replication but still replicated in $G_1$ phase.

## RESULTS

**For productive infection, AAV2 requires a helper virus and a cell in S/$G_2$ phase.** We examined the formation of AAV2 RCs in HeLa Fucci cells, which express fluorescent ubiquitination-based cell cycle indicators (Fucci) (45). Specifically, HeLa Fucci cells express green and red fluorescent proteins fused to geminin and Cdt1, respectively. In the $G_1$ phase of the cell cycle, geminin undergoes proteasome-dependent degradation, and the cells appear red. In the S, $G_2$, and M phases of the cell cycle, Cdt1 is ubiquitinated and degraded; thus, the cells appear green. Cells in early S phase simultaneously express Cdt1 and geminin and appear orange. In early $G_1$ phase, no fluorescence marker is expressed.

In the first set of experiments, HeLa Fucci cells were infected with wild-type HSV-1 (wtHSV-1) alone or coinfected with wtAAV2 and wtHSV-1. After 24 h, viral RCs were visualized by confocal laser scanning microscopy (CLSM) with antibodies specific for the HSV-1 and AAV2 DNA-binding proteins ICP8 and Rep, respectively. In cells infected with HSV-1 alone, we detected HSV-1 RCs in both red fluorescent ($G_1$-phase) and green fluorescent (S/$G_2$-phase) cells (S/$G_2$-to-$G_1$-phase ratio, 1.11 $\pm$ 0.36) (Fig. 1A and C), which is consistent with data from previous studies showing that HSV-1 can replicate in $G_1$, S, and $G_2$ phases (5–9). In contrast, AAV2 RCs were identified predominantly in the nuclei of cells expressing the green fluorescent S/$G_2$-phase marker geminin (Fig. 1B and C) (S/$G_2$-to-$G_1$-phase ratio, 6.65 $\pm$ 1.01). The S/$G_2$-to-$G_1$-phase ratios of total mock-infected HeLa Fucci cells (not gated for RCs) were 1.75 $\pm$ 0.10 at 0 h postinfection (p.i.) and 1.20 $\pm$ 0.05 at 24 h p.i.; the S/$G_2$-to-$G_1$-phase ratios were 1.04 $\pm$ 0.02 for total wtHSV-1-infected and 0.93 $\pm$ 0.02 for wtAAV2- and wtHSV-1-coinfected HeLa Fucci cells. The preference of AAV2 for replication in the S/$G_2$ phase of the cell cycle was also confirmed by fluorescence *in situ* hybridization (FISH) with a probe specific for AAV2 DNA (Fig. 2A). While no FISH signal was detected in noninfected cells (Fig. 2A, top), in the cultures infected with wtAAV2 alone, fluorescent dots representing AAV2 genomes were observed in both S/$G_2$- as well as $G_1$-phase cells (Fig. 2A, middle). Coinfection with the helper virus supported the formation of AAV2 RCs, and these RCs were found predominantly in the nuclei of S/$G_2$-phase cells (Fig. 2A, bottom, and B). Of note, the AAV2 genomes that were observed in the absence of the helper virus (Fig. 2A, middle) were not visible in Fig. 2A (bottom) because the laser intensity was strongly reduced for the acquisition of the brightly fluorescent AAV2 RCs. Taken together, these data show that efficient AAV2 replication requires not only the presence of a helper virus but also that the cell be in the S/$G_2$ phase of the cell cycle. Therefore, HSV-1 cannot extend its ability to replicate in different phases of the cell cycle to AAV2.

**In coinfected cultures, HSV-1 DNA replication is inhibited specifically in S/$G_2$-phase cells.** In the above-described experiments, we monitored cell cycle phases and virus replication in nongated cells (Fig. 1A and B and 2A), and we also determined cell cycle phases of cells "gated" for viral replication markers (Fig. 1C and 2B). Next, we analyzed virus replication in cells gated for the cell cycle phase. Specifically, HeLa Fucci cells were infected with wtHSV-1 or coinfected with wtHSV-1 and wtAAV2. After 24 h, cells positive for Cdt1 ($G_1$ phase) (red) or geminin (S/$G_2$ phase) (green) were sorted by

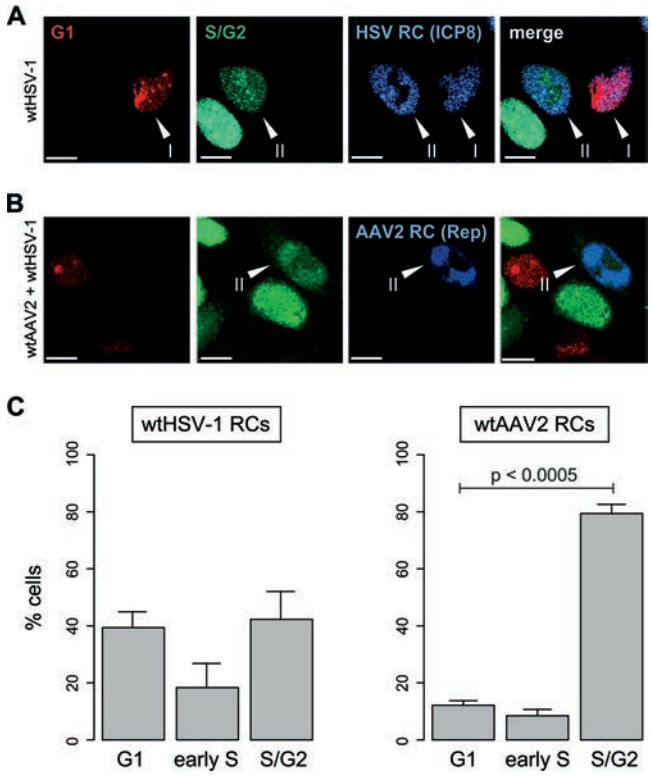


**FIG 1** Codetection of cell cycle phases and viral replication compartments. (A and B) HeLa Fucci cells were infected with wtHSV-1 (MOI of 3) or coinfected with wtAAV2 (MOI of 4,000) and wtHSV-1 (MOI of 3). After 24 h, the cells were fixed and processed for immunofluorescence analysis and CLSM. (A) HSV-1 RCs were visualized with a primary antibody specific for the HSV-1 major DNA-binding protein ICP8 and an AF-405-labeled secondary antibody (blue). (B) AAV2 RCs were visualized with a primary antibody specific for the AAV2 Rep proteins and an AF-405-labled secondary antibody (blue). Bars = 10 $\mu$m. Arrowheads in panels A and B indicate cells positive for HSV-1 or AAV2 RCs and either the red fluorescent $G_1$-phase marker Cdt1 (I) or the green fluorescent S/$G_2$-phase marker geminin (II). (C) From the cultures shown in panels A and B, approximately 30 cells containing HSV-1 or AAV2 RCs (blue) were analyzed for their cell cycle phase ($G_1$, early S, and S/$G_2$). The graphs show mean values from six independent experiments; error bars indicate standard deviations of the means.

fluorescence-activated cell sorter (FACS) analysis, and equal cell equivalents were analyzed by Southern blotting, Western blotting (WB), and quantitative PCR (qPCR). Consistent with the findings described above, the results of these assays showed that in the absence of AAV2, HSV-1 DNA replication was at least as efficient in S/$G_2$ phase as it was in $G_1$ phase (Fig. 3A and C), while AAV2 DNA replication in S/$G_2$ phase was at least 6-fold more efficient than in $G_1$ phase (Fig. 3A and D). HSV-1 replication in $G_1$-phase cells appeared to be equally efficient in the presence and absence of AAV2 (Fig. 3A and C). Interestingly, however, in the presence of AAV2, HSV-1 DNA was no longer detected by Southern blotting in S/$G_2$-phase cells (Fig. 3A), and qPCR revealed an approximately 4-fold reduction of HSV-1 DNA levels in S/$G_2$-phase cells compared to those in $G_1$-phase cells from coinfected cultures and an approximately 6-fold reduction compared to those in S/$G_2$-phase cells from cultures infected with HSV-1 alone (Fig. 3C). As an infection control, the HSV-1 ICP0 and AAV2 Rep proteins were detected by Western blotting (Fig. 3B). Of note, the levels of AAV2 DNA appear to directly correlate with the levels of AAV2 Rep proteins in the different cell cycle phases (Fig. 3A and B). Cell cycle phases of HeLa Fucci cells sorted into $G_1$ (Cdt1) (red), early S (Cdt1 and geminin) (orange), and S/$G_2$ (geminin) (green) populations by FACS analysis were confirmed by 4′,6-diamidino-2-phenylindole (DAPI) staining and flow cytometry (not shown).

These data show that the previously reported AAV2-mediated inhibition of HSV-1 replication (37, 38) is specific to the S/$G_2$ phase of the cell cycle and correlates with

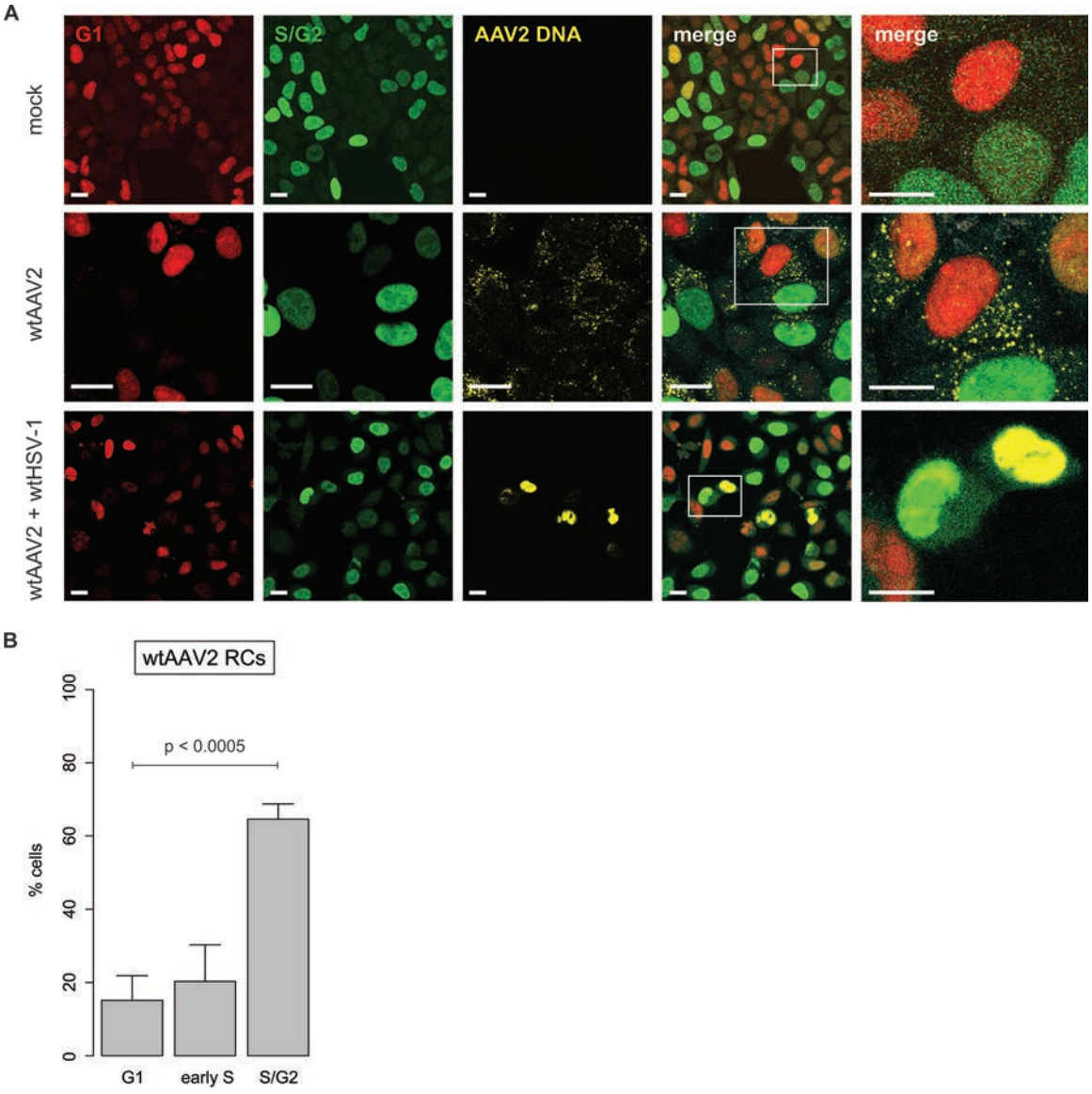


**FIG 2** Codetection of cell cycle phases and AAV2 genomes. HeLa Fucci cells were mock infected, infected with wtAAV2 alone (MOI of 4,000), or coinfected with wtAAV2 (MOI of 4,000) and wtHSV-1 (MOI of 3). After 24 h, the cells were fixed and processed for fluorescence *in situ* hybridization (FISH) and CLSM. (A) AAV2 DNA (yellow) was detected with an AF-647-labeled probe as described in Materials and Methods. The red and green signals indicate cells in $G_1$ (Cdt1) and $S/G_2$ (geminin) phases, respectively. The orange cells observed in some cultures are in early S phase, where they express both Cdt1 and geminin. Areas in the box were enlarged (right column). Bars = 10 $\mu$m. (B) From the wtAAV2- and wtHSV-1-coinfected cultures shown in panel A, approximately 30 cells containing AAV2 RCs were analyzed for their cell cycle phase ($G_1$, early S, and $S/G_2$). The graph shows mean values from six independent experiments; error bars indicate standard deviations of the means.

efficient AAV2 replication in these cell cycle phases. The next experiment was performed to investigate whether HSV-1 can replicate in $G_1$-phase cells despite the presence of AAV2 genomes or simply because AAV2 genomes are absent from these cells. For this, HeLa Fucci cells were coinfected with wtAAV2 and recombinant HSV-1 that encodes enhanced cyan fluorescent protein (ECFP) fused with the HSV-1 ICP4 protein (rHSV-1vECFP-ICP4), thus facilitating the observation of HSV-1 RCs due to the binding of the fluorescent ICP4 fusion protein to the replicating HSV-1 DNA in the cell nucleus (46). After 24 h, the cells were fixed, and FISH staining was performed by using an Alexa Fluor 647 (AF-647)-labeled AAV2 DNA probe. The micrographs shown in Fig. 4 demonstrate that HSV-1 RCs are formed in $G_1$-phase cells despite the presence of AAV2 genomes.

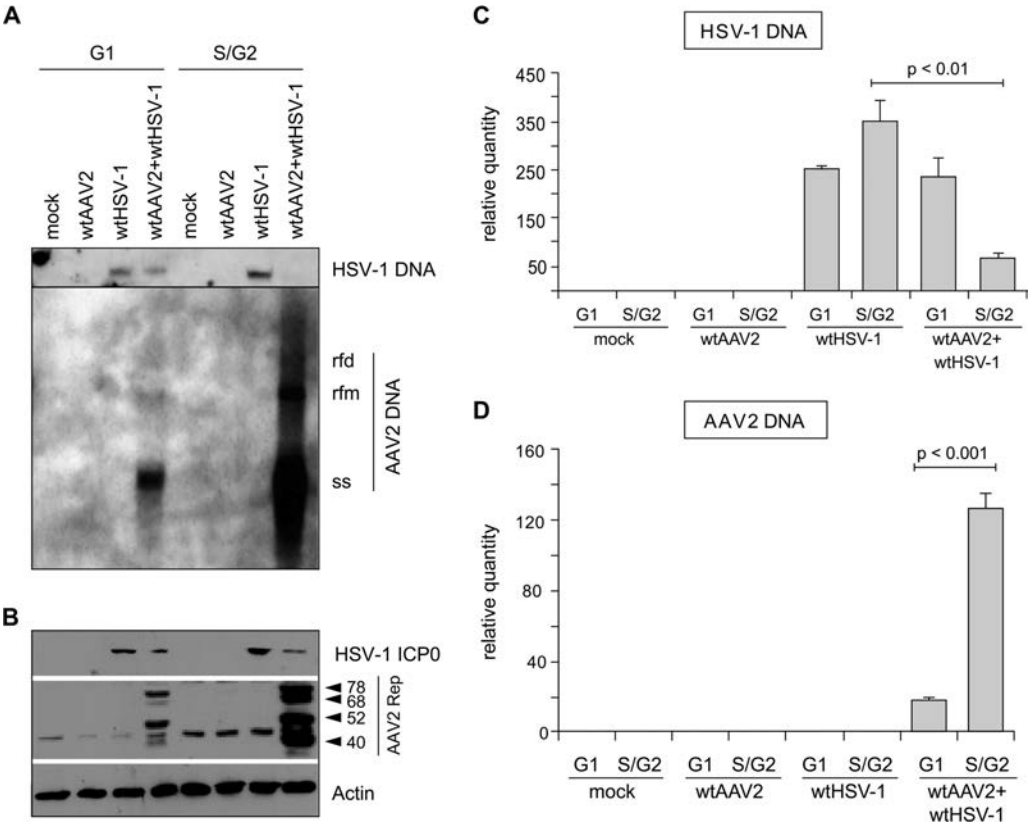


**FIG 3** Viral DNA replication in different phases of the cell cycle. HeLa Fucci cells were mock infected, infected with either wtAAV2 (MOI of 8,000) or wtHSV-1 (MOI of 3), or coinfected with wtAAV2 (MOI of 8,000) and wtHSV-1 (MOI of 3). After 24 h, cells positive for Cdt1 ($G_1$ phase) (red) or geminin ($S/G_2$ phase) (green) were sorted by FACS analysis and subjected to Southern and Western blot analyses. (A) Southern blot analysis for detection of HSV-1 and AAV2 DNA (equal cell equivalents were loaded into the different lanes) (ss, single stranded; rfm, replication-form monomer; rfd, replication-form dimer). (B to D) Western blot analysis to control for virus infection (HSV-1 ICP0 and AAV2 Rep; actin was used as a loading control) (B) and qPCR to quantify viral DNA (C and D). Graphs in panels C and D show mean values for relative HSV-1 or AAV2 DNA quantities from triplicate experiments; error bars indicate standard deviations of the means.

**Cell cycle-dependent AAV2 DNA replication is controlled by cell cycle-dependent AAV2 *rep* expression.** In the absence of a helper virus, gene expression from replication-defective recombinant AAV2 vectors was previously shown to occur preferentially in the S phase of the cell cycle (47, 48). To address the question of whether this also applies when a helper virus is present, we coinfected HeLa Fucci cells with wtHSV-1 and recombinant AAV2 vectors encoding fluorescent reporter proteins fused in frame with AAV2 Rep (rAAVCFPRep and rAAVYFPRep). The AAV2 p5 promoter used in these vectors for the transcriptional control of reporter gene expression is highly regulated during coinfection; in particular, its activity is very low in the absence of HSV-1. Therefore, we also used a recombinant AAV2 vector that expresses a reporter gene from the constitutively active human cytomegalovirus (CMV) IE1 enhancer/promoter (rAAVCFPNeo) to exclude a potential promoter effect responsible for the observed cell cycle-dependent AAV2 DNA replication/gene expression. Viral gene expression and the cell cycle phase were determined by fluorescence microscopy or flow cytometry. Upon coinfection of HeLa Fucci cells with rAAVCFPNeo and wtHSV-1, the majority of the cyan fluorescent cells was indeed in $S/G_2$ phase, approximately 10% of the cells were in $G_1$ phase, and 10% were in early S phase (Fig. 5A and B). A similar distribution was observed upon coinfection of HeLa Fucci cells with rAAVCFPRep and wtHSV-1: approximately 81% of the AAV2-transduced (ECFP-positive) cells were in $S/G_2$ phase, while only 19% were in $G_1$ phase, as determined by flow cytometry (Table 1). The inefficient AAV2 gene expression in $G_1$ phase was also observed in other cell lines, including AT22, HCT116, and normal human fibroblast (NHF) cells (Table 1). For

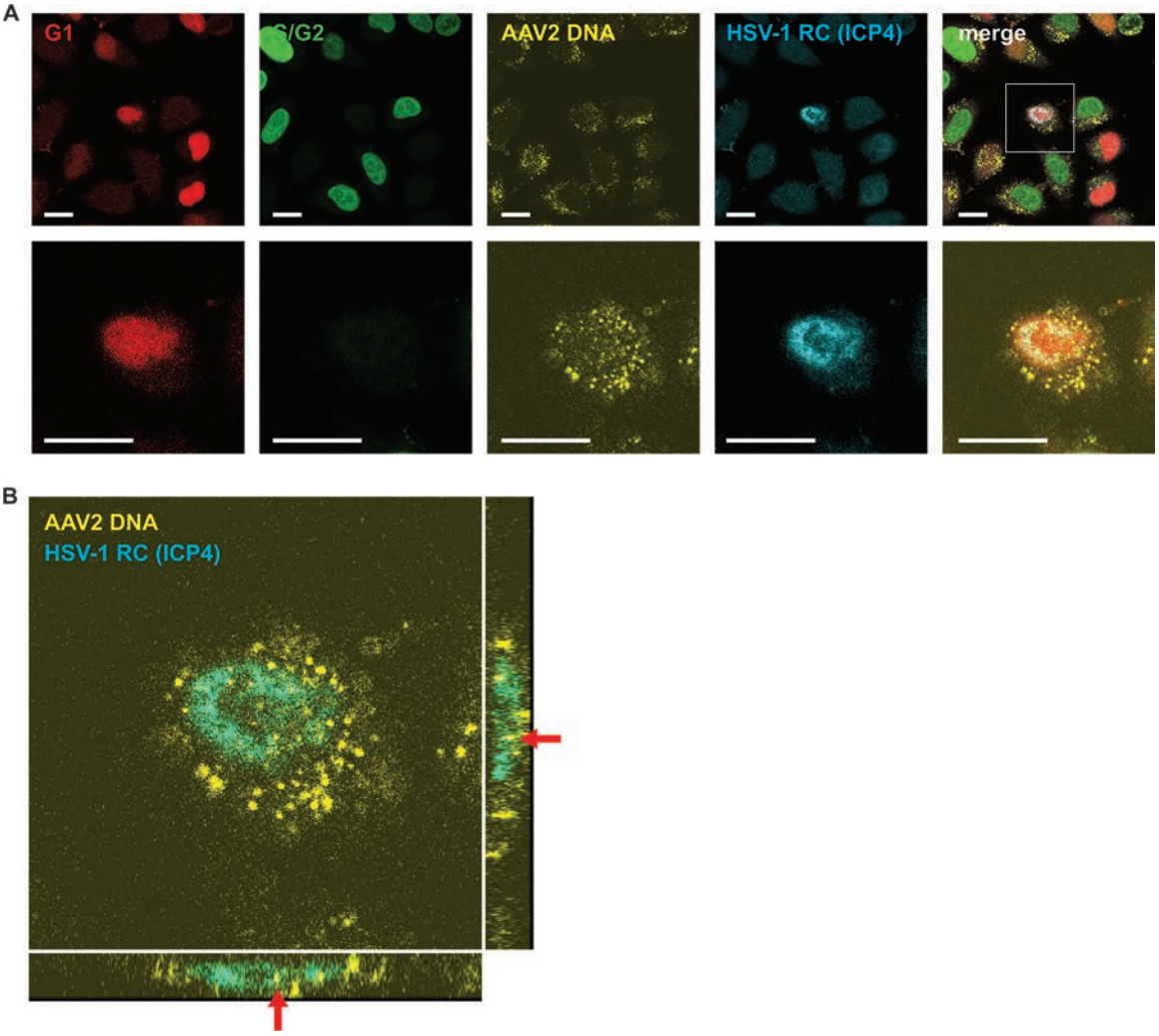


**FIG 4** Codetection of AAV2 genomes, HSV-1 RCs, and cell cycle phases. HeLa Fucci cells were coinfected with wtAAV2 (MOI of 4,000) and rHSV-1vECFP-ICP4 (MOI of 3). After 24 h, the cells were fixed and processed for FISH and CLSM. (A) AAV2 DNA (yellow) was detected with an AF-647-labeled probe as described in Materials and Methods. HSV-1 RCs were detected by the binding of the HSV-1 ECFP-ICP4 fusion protein to HSV-1 DNA (blue). The red and green signals indicate cells in $G_1$ (Cdt1) and $S/G_2$ (geminin) phases, respectively. The area in the box (top row, merge) is enlarged in the second row and in panel B. Bars = 20 $\mu$m. (B) Enlargement and sectioning of the HSV-1 RC-positive cell shown in panel A (box in the top row) reveal the subcellular localization of AAV2 genomes (red arrows). For clarity, the red and green channels were omitted.

example, in AT22 fibroblast cultures coinfected with rAAVYFPRep and wtHSV-1, more than 80% of AAV2-transduced (enhanced yellow fluorescent protein [EYFP]-positive) cells were in S or $G_2$ phase, while only approximately 16% of these cells were in $G_1$ phase (Table 1), although the majority (approximately 60%) of the nongated cells in the culture was in $G_1$ phase (not shown). Therefore, HSV-1 helper functions appear to support neither AAV2 replication nor AAV2 (*rep*) gene expression in $G_1$ cells, independent of the promoter, p5 or CMV. Inefficient AAV2 gene expression in $G_1$ phase and, consequently, low levels of AAV2 Rep proteins (as indeed shown in Fig. 3B) are likely responsible for the inefficient AAV2 replication and the inefficient inhibition of HSV-1 replication in this cell cycle phase, as AAV2 Rep proteins are known to be essential for AAV2 replication and also responsible for the inhibition of HSV-1 replication (43, 49).

Next, we addressed the question of whether, in coinfected cultures, HSV-1 replication is allowed in $G_1$-phase cells and inhibited in $S/G_2$-phase cells, because AAV2 *rep* is expressed efficiently only in $S/G_2$-phase but not in $G_1$-phase cells. For this, we used recombinant HSV-1 that encodes the VP16 protein fused with EYFP (rHSV48EYFP) (50). EYFP-VP16 accumulates on HSV-1 DNA and hence is a marker for HSV-1 RCs (50, 51). To

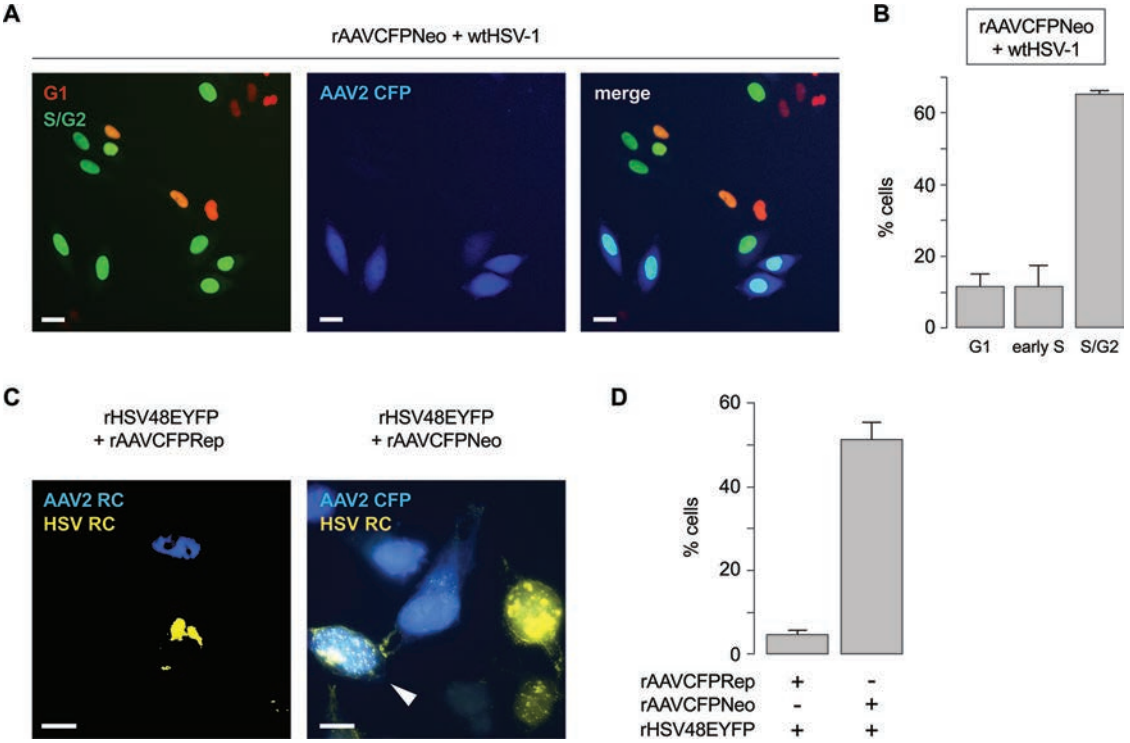


**FIG 5** Cell cycle-dependent AAV2 gene expression controls the replication of both AAV2 and HSV-1 in coinfected cultures. (A) HeLa Fucci cells were coinfected with rAAVCFPNeo (MOI of 4,000) and wtHSV-1 (MOI of 3). Images were acquired by automated epifluorescence microscopy using ImageXpress Micro XL (Molecular Devices) and fluorescence filters (Semrock) for ECFP (AAV2 gene expression) (blue), EGFP ($S/G_2$ phase) (green), and TRITC ($G_1$ phase) (red). Bars = 20 $\mu$m. (B) HeLa Fucci cells were coinfected with rAAVCFPNeo (MOI of 1,000) and wtHSV-1 (MOI of 3), and 20 h later, the cell cycle phase ($G_1$, early S, and $S/G_2$) of rAAVCFPNeo-transduced cells was determined by the expression of Ctd1 (red) and geminin (green). A total of 40,000 cells (events) per sample were counted by flow cytometry. The graph shows mean values from triplicate experiments; error bars indicate standard deviations of the means. (C) HeLa cells were coinfected with rHSV48EYFP (MOI of 3) and either rAAVCFPRep (MOI of 4,000) or rAAVCFPNeo (MOI of 4,000). After 24 h, cells were examined by using a standard fluorescence microscope. Bars = 10 $\mu$m. (D) From the cultures shown in panel C, 50 cells containing yellow fluorescent HSV-1 RCs were analyzed for the presence of AAV2 RCs in rHSV48EYFP- and rAAVCFPRep-coinfected cultures or ECFP fluorescence in rHSV48EYFP- and rAAVCFPNeo-coinfected cultures. The graph shows mean values from triplicate experiments; error bars indicate standard deviations of the means.

simultaneously visualize AAV2 Rep, we used rAAVCFPRep, which encodes an ECFP-Rep fusion protein from the viral p5 promoter and allows not only cell cycle-dependent replication of the viral genome in the presence of a helper virus but also monitoring of AAV2 RCs via interactions of the fluorescent Rep fusion protein with replicating viral DNA (31) (see Movie S1 in the supplemental material). As expected, in cultures coinfected with rHSV48EYFP and rAAVCFPRep, HSV-1 RCs and AAV2 RCs were not codetected in individual cells (Fig. 5C, left). However, in cells coinfected with rHSV48EYFP and rAAVCFPNeo, which encodes ECFP but no AAV2 Rep proteins, yellow fluorescent HSV-1 RCs were readily detected in both ECFP-positive and ECFP-negative cells

**TABLE 1** Cell cycle phases of AAV2-transduced cells

| Cell line | Infection[d] | % of cells in phase | | | |
|---|---|---|---|---|---|
| | | $G_1$ | S | $S/G_2$ | $G_2$ |
| HeLa Fucci[a] | rAAVCFPRep | 19 | | 81 | |
| AT22[b] | rAAVYFPRep | 16 | 40 | | 44 |
| HCT116[c] | rAAVYFPRep | 20 | 33 | | 47 |
| NHF[b] | rAAVCFPRep | 17 | 35 | | 48 |

[a]Cell cycle phases were determined by flow cytometry with fluorescent ubiquitination-based cell cycle indicators (Fucci).
[b]Cell cycle phases were determined by flow cytometry with propidium iodide.
[c]Cell cycle phases were determined by flow cytometry with DAPI.
[d]Coinfected with HSV-1.

(Fig. 5C, right). By using an epifluorescence microscope, cells positive for yellow fluorescent HSV-1 RCs were examined for ECFP fluorescence (Fig. 5D). In the rHSV48EYFP- and rAAVCFPRep-coinfected cultures, less than 5% of the cells containing HSV-1 RCs were ECFP-Rep positive. In contrast, in rHSV48EYFP- and rAAVCFPNeo-coinfected cultures, approximately 50% of the cells containing HSV-1 RCs were also positive for the AAV2 marker ECFP. Since rAAVCFPNeo transduction was observed predominantly in the $S/G_2$ phase of the cell cycle (Fig. 5A and B), these data suggest that AAV2 infection or nonreplicating AAV2 DNA *per se* is not sufficient to inhibit HSV-1 replication in $S/G_2$ phase but that *rep* expression is required. This is also supported by a previous finding that UV-inactivated wtAAV2 genomes, which do not express any AAV2 genes, did not inhibit HSV-1 replication (43). In conclusion, cell cycle-dependent AAV2 *rep* expression seems to be responsible for the observed negative correlation between HSV-1 and AAV2 replication efficiencies in different phases of the cell cycle. Low Rep levels in $G_1$ phase allow HSV-1 but not AAV2 to replicate, while high Rep levels in $S/G_2$ phase support AAV2 replication and block HSV-1 replication.

**Both single-stranded and double-stranded AAV2 vectors predominantly transduce cells in $S/G_2$ phase, independent of the presence or absence of a helper virus.** We used two different approaches to test whether the single-stranded nature of AAV2 DNA plays a role in cell cycle-dependent AAV2 gene expression: transfection of plasmid-cloned AAV2 genomes and infection with self-complementary recombinant AAV2 (scAAV2) vectors, which can form double-stranded DNA by self-annealing and therefore do not depend on second-strand synthesis for viral gene expression. Specifically, HeLa Fucci cells were transfected with plasmids containing *rep*-positive (pAAVCFPRep) or *rep*-negative (pAAVCFPp5) recombinant AAV2 genomes and 4 h later were mock infected or infected with wtHSV-1. After 24 h, the cells were examined by CLSM. The results are shown in Fig. 6 and are summarized as follows: ECFP fluorescent AAV2 RCs were readily detected in both $G_1$- and in $S/G_2$-phase cells of cultures transfected with pAAVCFPRep and infected with the helper virus (Fig. 6A). In the presence of HSV-1, ECFP fluorescence was also detected both in $G_1$- and in $S/G_2$-phase cells of cultures transfected with pAAVCFPp5, but in these cells, ECFP fluorescence was diffuse, and AAV2 RCs were not observed because of the absence of *rep* (Fig. 6B). No ECFP fluorescence was observed in the absence of HSV-1, as both plasmids use the helper virus-dependent AAV2 p5 promoter for transgene expression (not shown).

To confirm that HSV-1-supported AAV2 DNA replication can indeed take place in $G_1$ phase when the template is a circular double-stranded DNA, HeLa Fucci cells were transfected with pAAVCFPRep and 4 h later were mock infected or infected with wtHSV-1. After 24 h, episomal DNA was prepared from $G_1$- and $S/G_2$-phase cells according to methods described previously by Hirt (52) and subjected to qPCR with primers specific for *rep*. The graph in Fig. 6C shows that the relative AAV2 DNA content in $G_1$-phase cells is 80% larger in the presence of the helper virus, presumably because of DNA replication. We then tested whether HSV-1 DNA replication was also blocked in $G_1$-phase cells when *rep* is expressed from a plasmid-cloned recombinant AAV2 genome. The graph in Fig. 6D shows that this is clearly the case. The HSV-1 DNA content of ECFP (AAV2)- and Cdt1 ($G_1$-phase) (red)-double-positive HeLa Fucci cells transfected with pAAVCFPRep prior to HSV-1 infection was reduced by more than 60% compared to that in cells transfected with *rep*-negative pAAVCFPp5 plasmid DNA prior to infection with the helper virus. In summary, these data show that AAV2 (*rep*) gene expression, AAV2 genome replication, and the inhibition of HSV-1 replication can take place in $G_1$-phase cells when the AAV2 genome is provided as a circular double-stranded rather than a linear single-stranded DNA template.

These data suggest that AAV2 single-strand synthesis may be the limiting factor for efficient AAV2 gene expression/genome replication in $G_1$ phase, and accordingly, one would expect that scAAV2 vectors would support gene expression in this cell cycle phase. To investigate this possibility, we infected HeLa Fucci cells with scAAVCFP in presence or absence of the helper virus and monitored reporter gene expression (ECFP) and the cell cycle phase from 2 to 20 h after infection (Fig. 7). Indeed, 20 h after infection, many transgene-positive $G_1$-phase cells (purple) were observed in scAAVCFP-

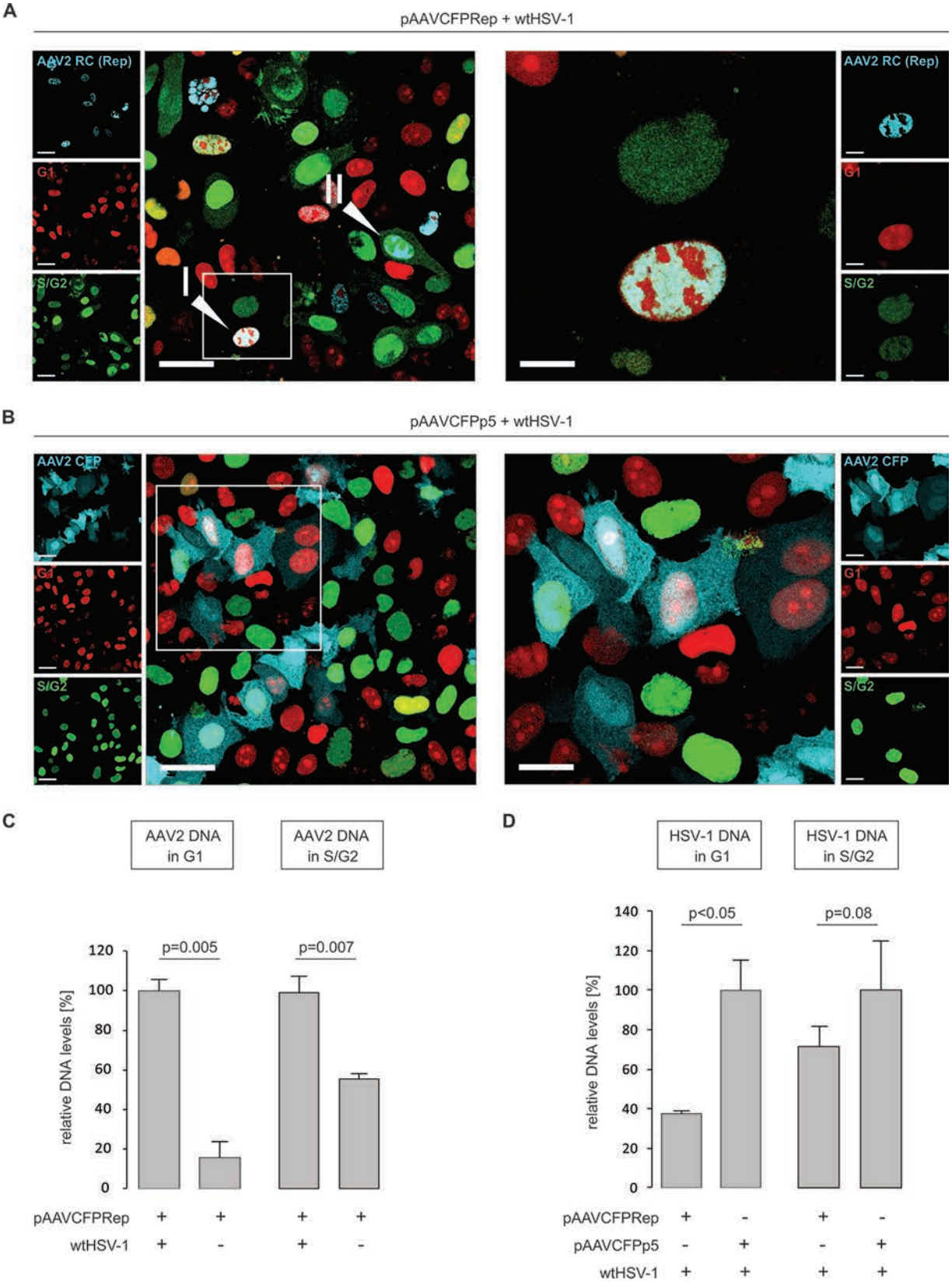


**FIG 6** Detection of cell cycle phases, AAV2 gene expression, and virus replication in cells transfected with circular, double-stranded *rep*-positive or *rep*-negative recombinant AAV2 genomes. (A and B) HeLa Fucci cells were transfected with pAAVCFPRep (A) or pAAVCFPp5 (B) and infected with wtHSV-1 (MOI of 2) 4 h later. After 24 h, cells were examined by CLSM with filters specific for Cdt1 ($G_1$ phase) (red), geminin ($S/G_2$ phase) (green), and ECFP (AAV2) (blue). The framed areas in panels A and B are shown at a higher magnification on the right. Arrowheads in panel A

(Continued on next page)

infected cultures in the absence of the helper virus (Fig. 7A, left). However, tracking of individual cells over time revealed that the transgene-positive $G_1$-phase cells observed 20 h after infection originated from cells that became transgene positive in S/$G_2$ phase and then went through mitosis (Fig. 7A, right, arrows; see also Movie S2 in the supplemental material). Occasionally, cells turned transgene positive in $G_1$ phase (not shown). Coinfection with wtHSV-1 largely prevented the generation of transgene-positive $G_1$ cells (Fig. 7A), presumably because of HSV-1-mediated $G_2$ arrest (5, 33). As expected from the above-described data, the vast majority of the cells infected with the single-stranded AAV2 vector (rAAVCFPNeo) turned transgene positive in S/$G_2$ phase and did not progress through mitosis, independent of the presence or absence of the helper virus (Fig. 7A and Movie S3). Also as expected from the above-described data, transgene-positive $G_1$-phase cells were also occasionally observed in rAAVCFPNeo-infected cultures in the absence of the helper virus. These cells often but not always originated from transgene-positive S/$G_2$-phase cells that progressed to $G_1$ phase, sometimes without division (Fig. 7A). To quantify the observations from live microscopy, we tracked and counted cells over time from the moment when AAV2 vector-encoded ECFP fluorescence became visible. The graph in Fig. 7B shows that more than 90% of the cells turned ECFP positive in S/$G_2$ phase, independent of the genome structure, whether single stranded or double stranded (self-complementary), or the presence or absence of the helper virus. However, in the absence of wtHSV-1, ECFP fluorescent S/$G_2$-phase cells progressed through mitosis to $G_1$ phase at a significantly higher frequency when infected with scAAVCFP than when infected with rAAVCFPNeo (Fig. 7C).

Overall, we conclude that (i) HSV-1 is not capable of extending its ability to replicate in all phases of the cell cycle to AAV2, (ii) cell cycle-dependent AAV2 DNA replication and inhibition of HSV-1 DNA replication are due to cell cycle-dependent AAV2 *rep* expression, and (iii) second-strand synthesis is likely not responsible for the cell cycle preference because both single-stranded and double-stranded linear AAV2 genomes preferentially transduce cells in S/$G_2$ phase.

## DISCUSSION

In this study, we addressed the question of how AAV2 and HSV-1 coordinate their replication programs. For this, we used a fluorescence microscopy approach, scoring different cell cycle stages and viral RCs on a single-cell level, and combined the results with biochemical virus replication measurements in isolated cells at the $G_1$ and S/$G_2$ stages. We find that AAV2 replication occurs predominantly in S/$G_2$ phase. Also, AAV2 gene expression was restricted to S/$G_2$-phase cells in both the presence and absence of the helper virus. HSV-1 replication was in turn restricted to $G_1$-phase cells in coinfected cultures, while it replicated efficiently in both $G_1$- and S/$G_2$-phase cells in the absence of AAV2 (for an overview, see Tables 2 and 3). On the other hand, HSV-1 RCs were readily detected in S/$G_2$-phase cells transduced with a *rep*-negative recombinant AAV2 vector. Therefore, as Rep proteins are essential for AAV2 replication and have been found to be at least partially responsible for the AAV2-mediated inhibition of HSV-1 replication (38, 43, 44), we conclude that cell cycle-dependent AAV2 *rep* expression is responsible for the observed restriction of AAV2 replication to S/$G_2$-phase cells and of HSV-1 replication to $G_1$-phase cells.

We have previously shown that the AAV2 Rep68/78 proteins, in particular the

**FIG 6** Legend (Continued)
indicate cells positive for AAV2 RCs and either the red fluorescent $G_1$-phase marker Cdt1 (I) or the green fluorescent S/$G_2$-phase marker geminin (II). Bars = 40 $\mu$m (left) and 10 $\mu$m (right). (C) HeLa Fucci cells were transfected with pAAVCFPRep and 4 h later were mock infected or infected with wtHSV-1 (MOI of 2). After 24 h, extrachromosomal DNA was prepared from Cdt1-positive $G_1$-phase cells (red) and geminin-positive S/$G_2$-phase cells (green), digested with DpnI, and subjected to qPCR with primers specific for AAV2 *rep*. (D) HeLa Fucci cells were transfected with pAAVCFPRep or pAAVCFPp5 and infected 4 h later with wtHSV-1 (MOI of 2). Total DNA extracted after 24 h from ECFP (AAV2)- and Cdt1 ($G_1$-phase) (red)- or ECFP- and geminin (S/$G_2$-phase) (green)-double-positive cells was subjected to qPCR with primers specific for HSV-1 DNA. Graphs in panels C and D show mean values for relative DNA quantities from triplicate experiments, and samples were prepared from equal numbers of cells; error bars indicate standard deviations of the means.

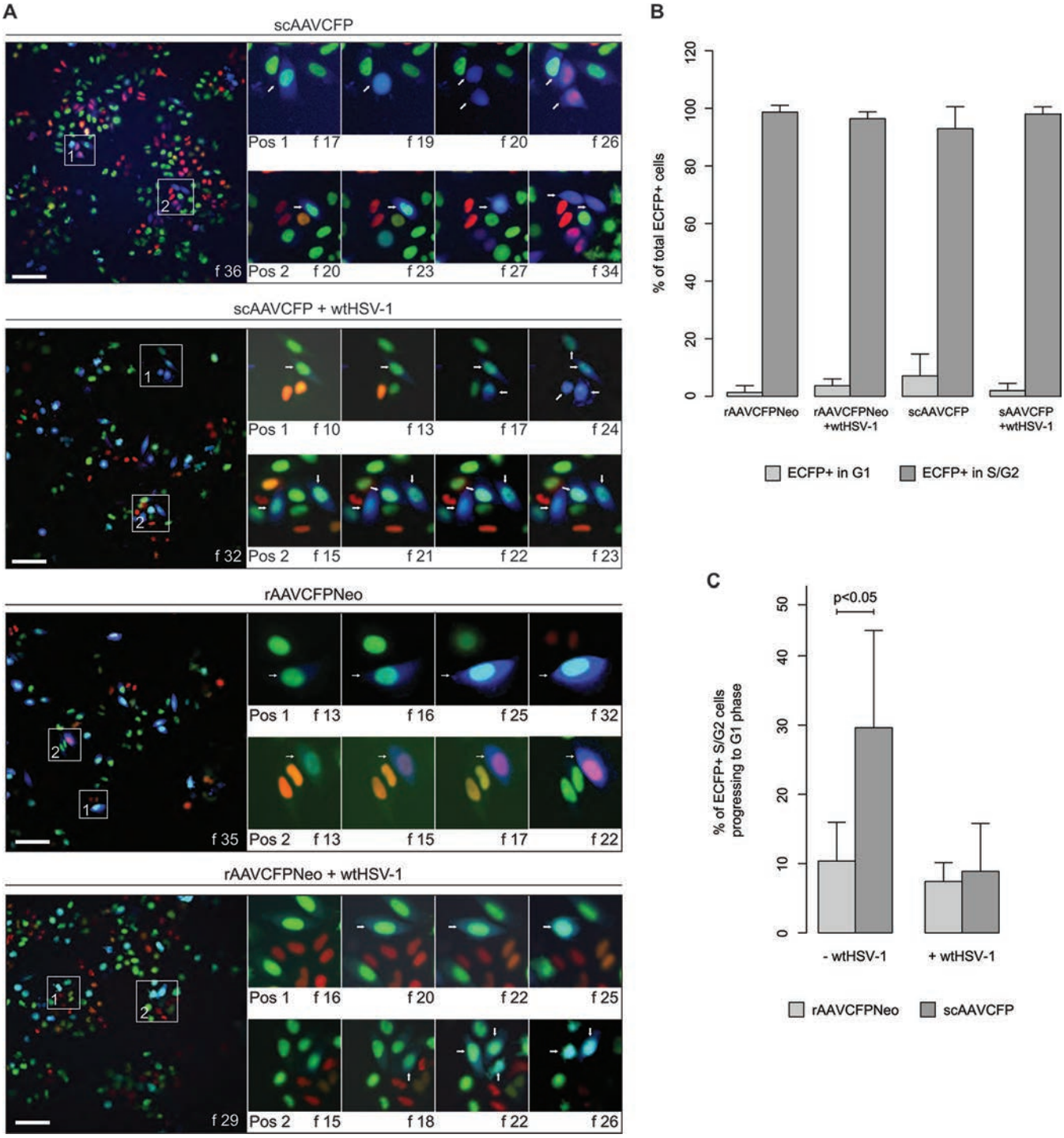


**FIG 7** Live-cell imaging of cell cycle-dependent AAV2 gene expression. (A) HeLa Fucci cells were infected with scAAVCFP (MOI of 3,000) or rAAVCFPNeo (MOI of 3,000) in the absence or presence of wtHSV-1 (MOI of 3), and images were acquired every 30 min from 2 to 20 h after infection by automated time-lapse (37°C with 5% $CO_2$, humidified) epifluorescence microscopy using ImageXpress Micro XL (Molecular Devices) and fluorescence filters (Semrock) for ECFP (AAV2 gene expression), GFP ($G_2$ phase), and TRITC ($G_1$ phase). A total of 36 frames was acquired, and the frame numbers are indicated. Overview images are shown in the left panels. Two different positions highlighted in each of the overview images (boxes 1 and 2) were enlarged and tracked over time (right panels). Arrows point to cells from the moment when ECFP fluorescence becomes visible. (B) Graph showing the percentage of cells that turned ECFP positive in either the $G_1$ or $S/G_2$ phase. (C) Graph showing the percentage of transgene-positive $S/G_2$-phase cells progressing to $G_1$ phase. Both graphs show mean values from at least 100 ECFP-positive cells tracked in at least 9 different infection-and-acquisition experiments; error bars indicate standard deviations of the means.

**TABLE 2** AAV2 and HSV-1 DNA replication in different cell cycle phases[a]

| Virus infection | Efficiency of DNA replication | | Fig. and/or supplemental material |
|---|---|---|---|
| | $G_1$ | $S/G_2$ | |
| HSV-1 | ++++ | ++++ | Fig. 1 + 3 |
| AAV2 | − | − | Fig. 2 + 3 |
| AAV2 (HSV-1 coinfection) | + | ++++ | Fig. 1–3, Movie S1 |
| HSV-1 (AAV2 coinfection) | ++++ | + | Fig. 3 + 4 |

[a]++++, efficient DNA replication; +, inefficient DNA replication; −, no DNA replication (AAV2 *rep* expression from the p5 promoter).

combined DNA-binding and ATPase/helicase activities, can block HSV-1 DNA replication on the level of DNA synthesis, even in the absence of AAV2 DNA. We also demonstrated that AAV2 Rep68 can bind to consensus Rep-binding sites on the HSV-1 genome and that the helicase activity can block the replication of any DNA if binding is facilitated (44). However, the conclusion from the present study, that the inhibition of HSV-1 replication is limited to $S/G_2$-phase cells because AAV2 *rep* is expressed efficiently only in this phase, inevitably begs the question of what controls the cell cycle-dependent expression of *rep*. Recombinant AAV2 vectors have been reported to transduce cells predominantly in S phase in the absence of a helper virus (47, 48). Our finding that HSV-1-provided helper functions do not support AAV2 replication and gene expression in $G_1$ phase, although HSV-1 itself can replicate in $G_1$ and $S/G_2$ phases and although the HSV-1 protein ICP0 strongly *trans*-activates AAV2 *rep* expression, indicates that a step prior to AAV2 transcription may be blocked. One obvious step is second-strand synthesis. For example, cellular proteins involved in second-strand synthesis such as polymerases or cofactors may not be available at sufficient concentrations in $G_1$ phase. Likewise, factors that block second-strand synthesis, such as DNA damage repair proteins, may be abundant or activated in $G_1$ but not in $S/G_2$ phase. We demonstrate that AAV2 transcription and replication are efficient in $S/G_2$- as well as in $G_1$-phase cells when the template is a circular double-stranded rather than a linear single-stranded DNA template, indicating that cell cycle-dependent *rep* expression may indeed be due to cell cycle-dependent second-strand synthesis. However, the circular versus linear state of the two template DNAs as well as the different means of delivery, transfection versus infection, may also affect transcription in a cell cycle-dependent manner, possibilities that were further explored by using scAAV2 vectors. If inefficient second-strand synthesis in $G_1$ phase was solely responsible for the observed cell cycle-dependent AAV2 replication and gene expression, one would expect that scAAV2 vectors, which can form double-stranded DNA by self-annealing and therefore do not depend on second-strand synthesis for gene expression, can transduce both $G_1$-and

**TABLE 3** Cell cycle-dependent gene expression from AAV2 vectors and the $G_2$-to-M-to-$G_1$-phase transition[a]

| AAV2 vector | Efficiency of gene expression in phase | | Efficiency of $G_2$–M–$G_1$ transition | Fig., supplemental material, and/or table |
|---|---|---|---|---|
| | $G_1$ | $S/G_2$ | | |
| ssAAV2cmv | + | ++++ | + | Fig. 7, Movie S3 |
| ssAAV2cmv (HSV-1 coinfection) | + | ++++ | + | Fig. 5 + 7 |
| ssAAV2p5 | + | ++++ | ND | Table 1 |
| dsAAV2cmv | + | ++++ | ++++ | Fig. 7, Movie S2 |
| dsAAV2cmv (HSV-1 coinfection) | + | ++++ | + | Fig. 7 |

[a]ssAAV2cmv, single-stranded AAV2 with a cytomegalovirus IE1 enhancer/promoter; dsAAV2cmv, double-stranded AAV2 with a cytomegalovirus IE1 enhancer/promoter; p5, AAV2 p5 promoter; ++++, efficient gene expression/G2-to-M-to-$G_1$-phase transition; +, inefficient replication/G2-to-M-to-$G_1$-phase transition; ND, not done.

$S/G_2$-phase cells efficiently. Indeed, in scAAV2 vector-transduced cell cultures, we observed a considerable proportion of AAV2 transgene-positive $G_1$-phase cells in the absence of the helper virus, but interestingly, high-throughput multichannel time-lapse microscopy of cell cycle progression and viral gene expression showed that the majority of the scAAV2-transduced $G_1$-phase cells originated from scAAV2-transduced $S/G_2$-phase cells that progressed through mitosis, an event that was observed at a significantly lower rate upon infection with the single-stranded rAAV2 vector (for an overview, see Table 3). We hypothesize that rAAV2 vectors, similar to wtAAV2 (53), can induce cell cycle arrest more efficiently than the scAAV2 vectors because of the single-stranded versus double-stranded nature of the genome. In the presence of the helper virus, neither single-stranded nor double-stranded AAV2 vector-transduced cells progressed through mitosis, presumably because of HSV-1-induced $G_2$ arrest (33). This hypothesis is supported by the finding that coinfection with an ICP0 deletion mutant of HSV-1, which is replication competent but does not induce cell cycle arrest in $G_2$ phase (33), allowed scAAV2 vector-transduced $G_2$-phase cells but not rAAV2 vector-transduced $G_2$-phase cells to progress through mitosis (data not shown).

The findings in this study may have important implications for AAV2-mediated gene therapy. Both single-stranded and double-stranded AAV2 vectors depend on cells in $S/G_2$ phase for efficient gene expression, which in fact may contribute to their low transduction efficiency, at least in postmitotic cells. However, when the target cells are mitotically active, the double-stranded AAV2 vectors may be preferred, as they allow the cells to go through mitosis, while the single-stranded AAV2 vectors do not. On the other hand, scAAV2 vectors have been shown to induce a more robust innate immune response in mouse liver than rAAV2 vectors (54). In any event, it would be interesting to compare the effects of scAAV2 and rAAV2 vectors on specific factors involved in cell cycle regulation, including p53, retinoblastoma protein, cyclin-dependent kinases (CDKs), and CDK inhibitors.

The observation that both single-stranded and double-stranded AAV2 vectors transduce cells predominantly in $S/G_2$ phase argues against second-strand synthesis as the mechanism responsible for cell cycle-dependent AAV2 gene expression/DNA replication and inhibition of HSV-1 DNA replication. Nevertheless, the preference of AAV2 to transduce cells in the $S/G_2$ phase of the cell cycle may likely be orchestrated by cellular factors other than those involved in second-strand synthesis. In fact, many different cellular proteins are recruited to AAV2 genomes (32, 55–57). Among these, the DNA damage response (DDR) proteins represent a very prominent group and may differentially affect specific phases in AAV2 genome processing, such as circularization, replication, and transcription. The DNA damage response is closely linked with the cell cycle through checkpoint proteins. Moreover, there is increasing evidence that CDKs, which are the master regulators of cell cycle progression, also have a role in the regulation of the DNA damage repair (for reviews, see reference 58–60), thereby coordinating DNA repair and cell cycle progression. For example, it has been shown that CDK1 activity regulates the choice between different double-strand break (DSB) repair pathways, homologous recombination (HR) and nonhomologous end joining (NHEJ). In $G_1$ phase, CDK1 activity is low, and NHEJ is used, while in $S/G_2/M$ phase, CDK1 activity is high, and HR is employed (61, 62). CDK1 activity stimulates HR by promoting the generation of the 3′ single-stranded DNA ends, which are necessary for HR and inhibitory for NHEJ (61–63). It has also been shown that CDK activity is essential for later steps in HR, specifically in the recruitment of Rad51 (64). Functional roles in DNA damage repair pathways have also been demonstrated for other CDKs in complex with cyclins (for a review, see reference 65).

The licensing factor that allows AAV2 gene expression/DNA replication in $S/G_2$ phase or the inhibitor that blocks it in $G_1$ phase remains to be identified. Nevertheless, the "partitioning" of the host cell population between the two different viruses is a novel concept of viral adaptation and a fascinating strategy to minimize competition,

allowing both AAV2 and HSV-1 to productively replicate although in distinct sets of cells.

## MATERIALS AND METHODS

**Cells.** NHF cells were obtained from X. O. Breakefield (Massachusetts General Hospital, Charlestown, MA, USA). HeLa Fucci cells were a gift from B. Kraus (University of Regensburg, Regensburg, Germany); these cells encode cell cycle-specific proteins fused with red fluorescent (Cdt1) ($G_1$-phase) or green fluorescent (geminin) (S/$G_2$-phase) fusion proteins (45). HCT116 cells were provided by E. Hendrickson (University of Minnesota, Minneapolis, MN, USA). NHF, HeLa Fucci, HCT116, and HeLa (ATCC) cells were cultured in Dulbecco's modified Eagle medium (DMEM) supplemented with 10% fetal bovine serum (FBS), 100 U/ml penicillin G, 100 $\mu$g/ml streptomycin, and 0.25 $\mu$g/ml amphotericin B (1% AB). AT22 IJE-T yZ5 cells (kindly provided by Y. Shiloh, Tel Aviv University, Tel Aviv, Israel) were cultured in DMEM supplemented with 10% FBS, 1% AB, and 100 $\mu$g/ml hygromycin B. Vero cells (ECACC) and 293T cells (kindly provided by J. Neidhardt, University of Zurich, Zurich, Switzerland) were grown in DMEM supplemented with 10% FBS and 1% AB. All cells were maintained at 37°C in a 95% air–5% $CO_2$ atmosphere. For all infection experiments, the virus was allowed to adsorb for 30 min at 4°C before the temperature was shifted to 37°C for 1 h. The cells were then washed with phosphate-buffered saline (PBS) and incubated with DMEM containing 2% FBS and 1% AB at 37°C for the indicated times after infection.

**Plasmids and viruses.** wtHSV-1 strain F was provided by B. Roizman (University of Chicago, Chicago, IL). Recombinant HSV-1 encoding ICP4 fused with ECFP (rHSV-1vECFP-ICP4) (46) was obtained from R. D. Everett (University of Glasgow, Glasgow, UK). Recombinant HSV-1 rHSV48EYFP encoding the VP16 protein fused with EYFP was described previously (50). wtHSV-1 and recombinant HSV-1 were grown and titrated on Vero cells. Plasmid pAAVtCR, which contains a recombinant AAV2 genome that lacks the *cap* gene and encodes unmodified Rep40/52 under the control of the p19 promoter and Rep68/78 fused at the N terminus with the fluorescent protein mCherry (31) under the control of the p5 promoter, was obtained from A. Salvetti (University of Lyon, Lyon, France). Plasmids containing recombinant AAV2 genomes, pAAVCFPRep and pAAVYFPRep, were constructed by replacing the mCherry coding sequence in the pAAVtCR plasmid with ECFP and EYFP coding sequences, respectively, as follows: pAAVtCR was treated first with BsrGI and then partially with BamHI, and the 5,169-bp fragment was ligated with the 738-bp BsrGI-BamHI fragment containing the ECFP or EYFP coding sequences from pECFP-N2 or pEYFP-N2 (Clontech), respectively. Plasmid pAAVCFPp5, which encodes ECFP from the AAV2 p5 promoter, was constructed by replacing the 1,885-bp BsrGI-SwaI fragment of pAAVCFPRep, which contains the AAV2 Rep coding sequence, with the BsrG1-SwaI adaptor oligonucleotide 5′-GTACAAGATCGATATT T-3′. The recombinant AAV2 genome rAAVCFPNeo was constructed by replacing the enhanced green fluorescent protein (EGFP) coding sequence in plasmid pAAVGFP (provided by M. Linden, King's College London School of Medicine, London, UK) with the ECFP coding sequence, as follows: pECFP-N2 was treated with PstI and NotI, and the 768-bp fragment was ligated with the 6,417-bp PstI-NotI fragment of pAAVGFP. Transgene expression from pAAVCFPNeo is controlled by the human CMV IE1 enhancer/promoter. Plasmid pscAAVCFP, which encodes the self-complementary recombinant AAV2 genome scAAVCFP, was constructed by replacing the EGFP coding sequence in pscAAVeGFP (kindly provided by J. Neidhardt, University of Zurich, Switzerland) with the ECFP coding sequence. Specifically, a DNA fragment containing the CMV enhancer/promoter-ECFP coding sequence was amplified by PCR from plasmid pCMVeCFP-PolyA (our unpublished data) using forward (5′-AAGATATCACTAGTTAGTTATTAATA GTAATCAATTACG-3′) and reverse (5′-CCGGTACCATGCAGTGAAAAAAATGC-3′) primers (PCR conditions were 30 s at 98°C; 35 cycles of 10 s at 98°C, 45 s at 58°C, and 60 s at 72°C; and 10 min at 72°C), digested with SpeI and NotI, and ligated between the SpeI and NotI sites of pscAAVeGFP. Recombinant AAV2 stocks were produced by transient transfection of 293T cells with pDG (66) and either pAAVCFPRep, pAAVYFPRep, pAAVCFPNeo, or pscAAVCFP. Virus stocks were purified by an iodixanol gradient, and titers were determined as described previously (67). wtAAV2 was grown and titrated as described previously (68).

**Antibodies.** The following primary antibodies were used: antiactin (catalog number SC-10731; Santa Cruz Biotechnology) (dilution for WB, 1:10,000), anti-ICP8 (catalog number Ab-20193; Abcam) (dilution for WB, 1:1,000; dilution for immunofluorescence [IF] assays, 1:200), anti-AAV2 Rep (catalog number 10R-A111A; Fitzgerald Industries) (dilution for WB, 1:200; dilution for IF assays, 1:50), and anti-ICP0 (catalog number ab6513) (dilution for WB, 1:2,000). The following secondary antibodies were used: rabbit anti-mouse IgG-horseradish peroxidase (HRP) (catalog number A9044; Sigma) (dilution, 1:10,000), goat anti-rabbit IgG-HRP (catalog number A6154; Sigma) (dilution, 1:10,000), and goat anti-mouse IgG(H+L)–AF-405 (catalog number A31556; Molecular Probes) (dilution, 1:500).

**FACS analysis followed by Western blotting, Southern blotting, or quantitative PCR.** For the experiments in Fig. 3, $5 \times 10^6$ HeLa Fucci cells were seeded onto 10-cm tissue culture plates and 24 h later were mock infected, infected with wtAAV2 (multiplicity of infection [MOI] of 8,000 genome-containing particles per cell) or wtHSV-1 (MOI of 3), or coinfected with wtAAV2 (MOI of 8,000) and wtHSV-1 (MOI of 3). After 24 h, cells positive for Cdt1 ($G_1$ phase) (red) or geminin (S/$G_2$ phase) (green) were sorted by using a FACSAria III sorter (BD Biosciences) and prepared for Western analysis, Southern blotting, or qPCR. For Western blot analysis, cells were trypsinized, washed once with PBS, resuspended in 1× loading buffer (4% SDS, 10% $\beta$-mercaptoethanol, 20% glycerol, 0.005% bromphenol blue, 0.125 M Tris-HCl [pH 6.8]), and boiled for 10 min. Cell lysates were separated on 10% SDS-polyacrylamide gels and transferred onto Protran nitrocellulose membranes (Whatman, Bottmingen, Switzerland). The membranes were blocked with PBS-T (PBS containing 0.3% Tween 20) supplemented with 5% nonfat dry milk

for 1 h at room temperature (RT). Incubation with antibodies was carried out with PBS-T supplemented with 2.5% nonfat dry milk. Primary antibodies were incubated overnight at 4°C, while secondary antibodies were incubated for 1 h at RT. Membranes were washed three times with PBS-T for 10 min after each antibody incubation step. HRP-conjugated secondary antibodies were detected with ECL detection reagent (ECL WB blotting systems; GE Healthcare, Zurich, Switzerland). The membranes were exposed to chemiluminescence detection films (Roche Diagnostics, Rotkreuz, Switzerland). Detection of antiactin served as a loading control for the lysate. For Southern blot analysis, extrachromosomal DNA was extracted according to protocols described previously by Hirt (52). The DNA was separated on 1% agarose gels and transferred onto nylon membranes (Hybond-$N^+$, catalog number RPN119B; Amersham). Hybridization with a digoxigenin (DIG)-labeled probe specific for the AAV2 Rep78- or the HSV-1 UL35-coding sequences and subsequent detection by an anti-DIG antibody conjugated with alkaline phosphatase and activation with the chemiluminescence substrate CDP Star were performed according to the manufacturer's protocols (Roche, Mannheim, Germany). The DIG-labeled probe was produced with the PCR DIG probe synthesis kit (Roche). For qPCR, total DNA was isolated by using the DNeasy blood and tissue kit (Qiagen, Hilden, Germany) according to the manufacturer's protocol. The viral DNA content was quantified by qPCR using the cellular telomerase reverse transcriptase (TERT) gene as an endogenous control (Applied Biosystems, Foster City, CA, USA) and primers and a TaqMan probe specific for the AAV2 Rep78-coding sequence (forward primer 5′-ATTGACGGAACTCAACGAC-3′, reverse primer 5′-CCTC AACCACGTCCTTT-3′, and TaqMan probe 5′-CATGATCCAGACGGCGGGTGA-3′) or primers specific for the HSV-1 UL42 gene (forward primer 5′-CCCTCAAGTTCTTCTTCCTCACG-3′ and reverse primer 5′-GGAGTCC TGGCTGTCTGTTG-3′) and SYBR green (Applied Biosystems, Foster City, CA, USA). AAV2 sequences were amplified under the following conditions: 2 min at 50°C; 15 min at 95°C; and 40 cycles of 15 s at 94°C, 30 s at 56°C, and 15 s at 72°C. HSV-1 sequences were amplified under the following conditions: 3 min at 95°C, 39 cycles of 15 s at 95°C and 60 s at 45°C, 10 s at 95°C, 5 s at 65°C, and 5 s at 95°C. For the experiments shown in Fig. 7C and D, $1.5 \times 10^6$ HeLa Fucci cells in 6-cm tissue culture plates were transfected with 0.5 $\mu$g of either pAAVCFPRep or pAAVCFPp5 by using Lipofectamine LTX according to the manufacturer's instructions (Life Technologies) and 4 h later were mock-infected or infected with wtHSV-1 (MOI of 2) as described in the legend. After 24 h, cells positive for the $G_1$-phase marker Cdt1 (red) or double positive for the $G_1$-phase marker and either CFP-Rep or CFP were sorted by using a FACSAria III sorter (BD Biosciences). Hirt DNA or total DNA was then prepared from the sorted cell populations. To determine the AAV2 DNA content, Hirt DNA was incubated with DpnI prior to qPCRs in order to degrade the transfected input plasmid DNA isolated from *Escherichia coli*. To determine the HSV-1 DNA content, total DNA was used for qPCR.

**Microscopy.** For microscopy, HeLa or HeLa Fucci cells were seeded onto coverslips (12-mm diameter; Glaswarenfabrik Karl Hecht GmbH & Co. KG, Sondheim, Germany) in 24-well tissue culture plates ($5 \times 10^4$ cells per well) or, specifically for epifluorescence live-cell microscopy, directly onto 96-well tissue culture plates ($10^4$ cells per well) (see also reference 69). The next day, the cells were infected as indicated in Results and the figure legends. For the experiments shown in Fig. 6, the cells were transfected with 0.5 $\mu$g of either pAAVCFPRep or pAAVCFPp5 4 h prior to infection. For live-cell microscopy of AAV2 gene expression/replication and cell cycle progression (Fig. 5A and 7A; see also Movies S1 to S3 in the supplemental material), images were acquired every 30 min from 2 to 20 h after infection by automated multisite multichannel live epifluorescence microscopy in a time-lapse mode (37°C with 5% $CO_2$, humidified) by using ImageXpress Micro XL (Molecular Devices) and fluorescence filters (Semrock) for ECFP (AAV2), GFP ($G_2$ phase), and tetramethylrhodamine isocyanate (TRITC) ($G_1$ phase) (69, 70); images were processed by using Fiji software (71). For standard fluorescence microscopy or CSLM, the cells were washed once with cold PBS 24 h after infection and then fixed with 3.7% paraformaldehyde (PFA) in PBS for 10 min at RT. The fixation process was stopped by incubation with 0.1 M glycine for 10 min at RT and two washes with cold PBS. For immunofluorescence analysis (Fig. 1A and B), the cells were permeabilized by treatment with precooled (−20°C) acetone for 2 min, followed by 3 washing steps with PBS. The cells were blocked for 30 min with 3% bovine serum albumin (BSA) in PBS. For staining, the cells were incubated with antibodies diluted in PBS-BSA (3%) in a humidified chamber at RT in the dark. The coverslips were placed onto droplets (40 $\mu$l) of a primary antibody solution. After incubation for 1 h, the cells were washed three times with PBS and once with $H_2O$. All coverslips (with and without antibody staining) were embedded in Glycergel (DakoCytomation, Carpinteria, CA) containing 1,4-diazabicyclo[2.2.2]octan (DABCO) (26 mg/ml; Fluka, Sigma-Aldrich Chemie GmbH, Munich, Germany), and cells were observed by using a confocal laser scanning microscope (Leica TCS SP2 acousto-optical beam splitter (AOBS); Leica Microsystems, Wetzlar, Germany) (Fig. 1A and B and 6A and B), an automated epifluorescence microscope using ImageXpress Micro XL (Molecular Devices) (Fig. 5A), or a standard fluorescence microscope (Axio Observer inverted microscope, Zeiss AG, Germany) (Fig. 5C). To prevent cross talk between the channels for the different fluorochromes, all channels were recorded separately, and fluorochromes with longer wavelengths were recorded first.

**Flow cytometry.** HCT116, AT22, NHF, or HeLa Fucci cells were seeded into wells of a 12-well tissue culture plate ($10^5$ cells per well) and 24 h later were coinfected with wtHSV-1 (MOI of 1.5 for AT22 cells and MOI of 3 for all other cell lines) and either rAAVCFPRep or rAAVYFPRep (MOI of 1,000 for HeLa Fucci cells and MOI of 4,000 for all other cell lines), as indicated in Table 1. All cells were incubated at 37°C with 5% $CO_2$ in DMEM supplemented with 2% FBS and 1% AB. After 20 to 24 h, the cells were trypsinized, washed once with PBS, centrifuged for 10 min at 1,000 $\times$ *g*, and resuspended in 1 ml PBS. The cells were fixed by the addition of 2.5 ml ethanol (EtOH) and incubation overnight at −20°C. To determine the cell cycle phases in HCT116, NHF, and AT22 cells, DNA was stained for 30 min with DAPI (1 $\mu$g/ml in PBS containing 0.1% Triton X-100) or propidium iodide (PI) (50 $\mu$g/ml in PBS containing 0.1% Triton X-100 and

0.1 mg/ml RNase A), as indicated in Table 1. A minimum of 40,000 events were scored for each sample by using a Gallios flow cytometer (Beckman Coulter), and data were analyzed by using Kaluza Flow Analysis software 1.3 (Beckman Coulter).

**Fluorescence *in situ* hybridization.** FISH was performed essentially as described previously by Lux et al. (68). Briefly, an ~3.9-kb DNA fragment containing the AAV2 genome without the inverted terminal repeats was amplified by PCR from plasmid pDG (66) using forward (5′-CGGGGTTTTACGAGATTGTG-3′) and reverse (5′-GGCTCTGAATACACGCCATT-3′) primers and the following conditions: 30 s at 95°C; 35 cycles of 10 s at 98°C, 15 s at 58°C, and 75 s at 72°C; and 10 min at 72°C. The PCR product was then digested with DpnI to cut the residual template DNA and purified with a Pure Link PCR purification kit (Qiagen). The DNA fragment was labeled with 5-(3-aminoallyl)dUTP by nick translation, and the incorporated dUTPs were labeled with amino-reactive Alexa Fluor 647 dye by using the Ares DNA labeling kit (Molecular Probes) according to the manufacturer's protocols. HeLa Fucci cells were plated onto glass coverslips in 24-well plates at a density of $1.4 \times 10^5$ cells per well and 24 h later were mock infected, infected with wtAAV2 (MOI of 4,000), or coinfected with wtAAV2 (MOI of 4,000) and either wtHSV-1 (MOI of 3) or rHSV-1vECFP-ICP4 (MOI of 3). Twenty-four hours after infection, the cells were washed with PBS, fixed for 30 min at RT with 2% PFA (in PBS), and then washed again with PBS. The cells were then quenched for 10 min with 50 mM $NH_4Cl$ (in PBS), washed with PBS, permeabilized for 10 min with 0.2% Triton X-100 (in PBS), blocked for 10 min with 0.2% gelatin (in PBS), and washed again with PBS. Hybridization solution (20 $\mu$l per coverslip) containing 1 ng/$\mu$l of the labeled DNA probe, 50% formamide, 7.3% dextran sulfate, 15 ng/$\mu$l salmon sperm DNA, and 0.74× SSC (1× SSC is 0.15 M NaCl plus 0.015 M sodium citrate) was denatured for 3 min at 95°C and shock cooled on ice. The coverslips with the fixed, and permeabilized cells facing down were placed onto a drop (20 $\mu$l) of the denatured hybridization solution and incubated overnight at 37°C in a humidified chamber. (Of note, the cells were not denatured, as the AAV2 genome is a single-stranded DNA.) The next day, the coverslips were washed three times with 2× SSC at 37°C, three times with 0.1× SSC at 60°C, and twice with PBS at RT. The cells were then embedded in ProLong Anti-Fade mountant (Molecular Probes) and imaged by confocal laser scanning microscopy (Leica SP8; Leica Microsystems, Wetzlar, Germany).

## SUPPLEMENTAL MATERIAL

Supplemental material for this article may be found at https://doi.org/10.1128/JVI.00357-17.

**SUPPLEMENTAL FILE 1,** MP4 file, 0.3 MB.
**SUPPLEMENTAL FILE 2,** MP4 file, 0.2 MB.
**SUPPLEMENTAL FILE 3,** MP4 file, 0.2 MB.
**SUPPLEMENTAL FILE 4,** PDF file, 0.1 MB.

## ACKNOWLEDGMENTS

We thank X. O. Breakefield, B. Kraus, E. Hendrickson, Y. Shiloh, J. Neidhardt, B. Roizman, R. Everett, A. Salvetti, and M. Linden for providing reagents and E. M. Schraner for assistance with the preparation of the figures.

This work was supported by grants 31003A_144094/1 and 31003A_166668/1 from the Swiss National Science Foundation to C.F.

We declare that we have no conflict of interest.

## REFERENCES

1. Adeyemi RO, Pintel DJ. 2014. Parvovirus-induced depletion of cyclin B1 prevents mitotic entry of infected cells. PLoS Pathog 10:e1003891. https://doi.org/10.1371/journal.ppat.1003891.
2. Berk AJ. 2007. Adenoviridae: the viruses and their replication, p 2355–2394. *In* Knipe DM, Howley PM, Griffin DE, Lamb RA, Martin MA, Roizman B, Straus SE (ed), Fields virology, 5th ed. Lippincott Williams & Wilkins, Philadelphia, PA.
3. Aubert M, Chen Z, Lang R, Dang CH, Fowler C, Sloan DD, Jerome KR. 2008. The antiapoptotic herpes simplex virus glycoprotein J localizes to multiple cellular organelles and induces reactive oxygen species formation. J Virol 82:617–629. https://doi.org/10.1128/JVI.01341-07.
4. Taylor TJ, Brockman MA, McNamee EE, Knipe DM. 2002. Herpes simplex virus. Front Biosci 7:d752–d764. https://doi.org/10.2741/A809.
5. Hobbs WE, II, DeLuca NA. 1999. Perturbation of cell cycle progression and cellular gene expression as a function of herpes simplex virus ICP0. J Virol 73:8245–8255.
6. Ehmann GL, McLean TI, Bachenheimer SL. 2000. Herpes simplex virus type 1 infection imposes a G(1)/S block in asynchronously growing cells and prevents G(1) entry in quiescent cells. Virology 267:335–349. https://doi.org/10.1006/viro.1999.0147.
7. Lomonte P, Everett RD. 1999. Herpes simplex virus type 1 immediate-early protein Vmw110 inhibits progression of cells through mitosis and from G(1) into S phase of the cell cycle. J Virol 73:9456–9467.
8. Song B, Liu JJ, Yeh KC, Knipe DM. 2000. Herpes simplex virus infection blocks events in the $G_1$ phase of the cell cycle. Virology 267:326–334. https://doi.org/10.1006/viro.1999.0146.
9. Song B, Yeh KC, Liu J, Knipe DM. 2001. Herpes simplex virus gene products required for viral inhibition of expression of $G_1$-phase functions. Virology 290:320–328. https://doi.org/10.1006/viro.2001.1175.
10. Muzyczka N, Berns KI. 2001. Parvoviridae: the viruses and their replication, p 2327–2346. *In* Knipe DM, Howley PM, Griffin DE, Lamb RA, Martin MA, Roizman B, Straus SE (ed), Fields virology, 4th ed, vol 2. Lippincott Williams & Wilkins, Philadelphia, PA.
11. Sonntag F, Schmidt K, Kleinschmidt JA. 2010. A viral assembly factor promotes AAV2 capsid formation in the nucleolus. Proc Natl Acad Sci U S A 107:10220–10225. https://doi.org/10.1073/pnas.1001673107.
12. Chejanovsky N, Carter BJ. 1989. Mutagenesis of an AUG codon in the adeno-associated virus rep gene: effects on viral DNA replication. Virology 173:120–128. https://doi.org/10.1016/0042-6822(89)90227-4.
13. Im DS, Muzyczka N. 1990. The AAV origin binding protein Rep68 is an ATP-dependent site-specific endonuclease with DNA helicase activity. Cell 61:447–457. https://doi.org/10.1016/0092-8674(90)90526-K.

14. Kotin RM, Menninger JC, Ward DC, Berns KI. 1991. Mapping and direct visualization of a region-specific viral DNA integration site on chromosome 19q13-qter. Genomics 10:831–834. https://doi.org/10.1016/0888-7543(91)90470-Y.
15. Samulski RJ, Zhu X, Xiao X, Brook JD, Housman DE, Epstein N, Hunter LA. 1991. Targeted integration of adeno-associated virus (AAV) into human chromosome 19. EMBO J 10:3941–3950. (Erratum, 11:1228, 1992).
16. King JA. 2001. DNA helicase-mediated packaging of adeno-associated virus type 2 genomes into preformed capsids. EMBO J 20:3282–3291. https://doi.org/10.1093/emboj/20.12.3282.
17. McCarty DM, Young SMJ, Samulski RJ. 2004. Integration of adeno-associated virus (AAV) and recombinant AAV vectors. Annu Rev Genet 38:819–845. https://doi.org/10.1146/annurev.genet.37.110801.143717.
18. Smith RH, Kotin RM. 1998. The Rep52 gene product of adeno-associated virus is a DNA helicase with 3′-to-5′ polarity. J Virol 72:4874–4881.
19. Wu J, Davis MD, Owens RA. 1999. Factors affecting the terminal resolution site endonuclease, helicase, and ATPase activities of adeno-associated virus type 2 Rep proteins. J Virol 73:8235–8244.
20. Zhou X, Zolotukhin I, Im DS, Muzyczka N. 1999. Biochemical characterization of adeno-associated virus rep68 DNA helicase and ATPase activities. J Virol 73:1580–1590.
21. Yoon-Robarts M, Linden RM. 2003. Identification of active site residues of the adeno-associated virus type 2 Rep endonuclease. J Biol Chem 278:4912–4918. https://doi.org/10.1074/jbc.M209750200.
22. Collaco RF, Kalman-Maltese V, Smith AD, Dignam JD, Trempe JP. 2003. A biochemical characterization of the adeno-associated virus Rep40 helicase. J Biol Chem 278:34011–34017. https://doi.org/10.1074/jbc.M301537200.
23. Hoggan MD, Blacklow NR, Rowe WP. 1966. Studies of small DNA viruses found in various adenovirus preparations: physical, biological, and immunological characteristics. Proc Natl Acad Sci U S A 55:1467–1474. https://doi.org/10.1073/pnas.55.6.1467.
24. Buller RM, Janik JE, Sebring ED, Rose JA. 1981. Herpes simplex virus types 1 and 2 completely help adenovirus-associated virus replication. J Virol 40:241–247.
25. Walz C, Deprez A, Dupressoir T, Dürst M, Rabreau M, Schlehofer JR. 1997. Interaction of human papillomavirus type 16 and adeno-associated virus type 2 co-infecting human cervical epithelium. J Gen Virol 78(Part 6):1441–1452.
26. Kotin RM, Linden RM, Berns KI. 1992. Characterization of a preferred site on human chromosome 19q for integration of adeno-associated virus DNA by non-homologous recombination. EMBO J 11:5071–5078.
27. Linden RM, Ward P, Giraud C, Winocour E, Berns KI. 1996. Site-specific integration by adeno-associated virus. Proc Natl Acad Sci U S A 93:11288–11294. https://doi.org/10.1073/pnas.93.21.11288.
28. Linden RM, Winocour E, Berns KI. 1996. The recombination signals for adeno-associated virus site-specific integration. Proc Natl Acad Sci U S A 93:7966–7972. https://doi.org/10.1073/pnas.93.15.7966.
29. Weindler FW, Heilbronn R. 1991. A subset of herpes simplex virus replication genes provides helper functions for productive adeno-associated virus replication. J Virol 65:2476–2483.
30. Ward P, Falkenberg M, Elias P, Weitzman M, Linden RM. 2001. Rep-dependent initiation of adeno-associated virus type 2 DNA replication by a herpes simplex virus type 1 replication complex in a reconstituted system. J Virol 75:10250–10258. https://doi.org/10.1128/JVI.75.21.10250-10258.2001.
31. Alazard-Dany N, Nicolas A, Ploquin A, Strasser R, Greco A, Epstein AL, Fraefel C, Salvetti A. 2009. Definition of herpes simplex virus type 1 helper activities for adeno-associated virus early replication events. PLoS Pathog 5:e1000340. https://doi.org/10.1371/journal.ppat.1000340.
32. Vogel R, Seyffert M, Strasser R, de Oliveira AP, Dresch C, Glauser DL, Jolinon N, Salvetti A, Weitzman MD, Ackermann M, Fraefel C. 2011. Adeno-associated virus type 2 modulates the host DNA damage response induced by herpes simplex virus 1 during coinfection. J Virol 86:143–155. https://doi.org/10.1128/JVI.05694-11.
33. Li H, Baskaran R, Krisky DM, Bein K, Grandi P, Cohen JB, Glorioso JC. 2008. Chk2 is required for HSV-1 ICP0-mediated $G_2$/M arrest and enhancement of virus growth. Virology 375:13–23. https://doi.org/10.1016/j.virol.2008.01.038.
34. Casto BC, Armstrong JA, Atchison RW, Hammon WM. 1967. Studies on the relationship between adeno-associated virus type 1 (AAV-1) and adenoviruses. II. Inhibition of adenovirus plaques by AAV; its nature and specificity. Virology 33:452–458. https://doi.org/10.1016/0042-6822(67)90120-1.
35. Casto BC, Atchison RW, Hammon WM. 1967. Studies on the relationship between adeno-associated virus type I (AAV-1) and adenoviruses. I. Replication of AAV-1 in certain cell cultures and its effect on helper adenovirus. Virology 32:52–59. https://doi.org/10.1016/0042-6822(67)90251-6.
36. Carter BJ, Laughlin CA, de la Maza LM, Myers M. 1979. Adeno-associated virus autointerference. Virology 92:449–462. https://doi.org/10.1016/0042-6822(79)90149-1.
37. Bantel-Schaal U, Zur Hausen H. 1988. Adeno-associated viruses inhibit SV40 DNA amplification and replication of herpes simplex virus in SV40-transformed hamster cells. Virology 164:64–74. https://doi.org/10.1016/0042-6822(88)90620-4.
38. Glauser DL, Strasser R, Laimbacher AS, Saydam O, Clément N, Linden RM, Ackermann M, Fraefel C. 2007. Live covisualization of competing adeno-associated virus and herpes simplex virus type 1 DNA replication: molecular mechanisms of interaction. J Virol 81:4732–4743. https://doi.org/10.1128/JVI.02476-06.
39. Chiorini JA, Zimmermann B, Yang L, Smith RH, Ahearn A, Herberg F, Kotin RM. 1998. Inhibition of PrKX, a novel protein kinase, and the cyclic AMP-dependent protein kinase PKA by the regulatory proteins of adeno-associated virus type 2. Mol Cell Biol 18:5921–5929. https://doi.org/10.1128/MCB.18.10.5921.
40. Di Pasquale G, Stacey SN. 1998. Adeno-associated virus Rep78 protein interacts with protein kinase A and its homolog PRKX and inhibits CREB-dependent transcriptional activation. J Virol 72:7916–7925.
41. Schmidt M, Chiorini JA, Afione S, Kotin R. 2002. Adeno-associated virus type 2 Rep78 inhibition of PKA and PRKX: fine mapping and analysis of mechanism. J Virol 76:1033–1042. https://doi.org/10.1128/JVI.76.3.1033-1042.2002.
42. Di Pasquale G, Chiorini JA. 2003. PKA/PrKX activity is a modulator of AAV/adenovirus interaction. EMBO J 22:1716–1724. https://doi.org/10.1093/emboj/cdg153.
43. Glauser DL, Seyffert M, Strasser R, Franchini M, Laimbacher AS, Dresch C, de Oliveira AP, Vogel R, Büning H, Salvetti A, Ackermann M, Fraefel C. 2010. Inhibition of herpes simplex virus type 1 replication by adeno-associated virus Rep proteins depends on their combined DNA-binding and ATPase/helicase activities. J Virol 84:3808–3824. https://doi.org/10.1128/JVI.01503-09.
44. Seyffert M, Glauser DL, Tobler K, Georgiev O, Vogel R, Vogt B, Agúndez L, Linden M, Büning H, Ackermann M, Fraefel C. 2015. Adeno-associated virus type 2 Rep68 can bind to consensus Rep-binding sites on the herpes simplex virus 1 genome. J Virol 89:11150–11158. https://doi.org/10.1128/JVI.01370-15.
45. Sakaue-Sawano A, Kurokawa H, Morimura T, Hanyu A, Hama H, Osawa H, Kashiwagi S, Fukami K, Miyata T, Miyoshi H, Imamura T, Ogawa M, Masai H, Miyawaki A. 2008. Visualizing spatiotemporal dynamics of multicellular cell-cycle progression. Cell 132:487–498. https://doi.org/10.1016/j.cell.2007.12.033.
46. Everett RD, Sourvinos G, Orr A. 2003. Recruitment of herpes simplex virus type 1 transcriptional regulatory protein ICP4 into foci juxtaposed to ND10 in live, infected cells. J Virol 77:3680–3689. https://doi.org/10.1128/JVI.77.6.3680-3689.2003.
47. Russell DW, Miller AD, Alexander IE. 1994. Adeno-associated virus vectors preferentially transduce cells in S phase. Proc Natl Acad Sci U S A 91:8915–8919. https://doi.org/10.1073/pnas.91.19.8915.
48. Russell DW, Alexander IE, Miller AD. 1995. DNA synthesis and topoisomerase inhibitors increase transduction by adeno-associated virus vectors. Proc Natl Acad Sci U S A 92:5719–5723. https://doi.org/10.1073/pnas.92.12.5719.
49. Glauser DL, Saydam O, Fraefel C. 2006. Parvovirus replication, p 71–99. *In* Hefferon KL (ed), Recent advances in DNA virus replication. Research Signpost, Kerala, India.
50. de Oliveira AP, Glauser DL, Laimbacher AS, Strasser R, Schraner EM, Wild P, Ziegler U, Breakefield XO, Ackermann M, Fraefel C. 2008. Live visualization of herpes simplex virus type 1 compartment dynamics. J Virol 82:4974–4990. https://doi.org/10.1128/JVI.02431-07.
51. La Boissiere S, Izeta A, Malcomber S, O'Hare P. 2004. Compartmentalization of VP16 in cells infected with recombinant herpes simplex virus expressing VP16-green fluorescent protein fusion proteins. J Virol 78:8002–8014. https://doi.org/10.1128/JVI.78.15.8002-8014.2004.
52. Hirt B. 1969. Replicating molecules of polyoma virus DNA. J Mol Biol 40:141–144. https://doi.org/10.1016/0022-2836(69)90302-7.
53. Hermanns J, Schulze A, Jansen-Dürr P, Kleinschmidt JA, Schmidt R, Zur Hausen H. 1997. Infection of primary cells by adeno-associated virus

type 2 results in a modulation of cell cycle-regulating proteins. J Virol 71:6020–6027.
54. Martino AT, Suzuki M, Markusic DM, Zolotukhin I, Ryals RC, Moghimi B, Ertl HC, Muruve DA, Lee B, Herzog RW. 2011. The genome of self-complementary adeno-associated viral vectors increases Toll-like receptor 9-dependent innate immune responses in the liver. Blood 117:6459–6468. https://doi.org/10.1182/blood-2010-10-314518.
55. Nash K, Chen W, McDonald WF, Zhou X, Muzyczka N. 2007. Purification of host cell enzymes involved in adeno-associated virus DNA replication. J Virol 81:5777–5787. https://doi.org/10.1128/JVI.02651-06.
56. Cervelli T, Palacios JA, Zentilin L, Mano M, Schwartz RA, Weitzman MD, Giacca M. 2008. Processing of recombinant AAV genomes occurs in specific nuclear structures that overlap with foci of DNA-damage-response proteins. J Cell Sci 121:349–357. https://doi.org/10.1242/jcs.003632.
57. Nicolas A, Alazard-Dany N, Biollay C, Arata L, Jolinon N, Kuhn L, Ferro M, Weller SK, Epstein AL, Salvetti A, Greco A. 2010. Identification of Rep-associated factors in herpes simplex virus type 1-induced adeno-associated virus type 2 replication compartments. J Virol 84:8871–8887. https://doi.org/10.1128/JVI.00725-10.
58. Branzei D, Foiani M. 2008. Regulation of DNA repair throughout the cell cycle. Nat Rev Mol Cell Biol 9:297–308. https://doi.org/10.1038/nrm2351.
59. You Z, Bailis JM. 2010. DNA damage and decisions: CtIP coordinates DNA repair and cell cycle checkpoints. Trends Cell Biol 20:402–409. https://doi.org/10.1016/j.tcb.2010.04.002.
60. Trovesi C, Manfrini N, Falcettoni M, Longhese MP. 2013. Regulation of the DNA damage response by cyclin-dependent kinases. J Mol Biol 425:4756–4766. https://doi.org/10.1016/j.jmb.2013.04.013.
61. Aylon Y, Liefshitz B, Kupiec M. 2004. The CDK regulates repair of double-strand breaks by homologous recombination during the cell cycle. EMBO J 23:4868–4875. https://doi.org/10.1038/sj.emboj.7600469.
62. Ira G, Pellicioli A, Balijja A, Wang X, Fiorani S, Carotenuto W, Liberi G, Bressan D, Wan L, Hollingsworth NM, Haber JE, Foiani M. 2004. DNA end resection, homologous recombination and DNA damage checkpoint activation require CDK1. Nature 431:1011–1017. https://doi.org/10.1038/nature02964.
63. Zhang Y, Shim EY, Davis M, Lee SE. 2009. Regulation of repair choice: Cdk1 suppresses recruitment of end joining factors at DNA breaks. DNA Repair (Amst) 8:1235–1241. https://doi.org/10.1016/j.dnarep.2009.07.007.
64. Caspari T, Murray JM, Carr AM. 2002. Cdc2-cyclin B kinase activity links Crb2 and Rqh1-topoisomerase III. Genes Dev 16:1195–1208. https://doi.org/10.1101/gad.221402.
65. Lim S, Kaldis P. 2013. Cdks, cyclins and CKIs: roles beyond cell cycle regulation. Development 140:3079–3093. https://doi.org/10.1242/dev.091744.
66. Grimm D, Kern A, Rittner K, Kleinschmidt JA. 1998. Novel tools for production and purification of recombinant adenoassociated virus vectors. Hum Gene Ther 9:2745–2760. https://doi.org/10.1089/hum.1998.9.18-2745.
67. Grieger JC, Choi VW, Samulski RJ. 2006. Production and characterization of adeno-associated viral vectors. Nat Protoc 1:1412–1428. https://doi.org/10.1038/nprot.2006.207.
68. Lux K, Goerlitz N, Schlemminger S, Perabo L, Goldnau D, Endell J, Leike K, Kofler DM, Finke S, Hallek M, Buning H. 2005. Green fluorescent protein-tagged adeno-associated virus particles allow the study of cytosolic and nuclear trafficking. J Virol 79:11776–11787. https://doi.org/10.1128/JVI.79.18.11776-11787.2005.
69. Yakimovich A, Gumpert H, Burckhardt CJ, Lutschg VA, Jurgeit A, Sbalzarini IF, Greber UF. 2012. Cell-free transmission of human adenovirus by passive mass transfer in cell culture simulated in a computer model. J Virol 86:10123–10137. https://doi.org/10.1128/JVI.01102-12.
70. Yakimovich A, Andriasyan V, Witte R, Wang IH, Prasad V, Suomalainen M, Greber UF. 2015. Plaque2.0—a high-throughput analysis framework to score virus-cell transmission and clonal cell expansion. PLoS One 10:e0138760. https://doi.org/10.1371/journal.pone.0138760.
71. Schindelin J, Arganda-Carreras I, Frise E, Kaynig V, Longair M, Pietzsch T, Preibisch S, Rueden C, Saalfeld S, Schmid B, Tinevez JY, White DJ, Hartenstein V, Eliceiri K, Tomancak P, Cardona A. 2012. Fiji: an open-source platform for biological-image analysis. Nat Methods 9:676–682. https://doi.org/10.1038/nmeth.2019.

## 5.2. Targeted image-based RNAi screen identifies host cell proteins with differential effects on the transduction efficiency of single-stranded and self-complementary AAV vectors

Francesca D. Franzoso, Artur Yakimovich, Kurt Tobler, Rebecca Vogel, Bernd Vogt, Hildegard Büning, Urs Greber, Cornel Fraefel

Submitted manuscript

**Own contributions:**

I have established an image-based high-throughput siRNA screening assay, I have performed a detailed analysis of the data and I have established the qRT-PCR assay and performed all the experiments (flow cytometry, microscopy, qPCR). I have performed statistical analyses, prepared the figures and wrote the first draft of the manuscript. This work is shown here as a manuscript that was recently submitted.

# Targeted image-based RNAi screen identifies host cell proteins with differential effects on the transduction efficiency of single-stranded and self-complementary AAV vectors

Francesca D. Franzoso[a,#], Artur Yakimovich[b,##], Kurt Tobler[a], Rebecca Vogel[a], Bernd Vogt[a], Hildegard Büning[c,d], Urs F. Greber[b], and Cornel Fraefel[a,*]

Institute of Virology, University of Zurich, Zurich, Switzerland[a]; Institute of Molecular Life Sciences, University of Zurich, Zurich, Switzerland[b]; Center for Molecular Medicine Cologne, University of Cologne, Cologne, Germany[c]; Institute for Experimental Hematology, Hannover Medical School, Hannover, Germany[d]

[*]Correspondence to: Institute of Virology, University of Zurich, Winterthurerstrasse 266a, CH-8057 Zurich, Switzerland. Email: cornel.fraefel@uzh.ch

[#]Present address: UMR 703 PAnTher INRA/ONIRIS, Anatomic Pathology and Gene Therapy Unit, Nantes-Atlantic College of Veterinary Medicine, Food Science and Engineering, Nantes, France

[##]Present address: MRC LMCB, University College London, London, United Kingdom

Number of Figures: 8

Number of Supplementary Figures: 1

Number of Supplementary Tables: 1

**Abstract**

Adeno-associated virus (AAV) based vectors attract significant interest for gene therapy. Here we performed a targeted, small interfering RNA (siRNA) screen for host factors implicated in AAV vector transduction. We identified cellular proteins, which affected the transduction efficiency of single-stranded (ss) and double-stranded (ds), self-complementary (sc) AAV vectors equally, as well as proteins with differential effects on the two vector types. In particular, knockdown of the ss DNA binding protein RPA1 resulted in differential transduction efficiencies of ss and sc AAV vectors. Knockdown of RPA2, another subunit of the RPA complex, had a similar effect as RPA1 on vector transduction. Interestingly however, RPA2 appeared to enhance HSV-1 mediated AAV2 DNA replication while RPA1 had no effect. Taken together, this study extends the list of host factors implicated in AAV vector transduction and AAV DNA replication and provides insight into a differential role of two components of the RPA complex.

**Key words:** adeno-associated virus (AAV), RNAi screen, recombinant (r) AAV vector, self-complementary (sc) AAV vector, replication protein A (RPA), herpes simplex virus type 1 (HSV-1)

## 1. Introduction

Adeno-associated virus 2 (AAV2) is the prototype member of the genus Dependoparvovirus within the *Parvoviridae*, a family of small, single-stranded (ss) DNA viruses. These viruses are powerful vectors in clinical gene therapy (Keeler et al., 2017). For productive replication AAV2 depends on the presence of a helper virus, such as herpes simplex virus type 1 (HSV-1), adenovirus 2 (AdV2) or human papillomavirus 16 (HPV-16) (Buller et al., 1981; Hoggan et al., 1966; Walz et al., 1997). In absence of the helper virus, AAV2 establishes a latent infection by maintaining its genome as an episome in the cell nucleus or by integrating it into the host cell genome, preferentially at a site termed AAVS1 on human chromosome 19 (Kotin et al., 1992; Kotin et al., 1991; Linden et al., 1996a; Linden et al., 1996b).

The AAV2 genome is a single-stranded DNA of 4.68 kb containing two clusters of genes, *rep* and *cap*, flanked by inverted terminal repeats (ITRs) of 145 nucleotides. The ITRs contain the viral origin of DNA replication and packaging signal. The *rep* genes encode four Rep isoforms, Rep40, Rep52, Rep68, and Rep78, due to alternative splicing and transcription from two different promoters, p5 and p19. The multifunctional Rep proteins are involved in diverse processes of the AAV2 life cycle, including DNA replication, regulation of gene expression, genome packaging, and genomic integration (Collaco et al., 2003; Im and Muzyczka, 1990; King, 2001; Smith and Kotin, 1998; Wu et al., 1999; Yoon-Robarts and Linden, 2003; Zhou et al., 1999). The *cap* genes are expressed from the p40 promoter and encode the VP1, VP2, and VP3 proteins, which differ in their N-termini due to alternative start codons; together they form an icosahedral capsid of 25 nm in diameter (Muzyczka and Berns, 2001). A nested open reading frame within the *cap* gene encodes the so called assembly-activating protein, which is believed to be required for AAV2 capsid assembly in the nucleolus (Sonntag et al., 2010).

The unique replication strategy of AAV2 is based on a rolling-hairpin mechanism in which the end of the 3'-ITR acts as primer for second-strand synthesis. The asymmetric leading-strand DNA synthesis results in a closed-end intermediate at the 3'-ITR. This structure is resolved by Rep68/78 which introduces a site- and strand-specific nick at the so called

terminal resolution signal (TRS), thereby creating a primer that allows completing the DNA replication process (Tattersall and Ward, 1976) (for a review see: (Muzyczka and Berns, 2001)).

Helper virus mediated AAV2 replication takes place in intranuclear replication compartments (RCs) that contain AAV2 DNA as well as viral and cellular proteins involved in AAV2 genome processing, including second-strand synthesis, transcription and DNA replication (Alazard-Dany et al., 2009; Cervelli et al., 2008; Fraefel et al., 2004; Franzoso et al., 2017; Glauser et al., 2005; Glauser et al., 2010; Glauser et al., 2007; Stracker et al., 2004; Weitzman et al., 1996). Proteomics and immunofluorescence analyses of cells co-infected with AAV2 and either AdV5 or HSV-1 revealed numerous cellular proteins that are recruited into AAV2 RCs or interact with Rep78 (Nash et al., 2009; Nicolas et al., 2010; Vogel et al., 2012) (for a review see: (Vogel et al., 2013)). Independent of the type of helper virus, the largest functional groups of cellular proteins recruited to AAV2 RCs belong to the DNA replication/repair machinery and transcription/RNA metabolism. While the majority of the cellular proteins in HSV-1 supported AAV2 RCs were found also in AdV5 supported AAV2 RCs, some proteins were associated with AAV2 RCs only in presence of either HSV-1 or AdV5.

The role of most of the cellular components of AAV2 RCs in AAV2 second-strand synthesis, transcription, and replication is not known. For example, replication protein A (RPA), a heterotrimeric single-stranded DNA binding protein complex composed of RPA1 (70 kDa), RPA2 (32 kDa) and RPA3 (14-kDa) subunits, is essential for cellular DNA replication, recombination and repair (for reviews see: (Fanning et al., 2006; Iftode et al., 1999; Stauffer and Chazin, 2004; Wold, 1997)). RPA is also required for the replication of simian virus 40 (SV40) DNA where it is involved in DNA unwinding in concert with the SV40 large T antigen (Fairman and Stillman, 1988; Ishimi et al., 1988; Wold and Kelly, 1988) (for reviews see: (Borowiec et al., 1990; Bullock, 1997; Fanning and Knippers, 1992)). While RPA has been identified as a component of AAV2 RCs and is known to interact with AAV2 Rep proteins (Nash et al., 2009; Nicolas et al., 2010; Nicolas et al., 2012; Stracker et al., 2004; Vogel et

al., 2012), studies to assess its requirement for AAV2 DNA replication yielded ambivalent results, depending on the assay (Nash et al., 2007; Nash et al., 2008; Nash et al., 2009; Ni et al., 1998; Ward et al., 1998).

Here, we performed a targeted image-based RNAi screen on a single cell level to investigate the effects of 62 cellular proteins previously identified as components of AAV2 RCs on the transduction efficiencies of ss and ds self-complementary (sc) AAV vectors. Targeted RNAi screens have previously been shown to be powerful exploratory tools for infectious agents, as well as in depth follow up studies (Prasad et al., 2014; Roulin et al., 2014; Snijder et al., 2012). The screen here was validated by confirming the posttranscriptional knockdown of selected genes and its consequence on vector transduction efficiency by reverse transcription quantitative PCR (RT-qPCR) and flow cytometry. Results showed that components of the MRN complex (MRE11-RAD50-NBS1) had the same effects on the transduction efficiency of ss and sc AAV2 vectors while other proteins, such as RPA1, had a differential effect on the transduction efficiency of the two different vectors. Specifically, the knock-down of RPA1 or RPA2 inhibited ss AAV vector transduction but enhanced sc AAV vector transduction. Interestingly however, only RPA2 but not RPA1 enhanced HSV-1 mediated AAV2 DNA replication.

## 2. RESULTS

### 2.1. Targeted RNAi screen identifies cellular proteins differentially affecting single-stranded and double-stranded AAV vector transduction

We designed an siRNA library of 62 genes previously identified to interact with the AAV2 genome either directly or via the AAV2 Rep proteins (Nash et al., 2009; Nicolas et al., 2010; Vogel et al., 2013; Vogel et al., 2012). HeLa cells were transfected with individual siRNAs (three independent siRNAs per gene; see Supplementary Table 1) for 48 h, inoculated with ss recombinant (r) or ds (sc) AAV vectors, rAAVGFPNeo or scAAVGFP, expressing EGFP from the human cytomegalovirus (CMV) IE1 enhancer/promoter for 24 h. Cells were stained

with Hoechst, and EGFP positive cells and cell nuclei were visualized by high-throughput microscopy to determine transduction efficiencies (Fig. 1, A-C). The screen was carried out in triplicate and for each siRNA means of the transduction fraction (number of EGFP positive cells divided by total number of cells) were determined and used for bioinformatical analyses as described in Materials and methods (see also (Carpenter et al., 2006; Ramo et al., 2014; Yakimovich et al., 2015; Yakimovich et al., 2012)). The results are shown as heat maps in Fig. 1C and can be summarized as follows: cellular proteins that have a negative effect on vector transduction (transduction rate increased upon siRNA knockdown) are at the top of the list, proteins that have a positive effect on vector transduction (transduction rate reduced upon knockdown) are listed at the bottom. Some cellular proteins were found to inhibit transduction, e.g. MRE11, NBN, RAD50, MSH3, PCNA, others, such as EEF1A1 were found to enhance transduction by both ss and sc AAV2 vectors. Yet other proteins were observed to enhance or inhibit transduction by one but not the other vector; for example, the knockdown of RFC2 inhibited the transduction by the ss AAV2 vector but had no effect on that of the sc AAV2 vector. An interesting group of proteins includes RPA1, MSH2, and MSH6, where siRNA knockdown led to opposite effects for ss and sc AAV2 vectors. For a selected set of proteins, including MSH2, MSH3, MSH6, RPA1, and RFC2, the post-transcriptional knockdown was confirmed (Supplementary Fig. 1) and the effect on transduction efficiency validated by RT-qPCR (Fig. 2).

**2.2. Ectopic expression of RPA1 or RPA2 inhibits transduction by ssAAV vectors.**

The influence of RPA1 on transduction by ss and sc AAV vectors was further investigated because it showed the most differential effect in the RNAi screen. We analyzed also the effect of RPA2 on AAV transduction. Cells were reverse transfected with siRNA, inoculated 48h later with rAAVGFPNeo or scAAVGFP, and analyzed at 24h after infection by flow cytometry to determine the percentage and the mean fluorescence intensities of EGFP-positive cells. As shown in Fig. 3, RPA1 and RPA2 both appear to significantly inhibit transduction by the ss AAV vector but enhance transduction by the sc AAV vector.

To validate the RPA1 and RPA2 effects, we first established an assay that allowed to specifically knock-down endogenous RPA1 and RPA2 and complement it with exogenous, plasmid encoded protein. In particular, we transfected cells first with siRNAs against the 5' untranslated region (utr) of the endogenous RPA1 or RPA2 transcripts and, 24h later, with expression plasmids encoding RPA1 or RPA2 cDNAs lacking the 5'utr (Fig. 4). At 24h after plasmid transfection, we performed RT-qPCR with primers specific for the coding sequences, which detect both endogenous and exogenous RPA1 and RPA2 transcripts, or primers specific for the 5'utr regions, which detect only the endogenous transcripts. Fig 4A shows that the relative RPA1 mRNA levels of cells treated with the 5'utr-specific siRNA significantly increased upon transfection of the RPA1 encoding plasmid when using the coding sequence-specific primers (graph on left) but not when using the 5'utr-specific primers (graph on right). This demonstrates that endogenous RPA1 is indeed knocked-down and that the increased RPA1 mRNA levels detected with the coding sequence-specific primers originate largely from the expression plasmid. Likewise, Fig. 4B shows that this assay can also differentiate between endogenous and exogenous RPA2.

We then determined transduction efficiencies of ss and sc AAV vectors. For this, cells were transfected with siRNAs and the expression plasmids as described above and infected 24h later with rAAVGFPNeo or scAAVGFP. At 24h after infection, the cells were processed for RT-qPCR to detect AAV vector-mediated EGFP expression (Fig. 5, A and B) or assessed by fluorescence microscopy (Fig. 5C). The increased rAAVGFPNeo-mediated EGFP expression levels observed upon knockdown of endogenous RPA1 or RPA2 were reversed to control levels when exogenous RPA1 or RPA2 was provided (Fig 5, A and C). Inversely, the reduced scAAVGFP-mediated EGFP expression levels upon knock-down of endogenous RPA1 or RPA2 were also reversed to control levels when exogenous RPA1 or RPA2 was provided (Fig. 5B). Similar results were obtained also when using flow cytometry to determine percentage and mean fluorescence intensities of EGFP-positive cells as read-out (Fig. 6). These results demonstrate that the differential effects of RPA1 and RPA2 on the transduction efficiencies of ss and sc AAV vectors are not due to an off-target effect.

We next designed an assay that allowed the direct monitoring of the differential effects of RPA1 and RPA2 on the transduction by ss and sc AAV vectors in co-infected cells. Specifically, cells were transfected with RPA1- or RPA2-specific siRNAs and with expression plasmids as described above and then co-infected with rAAVRFPNeo and scAAVCFP. The transduction efficiencies (mean fluorescence intensities) were determined by flow cytometry at 24h after infection to calculate the RFP/ECFP ratios. The results are shown in Fig. 7 and can be summarized as follows: The RFP/CFP (ssAAV/scAAV) ratios of the mean fluorescence intensities were increased up to 2-fold upon siRNA-mediated knock-down of RPA1 or RPA2, but were reversed to control levels (scr2 siRNA) in presence of exogenous RPA1 or RPA2 (Fig. 7).

### 2.3. RPA2 but not RPA1 appears to enhance AAV2 DNA replication.

To investigate the role of RPA1 and RPA2 in AAV2 DNA replication we used a variation of the assays described above. Specifically, cells were transfected with siRNAs and expression plasmids as described above and then infected with wtAAV2 or co-infected with wtAAV2 and wtHSV-1 as the helper virus. At 24h after infection, cells were processed for qPCR to quantify AAV2 DNA (Fig. 8A) or Southern blot (Fig. 8B). Interestingly, posttranscriptional knockdown of RPA2 but not RPA1 significantly inhibited AAV2 DNA replication. The effect of RPA2 knockdown was reversed upon expression of exogenous RPA2. We conclude that the RPA subunits RPA1 and RPA2 both affected AAV2 vector transduction, although the effects were differential for ss and sc vectors, whereas only RPA2 enhanced AAV2 DNA replication.

## 3. Discussion

AAV vectors are extensively used in gene therapy applications (Keeler et al., 2017). Nevertheless, a better understanding of their mechanisms of transduction is necessary to enhance their applicability. In this work we used a limited RNAi screening strategy to examine the effects of 62 known cellular components of AAV2 RCs on the transduction

efficiency of ss and ds (sc), EGFP-encoding AAV vectors on a single cell level. For validation of the RNAi screen, the knockdown of selected genes as well as the effect on the transduction efficiency was determined by RT-qPCR and flow cytometry. We found many cellular proteins, including MRE11, RAD50, PCNA, PRKDC (DNA-PKcs), MSH3, and SMC1A with a negative effect on the transduction efficiency of both ss and sc AAV vectors. MRE11, Rad50 and NBS1 together form the MRN complex which has previously been shown to inhibit the transduction efficiency of AAV vectors (Cervelli et al., 2008; Lentz and Samulski, 2015; Schwartz et al., 2007). Inhibition of gene expression was observed with both ss and sc AAV vectors and was described to depend on the physical interaction between the MRN complex and the vector genomes rather than on the nuclease activity of MRE11 (Lentz and Samulski, 2015).

We also found proteins, such as the eukaryotic translation elongation factor 1 alpha 1 (EEF1A1), which appear to enhance the transduction efficiencies of ss and sc AAV vectors. Other proteins had an apparent effect only on either ss or sc AAV vectors. For example, the knockdown of replication factor C subunit 2 (RFC2) and heterogeneous nuclear ribonucleoprotein D0 (HNRNPD) specifically augmented the transduction efficiency of ss AAV vectors.

Of all the proteins investigated, RPA1 showed the strongest differential effects on the transduction efficiency of ss and sc AAV vectors. While the knockdown of RPA1 lead to the largest increase in the transduction efficiency of the ss AAV vector, that of the sc AAV vector was strongly reduced. The same effect was observed also when treating the cells with siRNAs specific for RPA2 and was reversed upon delivery of plasmid encoded exogenous RPA1 or RPA2.

RPA1, RPA2 and RPA3 together form a heterotrimer which binds to ss DNA and plays essential roles in genome processing and maintenance (for a review see: (Fanning et al., 2006; Liu and Huang, 2016)). DNA binding is mediated mainly by RPA1, which contains three of the four ssDNA binding domains (DBD-A, -B, -C) (Brill and Bastin-Shanower, 1998; Wold and Kelly, 1988). RPA2 also contains a ssDNA binding domain (DBD-D) but may

nevertheless depend on RPA1 for efficient ssDNA binding (Bochkareva et al., 1998). As RPA has an approximately 1000-fold higher affinity for ssDNA than for dsDNA (Kim et al., 1994) and directly binds to ssDNA (Kenny et al., 1990), the differential effect on the transduction efficiency of ss and sc AAV vectors is not surprising. Moreover, as RPA is a protein complex, it was expected that the knock-down of either component RPA1 or RPA2 can affect the transduction efficiencies of the two different vectors.

More surprising was the observation that only RPA2 enhanced HSV-1 mediated AAV2 replication while RPA1 had no significant positive or negative effect on virus replication. Previous studies on the role of RPA in AAV2 replication showed contrasting results. For example, using a crude cytoplasmic extract of AdV-infected cells, Ni et al., (Ni et al., 1998) identified several cellular proteins involved in AAV2 DNA replication, including RPA, RFC, and PCNA. Moreover, Ward et al. (Ward et al., 1998) demonstrated that both the AdV DNA-binding protein (Ad-DBP) and the cellular RPA can enhance the processivity of AAV2 DNA replication. By contrast, Nash et al. (Nash et al., 2007) found that fractions of AdV-infected crude cell extracts that contained RFC and PCNA but not RPA can support AAV2 DNA replication. The minimal set of cellular proteins required for the reconstitution of efficient AAV2 DNA replication in vitro was subsequently found to include polymerase delta, RFC, PCNA, and the minichromosome maintenance (MCM) complex, but not RPA (Nash et al., 2008).

RPA may not be essential for AAV2 replication because the ssDNA binding proteins of the helper viruses, such as HSV-1 ICP8, which is required for AAV2 DNA replication (Alazard-Dany et al., 2009; Weindler and Heilbronn, 1991), can complement its activity. While our data indicate that at least RPA2 can enhance HSV-1 supported AAV2 DNA replication, it was rather unexpected that RPA1 did not show the same effect, although it forms a complex with RPA2 and although it is believed to be responsible for ssDNA binding. RPA has been shown to interact with the SV40 large T antigen and to be essential for viral DNA replication (Fairman and Stillman, 1988; Ishimi et al., 1988; Wold and Kelly, 1988) (for reviews see: (Borowiec et al., 1990; Bullock, 1997; Fanning and Knippers, 1992)). In particular, RPA1 has

been shown to be required for unwinding of SV40 DNA (Kenny et al., 1990) but not for the complete replication process, as a monoclonal antibody directed against RPA2 resulted in the inhibition of SV40 DNA replication (Erdile et al., 1991a; Erdile et al., 1991b). This provides evidence that the RPA2 activity is important for viral DNA replication and that the two subunits have differential functions. However, the divergent effects of RPA1 and RPA2 knockdown (or ectopic expression) on AAV2 replication may not be directly related to DNA binding or unwinding activities but rather to differential interactions with viral proteins, such as AAV Rep or HSV-1 ICP8, and cellular factors, e.g. RFC or components of the MRN complex. These interacting proteins are involved in DNA processing. A large number of different proteins bind to RPA (for reviews see: (Fanning et al., 2006; Iftode et al., 1999)). While some of these proteins, such as RAD9 or RAD52, can bind to both subunits, other proteins bind specifically to either RPA1 (e.g. P53, RFC, RAD51) or RPA2 (activation induced cytidine deaminase, Uracil-DNA glycosylase). These different activities could be regulated by DNA protein kinase or the ataxia telangiectasia-mutated (ATM) protein kinase, both of which target RPA (Iftode et al., 1999).

The mechanisms responsible for the observed differential requirement of RPA1 and RPA2 for AAV2 replication as well as for the apparent enhancement of the transduction efficiency of sc AAV vectors and inhibition of that of ss AAV vectors remain to be investigated. The present study nevertheless provides a useful strategy to screen the role of selected functional groups of proteins in specific phases of the viral life cycle and to validate the data by reversing the effects through ectopic expression of the corresponding genes. In particular, the observed differential effects of specific cellular proteins on vector transduction, depending on the conformation of the vector genome, may allow to draw conclusions concerning their involvement in specific viral genome processing steps, including second-strand synthesis and transcription.

## 4. Materials and Methods

**4.1. Cells.** HeLa cells (ATCC), 293T cells (kindly provided by J. Neidhardt, University of Zürich, Switzerland), and Vero cells (ECACC) were maintained in growth medium containing Dulbecco's modified Eagle medium (DMEM) supplemented with 10% fetal bovine serum (FBS), 100 units/ml penicillin G and 100 µg/ml streptomycin (1% AB) at 37°C in a 95% air-5% $CO_2$ atmosphere. For all infection experiments, virus and vectors were allowed to adsorb for 30min at 4°C and 1h at 37°C. The cells were then washed with phosphate-buffered saline (PBS) and incubated with DMEM containing 2% FBS and 1% AB at 37°C.

**4.2. Viruses and plasmids.** HSV-1 strain F (kindly provided by B. Roizman, Marjorie B. Kovler Viral Oncology Laboratories, University of Chicago, Chicago, USA) was grown and titrated on Vero cells. Wild-type (wt) AAV2 was grown and titrated as described previously (Lux et al., 2005). Plasmids pAAVGFPneo and pscAAVGFP containing the recombinant (r)AAVGFPNeo and self-complementary (sc)AAVGFP vectors were kindly provided by M. Linden (King's College London School of Medicine, London, UK) and J. Neidhardt (University of Zürich, Switzerland), respectively.

rAAVRFPNeo was constructed by replacing the EGFP coding sequence in plasmid pAAVGFPneo with the mRFP coding sequence as follows: pcDNA-mRFP1-N (kindly provided by M. Gastadelli, Institute of Molecular Life Sciences, University of Zurich, Switzerland) was digested with *Bam*HI and *Not*I, and the 711 bp fragment containing the mRFP coding sequence was ligated with the 6491 bp *Bam*HI-*Not*I fragment of pAAVGFPneo. The resulting plasmid was termed prAAVRFPNeo. scAAVCFP was constructed by replacing the EGFP coding sequence in plasmid pscAAVGFP with the ECFP coding sequence as follows: a DNA fragment containing the CMV enhancer/promoter-ECFP coding sequence was amplified by PCR from plasmid pCMVeCFP-PolyA (unpublished material) using forward (5'-AAGATATCACTAGTTAGTTATTAATAGTAATCAATTACG-3') and reverse (5'-CCGGTACCATGCAGTGAAAAAAATGC-3') primers (PCR conditions: 30 sec 98°C, 35x (10 sec 98°C, 45 sec 58°C, 60 sec 72°C), 10 min 72°C), digested with *Spe*I

and *Not*I, and ligated between the *Spe*I and *Not*I sites of pscAAVGFP. The resulting plasmid was termed pscAAVCFP. Transgene expression from all AAV vectors used in this study is controlled by the human cytomegalovirus IE1 enhancer/promoter (CMV promoter). AAV vector stocks were produced by transient transfection of 293T cells with pDG (Grimm et al., 1998) and either pAAVGFPNeo, pAAVRFPNeo, pscAAVGFP or pscAAVCFP. Virus stocks were purified by Iodixanol gradient, and titers were determined as described elsewhere (Grieger et al., 2006).

Plasmids encoding RPA1 (p11d-RPA70; (Haring et al., 2008)) and RPA2 (pERPA2wt; (Vassin et al., 2004)) were kindly provided by M. Wold (University of Iowa, Iowa, USA) and J.A. Borowiec (New York University School of Medicine, New York, USA), respectively. As empty vector control we used pUC19 (Clontech, Takara Bio USA, Inc).

**4.3. RNAi screening.** An siRNA library of 62 cellular genes with three independent siRNAs for each gene was designed and provided by Ambion (Silencer Select siRNAs from Thermo Fischer Scientific, Switzerland; see Supplementary Table 1). All experiments were conducted in 96-well tissue culture plates. For screening, the plates contained one of the three different siRNAs for the selected cellular genes and the following controls: KIF11 siRNA (transfection efficiency), two different scrambled siRNAs (scrambled 1, scrambled 2), no siRNA.

For transfection, 0.2 µl of Lipofectamine RNAiMAX and 13.8 µl OptiMEM (Life Technologies) mixture was added to each well of the screening plates containing 1.6 pmol siRNA diluted in 14 µl OptiMEM (final concentration 10nM). After incubation for 20min at room temperature (RT), $2.5x10^3$ HeLa cells in 80 µl DMEM/10% FBS were added per well. After 48h incubation at 37°C, the cells were infected with either rAAVGFPNeo (MOI 3000) or scAAVGFP (MOI 3000) in DMEM containing 2% FBS. At 24h after infection, the cells were fixed with paraformaldehyde (PFA; 4%) for 20min at RT and stained with Hoechst to visualize nuclei. Screening plates were sealed prior to imaging.

Numbers of cell nuclei and numbers of EGFP-positive cells were recorded by using an ImageXpress Micro or ImageXpress XL Micro High-Content Screening System (Molecular Devices, Sunnyvale, CA, USA) equipped with 10x Nikon Plan Fluor objectives with a 0.3 NA (2x binning) or 20x Nikon S Plan Fluor ELWD ADM with a 0.45 NA, respectively. Multiple wavelength acquisition was enabled through respective excitation/emission filter assemblies (Semrock). Images were further analyzed with CellProfiler software (BROAD Institute, Cambridge, MA, USA; (Carpenter et al., 2006)) and KNIME (KNIME.COM AG, Zurich Switzerland). Transduction rates from triplicate experiments $x_n{}^k{}_{1,2,3}$ ($n \in \{genes\}$, $k \in \{siRNAs\ 1, 2, 3\}$) and controls ($x_{scr1}{}^k{}_{1,2,3}$ , $x_{scr2}{}^k{}_{1,2,3}$ and $x_{no\_siRNA}{}^k{}_{1,2,3}$) were calculated by dividing the number of EGFP-positive cells by the number of cell nuclei. The mean $x_n{}^k$, $x_{scr1}{}^k$, $x_{scr2}{}^k$ and $x_{no\_siRNA}{}^k$ of each triplicate was calculated. The control transduction rate $x_{control}{}^k$ was calculated as mean of $x_{scr1}{}^k$, $x_{scr2}{}^k$ and $x_{no\_siRNA}{}^k$. Relative transduction rates for each gene and each siRNA was calculated by $X_n{}^k = [x_n{}^k - x_{control}{}^k]/x_{control}{}^k$.

**4.4. Transfection and infection experiments for quantitative PCR, flow cytometry and Southern analysis.** 1 µl Lipofectamine RNAiMAX in 99 µl OptiMEM was incubated for 5 min at RT and then added to each well of a 24 well plate containing 100 µl of an siRNA/OptiMEM mixture (final concentration 30 nM). Following incubation for 20min at RT, $6x10^4$ HeLa cells in 300 µl DMEM/10% were added per well. For some experiments, the cultures were transfected at 24h after siRNA transfection with empty vector DNA (pUC19) or expression plasmids encoding RPA1 or RPA2 (50 ng DNA, 5 µl Lipofectamine 2000; Invitrogen) according to the manufacturer's protocol. At 48h after siRNA transfection, the cells were infected with rAAV vectors, scAAV vectors, or wtAAV2 (MOI 3000) alone or in presence of wtHSV-1 (MOI 3) as described above and in the figure legends. At 72h after siRNA transfection, the cells were observed using a fluorescence microscope or processed for quantitative PCR, flow cytometry, or Southern analysis.

**4.5. Quantitative real-time PCR.** For quantifying AAV2 DNA, total DNA was isolated using the DNeasy Blood & Tissue Kit (Qiagen, Hilden, Germany) according to the manufacturer's protocol. AAV2 DNA was quantified by PCR using the cellular TERT gene as endogenous control (Applied Biosystems, Fostercity, CA, USA), primers and TaqMan probe specific for the AAV2 *rep78*-coding sequence (fw: 5'-ATTGACGGGAACTCAACGAC-3'; rev: 5'-CCTCAACCACGGATCCTTT-3'; TaqMan probe: 5'-CATGATCCAGACGGCGGGTGA-3'), and the following conditions: 2 min 50$^{o}$C, 15 min 95$^{o}$C, 40x (15 sec 94$^{o}$C, 30 sec 56$^{o}$C, 15 sec 72$^{o}$C).

For gene expression analysis, the cells were lysed with TRIZOL (Life Technologies), and total RNA was isolated and treated with DNAse using Direct-zol RNA kit (Zymo Research, Irvine, CA, USA), and reverse-transcribed with random hexamer primers (Promega, Madison, WI, USA) and the Reverse Transcription System kit from Promega. Quantitative PCR was performed using SYBR Green (Life Technologies) in a CFX96 Real-Time system (Bio-Rad, Hemel, UK) with primers specific for individual genes and GAPDH as internal control. Control reactions were performed without the reverse transcription step (not shown). The primer sequences were as follows (5'-3'):

EGFP forward (fw): CCG AGG TGA AGT TCG AGG

EGFP reverse (rev): GCC GTT CTT CTG CTT GTC

RPA1cs fw: GCAGAAGGGGGATACAAACA;

RPA1cs rev: CCGTAGTAATGGGACGGATG;

RPA1utr fw: ACTTCTCGGGCCAATAACTG;

RPA1utr rev: CTCCACCGCCAAGACTTC;

RPA2cs fw: GATTGGTTGATTTCTTGCGATA;

RPA2cs rev: CAAAACCCTCCGCACTAGC;

RPA2utr fw: AACCUAGUUUCACAAUCUGUUUU;

RPA2utr rev: AAAACAGAUUGUGAAACUAGGUU;

GAPDH fw: GAAGATGGTGATGGGATTTC;

GAPDH rev: GAAGGTGAAGGTCGGAGTC.

Results were normalized to GAPDH, and fold changes to the control (scr2) were calculated. Means from triplicate experiments with error bars showing standard error of the mean are shown.

**4.6. Flow cytometry.**

Cells were trypsinized and washed once with PBS. Flow cytometry was performed on a FACScalibur (Becton-Dickinson). A minimum of 40`0000 events was scored for each sample. The percentage and the mean fluorescence intensities of EGFP-positive cells was determined using Kaluza analysis software (Beckman Coulter, Inc., USA).

**4.7. Southern analysis**

Extrachromosomal DNA was extracted according to the protocol described by Hirt (Hirt, 1969). The DNA was separated on 1% agarose gels and transferred to nylon membranes (Amersham Hybond-N+ RPN119B). Hybridization with a digoxigenin (DIG)-labeled probe specific for AAV2 *rep78*, detection by an anti-DIG antibody conjugated with alkaline phosphatase, and activation with the chemiluminescence substrate CDP Star was performed according to the manufacturer's protocol (Roche, Mannheim, Germany). The DIG-labeled probe was produced with the PCR DIG probe synthesis kit (Roche) as follows: a 744-bp fragment within the *rep78* coding sequence was amplified using primers 5'-GAACGCGATATCGCAGCCGCCATGCCGGG-3' and 5'-GGATCCGAATTCACTGCTTCTCCGAGGTAATC-3'.

**4.8. Statistical analysis.** For the statistical analysis of the RNAi screening data, R statistical program was used. All the other data was statistically analyzed using Prism Software (GraphPad) using Grouped Analysis and multiple Student's *t*-tests.

**Acknowledgements**

We would like to thank J. Neidhardt, B. Roizman, M. Linden, M. Gastadelli, M. Wold, and J.A. Borowiec for providing reagents, A. Man and E. Yàngüez López-Cano for technical help, and S. Stertz, N. Wolfrum, M. Seyffert, S. Sutter and A. Meier for critical discussions. This work was supported by grants from the Swiss National Science Foundation, No. 31003A_144094/1 and No. 31003A_166668/1, to CF.

**References**

Alazard-Dany, N., Nicolas, A., Ploquin, A., Strasser, R., Greco, A., Epstein, A.L., Fraefel, C., Salvetti, A., 2009. Definition of herpes simplex virus type 1 helper activities for adeno-associated virus early replication events. PLoS Pathogens 5, e1000340.

Bochkareva, E., Frappier, L., Edwards, A.M., Bochkarev, A., 1998. The RPA32 subunit of human replication protein A contains a single-stranded DNA-binding domain. J Biol Chem 273, 3932-3936.

Borowiec, J.A., Dean, F.B., Bullock, P.A., Hurwitz, J., 1990. Binding and unwinding--how T antigen engages the SV40 origin of DNA replication. Cell 60, 181-184.

Brill, S.J., Bastin-Shanower, S., 1998. Identification and characterization of the fourth single-stranded-DNA binding domain of replication protein A. Mol Cell Biol 18, 7225-7234.

Buller, R.M., Janik, J.E., Sebring, E.D., Rose, J.A., 1981. Herpes simplex virus types 1 and 2 completely help adenovirus-associated virus replication. J. Virol. 40, 241-247.

Bullock, P.A., 1997. The initiation of simian virus 40 DNA replication in vitro. Crit Rev Biochem Mol Biol 32, 503-568.

Carpenter, A.E., Jones, T.R., Lamprecht, M.R., Clarke, C., Kang, I.H., Friman, O., Guertin, D.A., Chang, J.H., Lindquist, R.A., Moffat, J., Golland, P., Sabatini, D.M., 2006. CellProfiler: image analysis software for identifying and quantifying cell phenotypes. Genome Biol 7, R100.

Cervelli, T., Palacios, J.A., Zentilin, L., Mano, M., Schwartz, R.A., Weitzman, M.D., Giacca, M., 2008. Processing of recombinant AAV genomes occurs in specific nuclear structures that overlap with foci of DNA-damage-response proteins. Journal of cell science 121, 349-357.

Collaco, R.F., Kalman-Maltese, V., Smith, A.D., Dignam, J.D., Trempe, J.P., 2003. A biochemical characterization of the adeno-associated virus Rep40 helicase. J Biol Chem 278, 34011-34017.

Erdile, L.F., Collins, K.L., Russo, A., Simancek, P., Small, D., Umbricht, C., Virshup, D., Cheng, L., Randall, S., Weinberg, D., et al., 1991a. Initiation of SV40 DNA replication: mechanism and control. Cold Spring Harb Symp Quant Biol 56, 303-313.

Erdile, L.F., Heyer, W.D., Kolodner, R., Kelly, T.J., 1991b. Characterization of a cDNA encoding the 70-kDa single-stranded DNA-binding subunit of human replication protein A and the role of the protein in DNA replication. J Biol Chem 266, 12090-12098.

Fairman, M.P., Stillman, B., 1988. Cellular factors required for multiple stages of SV40 DNA replication in vitro. EMBO J 7, 1211-1218.

Fanning, E., Klimovich, V., Nager, A.R., 2006. A dynamic model for replication protein A (RPA) function in DNA processing pathways. Nucleic Acids Res 34, 4126-4137.

Fanning, E., Knippers, R., 1992. Structure and function of simian virus 40 large tumor antigen. Annu Rev Biochem 61, 55-85.

Fraefel, C., Bittermann, A.G., Bueler, H., Heid, I., Bachi, T., Ackermann, M., 2004. Spatial and temporal organization of adeno-associated virus DNA replication in live cells. J. Virol. 78, 389-398.

Franzoso, F.D., Seyffert, M., Vogel, R., Yakimovich, A., de Andrade Pereira, B., Meier, A.F., Sutter, S.O., Tobler, K., Vogt, B., Greber, U.F., Buning, H., Ackermann, M., Fraefel, C., 2017. Cell cycle-dependent expression of AAV2 Rep in HSV-1 co-infections gives rise to a mosaic of cells replicating either AAV2 or HSV-1. J Virol.

Glauser, D.L., Saydam, O., Balsiger, N.A., Heid, I., Linden, R.M., Ackermann, M., Fraefel, C., 2005. Four-dimensional visualization of the simultaneous activity of alternative adeno-associated virus replication origins. J. Virol. 79, 12218-12230.

Glauser, D.L., Seyffert, M., Strasser, R., Franchini, M., Laimbacher, A.S., Dresch, C., Oliveira, A.P.d., Vogel, R., Büning, H., Salvetti, A., Ackermann, M., Fraefel, C., 2010. Inhibition of herpes simplex virus type 1 replication by adeno-associated virus rep proteins depends on their combined DNA-binding and ATPase/helicase activities. J. Virol. 84, 3808-3824.

Glauser, D.L., Strasser, R., Laimbacher, A.S., Saydam, O., Clément, N., Linden, R.M., Ackermann, M., Fraefel, C., 2007. Live covisualization of competing adeno-associated virus and herpes simplex virus type 1 DNA replication: molecular mechanisms of interaction. J. Virol. 81, 4732-4743.

Grieger, J.C., Choi, V.W., Samulski, R.J., 2006. Production and characterization of adeno-associated viral vectors. Nat Protoc 1, 1412-1428.

Grimm, D., Kern, A., Rittner, K., Kleinschmidt, J.A., 1998. Novel tools for production and purification of recombinant adenoassociated virus vectors. Human Gene Therapy 9, 2745-2760.

Haring, S.J., Mason, A.C., Binz, S.K., Wold, M.S., 2008. Cellular functions of human RPA1. Multiple roles of domains in replication, repair, and checkpoints. J Biol Chem 283, 19095-19111.

Hirt, B., 1969. Replicating molecules of polyoma virus DNA. Journal of Molecular Biology 40, 141-144.

Hoggan, M.D., Blacklow, N.R., Rowe, W.P., 1966. Studies of small DNA viruses found in various adenovirus preparations: physical, biological, and immunological characteristics. Proceedings of the National Academy of Sciences of the United States of America 55, 1467-1474.

Iftode, C., Daniely, Y., Borowiec, J.A., 1999. Replication protein A (RPA): the eukaryotic SSB. Crit Rev Biochem Mol Biol 34, 141-180.

Im, D.S., Muzyczka, N., 1990. The AAV origin binding protein Rep68 is an ATP-dependent site-specific endonuclease with DNA helicase activity. Cell 61, 447-457.

Ishimi, Y., Claude, A., Bullock, P., Hurwitz, J., 1988. Complete enzymatic synthesis of DNA containing the SV40 origin of replication. J Biol Chem 263, 19723-19733.

Keeler, A.M., ElMallah, M.K., Flotte, T.R., 2017. Gene Therapy 2017: Progress and Future Directions. Clin Transl Sci.

Kenny, M.K., Schlegel, U., Furneaux, H., Hurwitz, J., 1990. The role of human single-stranded DNA binding protein and its individual subunits in simian virus 40 DNA replication. J Biol Chem 265, 7693-7700.

Kim, C., Paulus, B.F., Wold, M.S., 1994. Interactions of human replication protein A with oligonucleotides. Biochemistry 33, 14197-14206.

King, J.A., 2001. DNA helicase-mediated packaging of adeno-associated virus type 2 genomes into preformed capsids. The EMBO Journal 20, 3282-3291.

Kotin, R.M., Linden, R.M., Berns, K.I., 1992. Characterization of a preferred site on human chromosome 19q for integration of adeno-associated virus DNA by non-homologous recombination. EMBO Journal 11, 5071-5078.

Kotin, R.M., Menninger, J.C., Ward, D.C., Berns, K.I., 1991. Mapping and direct visualization of a region-specific viral DNA integration site on chromosome 19q13-qter. Genomics 10, 831-834.

Lentz, T.B., Samulski, R.J., 2015. Insight into the mechanism of inhibition of adeno-associated virus by the Mre11/Rad50/Nbs1 complex. J Virol 89, 181-194.

Linden, R.M., Ward, P., Giraud, C., Winocour, E., Berns, K.I., 1996a. Site-specific integration by adeno-associated virus. Proceedings of the National Academy of Sciences of the United States of America 93, 11288-11294.

Linden, R.M., Winocour, E., Berns, K.I., 1996b. The recombination signals for adeno-associated virus site-specific integration. Proceedings of the National Academy of Sciences of the United States of America 93, 7966-7972.

Liu, T., Huang, J., 2016. Replication protein A and more: single-stranded DNA-binding proteins in eukaryotic cells. Acta Biochim Biophys Sin (Shanghai) 48, 665-670.

Lux, K., Goerlitz, N., Schlemminger, S., Perabo, L., Goldnau, D., Endell, J., Leike, K., Kofler, D.M., Finke, S., Hallek, M., Buning, H., 2005. Green fluorescent protein-tagged adeno-associated virus particles allow the study of cytosolic and nuclear trafficking. J. Virol. 79, 11776-11787.

Muzyczka, N., Berns, K.I., 2001. Parvoviridae: The viruses and their replication. Fields Virology 2, 2327-2346.

Nash, K., Chen, W., McDonald, W.F., Zhou, X., Muzyczka, N., 2007. Purification of host cell enzymes involved in adeno-associated virus DNA replication. J. Virol. 81, 5777-5787.

Nash, K., Chen, W., Muzyczka, N., 2008. Complete in vitro reconstitution of adeno-associated virus DNA replication requires the minichromosome maintenance complex proteins. J. Virol. 82, 1458-1464.

Nash, K., Chen, W., Salganik, M., Muzyczka, N., 2009. Identification of cellular proteins that interact with the adeno-associated virus rep protein. J Virol 83, 454-469.

Ni, T.H., McDonald, W.F., Zolotukhin, I., Melendy, T., Waga, S., Stillman, B., Muzyczka, N., 1998. Cellular proteins required for adeno-associated virus DNA replication in the absence of adenovirus coinfection. J. Virol. 72, 2777-2787.

Nicolas, A., Alazard-Dany, N., Biollay, C., Arata, L., Jolinon, N., Kuhn, L., Ferro, M., Weller, S.K., Epstein, A.L., Salvetti, A., Greco, A., 2010. Identification of Rep-Associated Factors in Herpes Simplex Virus Type 1-Induced Adeno-Associated Virus Type 2 Replication Compartments. J. Virol. 84, 8871-8887.

Nicolas, A., Jolinon, N., Alazard-Dany, N., Barateau, V., Epstein, A.L., Greco, A., Büning, H., Salvetti, A., 2012. Factors influencing helper-independent adeno-associated virus replication. Virology 432, 1-9.

Prasad, V., Suomalainen, M., Pennauer, M., Yakimovich, A., Andriasyan, V., Hemmi, S., Greber, U.F., 2014. Chemical induction of unfolded protein response enhances cancer cell killing through lytic virus infection. J Virol 88, 13086-13098.

Ramo, P., Drewek, A., Arrieumerlou, C., Beerenwinkel, N., Ben-Tekaya, H., Cardel, B., Casanova, A., Conde-Alvarez, R., Cossart, P., Csucs, G., Eicher, S., Emmenlauer, M., Greber, U., Hardt, W.D., Helenius, A., Kasper, C., Kaufmann, A., Kreibich, S., Kuhbacher, A., Kunszt, P., Low, S.H., Mercer, J., Mudrak, D., Muntwiler, S., Pelkmans, L., Pizarro-Cerda, J., Podvinec, M., Pujadas, E., Rinn, B., Rouilly, V., Schmich, F., Siebourg-Polster, J., Snijder, B., Stebler, M., Studer, G., Szczurek, E., Truttmann, M., von Mering, C., Vonderheit, A., Yakimovich, A., Buhlmann, P., Dehio, C., 2014. Simultaneous analysis of large-scale RNAi screens for pathogen entry. BMC Genomics 15, 1162.

Roulin, P.S., Lotzerich, M., Torta, F., Tanner, L.B., van Kuppeveld, F.J., Wenk, M.R., Greber, U.F., 2014. Rhinovirus uses a phosphatidylinositol 4-phosphate/cholesterol counter-current for the formation of replication compartments at the ER-Golgi interface. Cell Host Microbe 16, 677-690.

Schwartz, R.A., Palacios, J.A., Cassell, G.D., Adam, S., Giacca, M., Weitzman, M.D., 2007. The Mre11/Rad50/Nbs1 complex limits adeno-associated virus transduction and replication. J. Virol. 81, 12936-12945.

Smith, R.H., Kotin, R.M., 1998. The Rep52 gene product of adeno-associated virus is a DNA helicase with 3'-to-5' polarity. J Virol 72, 4874-4881.

Snijder, B., Sacher, R., Ramo, P., Liberali, P., Mench, K., Wolfrum, N., Burleigh, L., Scott, C.C., Verheije, M.H., Mercer, J., Moese, S., Heger, T., Theusner, K., Jurgeit, A., Lamparter, D., Balistreri, G., Schelhaas, M., De Haan, C.A., Marjomaki, V., Hyypia, T., Rottier, P.J., Sodeik, B., Marsh, M., Gruenberg, J., Amara, A., Greber, U., Helenius, A., Pelkmans, L., 2012. Single-cell analysis of population context advances RNAi screening at multiple levels. Mol Syst Biol 8, 579.

Sonntag, F., Schmidt, K., Kleinschmidt, J.A., 2010. A viral assembly factor promotes AAV2 capsid formation in the nucleolus. Proceedings of the National Academy of Sciences of the United States of America 107, 10220-10225.

Stauffer, M.E., Chazin, W.J., 2004. Physical interaction between replication protein A and Rad51 promotes exchange on single-stranded DNA. J Biol Chem 279, 25638-25645.

Stracker, T.H., Cassell, G.D., Ward, P., Loo, Y.M., van Breukelen, B., Carrington-Lawrence, S.D., Hamatake, R.K., van der Vliet, P.C., Weller, S.K., Melendy, T., Weitzman, M.D., 2004. The Rep protein of adeno-associated virus type 2 interacts with single-stranded DNA-binding proteins that enhance viral replication. J. Virol. 78, 441-453.

Tattersall, P., Ward, D.C., 1976. Rolling hairpin model for replication of parvovirus and linear chromosomal DNA. Nature 263, 106-109.

Vassin, V.M., Wold, M.S., Borowiec, J.A., 2004. Replication protein A (RPA) phosphorylation prevents RPA association with replication centers. Mol Cell Biol 24, 1930-1943.

Vogel, R., Seyffert, M., Pereira Bde, A., Fraefel, C., 2013. Viral and Cellular Components of AAV2 Replication Compartments. Open Virol J 7, 98-120.

Vogel, R., Seyffert, M., Strasser, R., de Oliveira, A.P., Dresch, C., Glauser, D.L., Jolinon, N., Salvetti, A., Weitzman, M.D., Ackermann, M., Fraefel, C., 2012. Adeno-associated virus type 2 modulates the host DNA damage response induced by herpes simplex virus 1 during coinfection. J Virol 86, 143-155.

Walz, C., Deprez, A., Dupressoir, T., Dürst, M., Rabreau, M., Schlehofer, J.R., 1997. Interaction of human papillomavirus type 16 and adeno-associated virus type 2 co-infecting human cervical epithelium. J Gen Virol 78 ( Pt 6), 1441-1452.

Ward, P., Dean, F.B., O'Donnell, M.E., Berns, K.I., 1998. Role of the adenovirus DNA-binding protein in in vitro adeno-associated virus DNA replication. J. Virol. 72, 420-427.

Weindler, F.W., Heilbronn, R., 1991. A subset of herpes simplex virus replication genes provides helper functions for productive adeno-associated virus replication. J. Virol. 65, 2476-2483.

Weitzman, M.D., Fisher, K.J., Wilson, J.M., 1996. Recruitment of wild-type and recombinant adeno-associated virus into adenovirus replication centers. J. Virol. 70, 1845-1854.

Wold, M.S., 1997. Replication protein A: a heterotrimeric, single-stranded DNA-binding protein required for eukaryotic DNA metabolism. Annu Rev Biochem 66, 61-92.

Wold, M.S., Kelly, T., 1988. Purification and characterization of replication protein A, a cellular protein required for in vitro replication of simian virus 40 DNA. Proc Natl Acad Sci U S A 85, 2523-2527.

Wu, J., Davis, M.D., Owens, R.A., 1999. Factors affecting the terminal resolution site endonuclease, helicase, and ATPase activities of adeno-associated virus type 2 Rep proteins. J. Virol. 73, 8235-8244.

Yakimovich, A., Andriasyan, V., Witte, R., Wang, I.H., Prasad, V., Suomalainen, M., Greber, U.F., 2015. Plaque2.0-A High-Throughput Analysis Framework to Score Virus-Cell Transmission and Clonal Cell Expansion. PLoS One 10, e0138760.

Yakimovich, A., Gumpert, H., Burckhardt, C.J., Lutschg, V.A., Jurgeit, A., Sbalzarini, I.F., Greber, U.F., 2012. Cell-free transmission of human adenovirus by passive mass transfer in cell culture simulated in a computer model. J Virol 86, 10123-10137.

Yoon-Robarts, M., Linden, R.M., 2003. Identification of active site residues of the adeno-associated virus type 2 Rep endonuclease. Journal of Biological Chemistry 278, 4912-4918.

Zhou, X., Zolotukhin, I., Im, D.S., Muzyczka, N., 1999. Biochemical characterization of adeno-associated virus rep68 DNA helicase and ATPase activities. J. Virol. 73, 1580-1590.

**Figure Legends**

**Fig. 1. RNAi screening determines the differential effects of selected cellular genes on the transduction efficiencies of single-stranded (ss) and double-stranded (ds) self-complementary (sc) AAV vectors**. HeLa cells were treated with siRNAs targeting 62 cellular genes (3 different siRNAs per gene) or, as control, scrambled siRNAs or no siRNA. After 48h, the cultures were mock-infected or infected with either rAAVGFPNeo (MOI 3000) or scAAVGFP (MOI 3000) and, 24h later, subjected to high throughput widefield microscopy to determine transduction rates $x_n^k$ ($n \in$ {genes}, $k \in$ {siRNAs 1, 2, 3}) and $x_{control}$ (mean of $x_{scr1}$ , $x_{scr2}$ and $x_{no\ siRNA}$) and to calculate the relative transduction rates $X_n^k$ ($[x_n-x_{control}]/x_{control}$). (A) Primary screening workflow. (B) Representative high throughput widefield microscopy images of cells transfected with scrambled siRNA or siRNAs targeting RFC2, RPA1, or MSH6 at 24h after infection with rAAVGFPNeo. EGFP-fluorescent cells and total cell nuclei (Hoechst staining) are shown. Scale bar = 100 µm (C) Heat maps representing the relative transduction rates $X_n^k$ of the RNAi screening results. The order of the genes listed on the left and right is based on the median values of the relative transduction rates from the three gene-specific siRNAs. The weight and intensity of the grayscale of the connection lines between the genes reflect the order of the differential effects that the individual genes have on transduction by rAAVGFPNeo and scAAVGFP.

**Fig. 2. Validation of the RNAi screening results by reverse transcription quantitative PCR (RT-qPCR).** HeLa cells were treated with siRNAs targeting individual genes selected from the primary screen (MSH2, MSH3, MSH6, RPA1, RFC2; pools of three different siRNAs) or scrambled siRNA (scr2). After 48h, the cells were infected with (A) rAAVGFPNeo (MOI 3000) or (B) scAAVGFP (MOI 3000). At 24h after infection, total RNA was isolated and subjected to RT-qPCR with primers specific for EGFP and GAPDH (internal control). Relative EGFP/GAPDH mRNA levels of each sample normalized to scr2 siRNA are shown

as means from triplicate experiments. Error bars show standard deviations of the mean. *P<0.05, ***P<0.001.

**Fig. 3. Effects of RPA1 and RPA2 on the transduction efficiencies of ssAAV and scAAV vectors**. HeLa cells were treated with scrambled siRNA (scr2) or siRNAs targeting the coding sequences (cs) of RPA1 or RPA2, or left untreated (-). After 48h, the cells were mock-infected (-) or infected (+) with either (A) rAAVGFPNeo (MOI 3000) or (B) scAAVGFP (MOI 3000). At 24h after infection, the cells were harvested and subjected to flow cytometry to determine the percentage of EGFP positive cells (left panels) and mean fluorescence intensities (right panels). 40'000 events (cells) per sample were counted. The data represent mean values from triplicate experiments. Error bars show standard deviations of the mean. *P<0.05, **P<0.01, ***P<0.001.

**Fig. 4. Rescue of RPA knockdown by exogenous RPA**. HeLa cells were treated with scrambled siRNA (scr2) or siRNAs targeting the 5' untranslated region (utr) of either RPA1 (A) or RPA2 (B) and, 24h later, transfected with an empty vector (ev) or plasmids encoding either RPA1 (A) or RPA2 (B). After 24h, total RNA was isolated and subjected to RT-qPCR with primers specific for detection of transcription from either exogenous (coding sequence primers, cs; left panels) or endogenous (5'utr primers, right panel) RPA 1 and RPA2. GAPDH was used as internal control and the relative mRNA levels (RPA1/GAPDH, RPA2/GAPDH) normalized to scr2 siRNA are shown as means from triplicate experiments. Error bars show standard deviations of the mean. *P<0.05, ***P<0.001.

**Fig. 5. Exogenous RPA1 and RPA2 block transduction by ssAAV vectors: RT-qPCR and fluorescence microscopy**. HeLa cells were treated with scrambled siRNA (scr2) or siRNAs targeting the 5'utr of either RPA1 or RPA2. After 24h, the cells were transfected with an empty vector (ev) or plasmids encoding either RPA1 or RPA2 and, 24h later, infected with either (A) rAAVGFPNeo (MOI 3000) or (B) scAAVGFP (MOI 3000). At 24h after

infection, total RNA was isolated and subjected to RT-qPCR with primers specific for EGFP and GAPDH (internal control). EGFP/GAPDH mRNA levels of each sample normalized to scr2 siRNA is shown as means from triplicate experiments. Error bars show standard deviations of the mean. **P<0.01, ***P<0.001. (C) Representative photomicrographs of rAAVGFPNeo infected cells transfected with siRNAs and expression plasmid as indicated. Scale bar = 100 µm.

**Fig. 6. Exogenous RPA1 and RPA2 block transduction by ssAAV vectors: flow cytometry**. HeLa cells were treated with scrambled siRNA (scr2) or siRNAs targeting the 5'utr of either RPA1 or RPA2. After 24h, the cells were transfected with plasmids encoding either RPA1 or RPA2 or an empty vector (ev) and, 24h later, infected with either (A) rAAVGFPNeo (MOI 3000) or (B) scAAVGFP (MOI 3000). At 24h after infection, the cells were harvested and subjected to flow cytometry to determine the percentage of EGFP positive cells (left panels) and mean fluorescence intensities (right panels). 40'000 events (cells) per sample were counted. The data represent mean values from triplicate experiments. Error bars show standard deviations of the mean. **P<0.01, ***P<0.001.

**Fig. 7. Effects of RPA1 and RPA2 on the transduction efficiencies of ssAAV and scAAV vectors in co-infected cells.** HeLa cells were treated with scrambled siRNA (scr2) or siRNAs targeting the 5'utr of either RPA1 or RPA2. After 24h, the cells were transfected with an empty vector (ev) or plasmids encoding either RPA1 or RPA2 and, 24h later, co-infected with rAAVRFPNeo (MOI 3000) and scAAVCFP (MOI 3000). At 24h after infection, the cells were harvested and subjected to flow cytometry to determine RFP and ECFP mean fluorescence intensities. 40'000 events (cells) per sample were counted. The data represent ratios of mean fluorescence intensities (RFP/ECFP), normalized to the RFP/ECFP ratios of cells transfected with scr2 siRNA and empty vector, from triplicate experiments. Error bars show standard deviations of the mean. ***P<0.001.

**Fig. 8. Effects of RPA1 and RPA2 on AAV2 DNA synthesis**. HeLa cells were treated with scrambled siRNA (scr2) or siRNAs targeting the 5'utr of either RPA1 or RPA2. After 24h, the cells were transfected with an empty vector (ev) or plasmids encoding either RPA1 or RPA2 and, 24h later, infected with wtAAV2 alone (MOI 3000) or co-infected with wtAAV2 (MOI 3000) and wtHSV-1 (MOI 3). At 24h after infection, total DNA was isolated and subjected to quantitative PCR with primers specific for AAV2 *rep78* or TERT (endogenous control). The graph in (A) shows relative AAV2 DNA/TERT DNA levels as means from triplicate experiments, normalized to co-infected cells transfected with scr2 siRNA and empty vector. Error bars show standard deviations of the mean. *P<0.05. (B) Hirt DNA prepared from parallel cultures was subjected to Southern analysis with a *rep78* specific probe (ss=single stranded, rfm=replication form monomer, rfd=replication form dimer).

**Supplementary Fig. 1. Efficiency of siRNA knockdown**. HeLa cells were treated with siRNAs targeting individual genes selected from the primary screen (MSH2, MSH3, MSH6, RPA1, RFC2; three different siRNAs each) or scrambled siRNA (scr2). After 48h, the cells were lysed with TRIZOL (Life Technologies), and total RNA was isolated and treated with DNAse using Direct-zol RNA kit (Zymo Research, Irvine, CA, USA), and reverse-transcribed using random primers (Promega, Madison, WI, USA) and the Reverse Transcription System kit from Promega. Real-time quantitative PCR was performed using SYBR Green (Life Technologies) in a CFX96 Real-Time system (Bio-Rad, Hemel, UK) with primers specific for the individual genes and GAPDH as internal control. The primer sequences were as follows (5'-3'):

MSH2 fw: GCTTCGTGCGCTTCTTTCAG;

MSH2 rev: CAGATTCTTTGCTCCTGCCG;

MSH3-fw: GGCAACTCTGAGCCAAAGAAATG;

MSH3 rev: GAGGAAGGGCAGAATCGCAG;

MSH6 fw: ACTGAGAGCAATGCAACGTG;

MSH6 rev: AAGTTGTGCCTACCTCCATCTC;

RPA1 forward (fw): GCAGAAGGGGGATACAAACA;

RPA1 reverse (rev): CCGTAGTAATGGGACGGATG;

RFC2 fw: TACGAACTGCCGTGGGTTG;

RFC2 rev: AGGGCCCGCAATGATGATG;

GAPDH fw: GAAGATGGTGATGGGATTTC;

GAPDH rev: GAAGGTGAAGGTCGGAGTC.

Results were normalized to GAPDH, and fold changes to the control (scr2) were calculated. Means from triplicate experiments with error bars showing standard deviations of the mean are shown. ***P<0.001.

**Figure 1**

Click here to download Figure: Franzoso et al. Fig. 1.pdf

**Franzoso et al., Fig. 1**

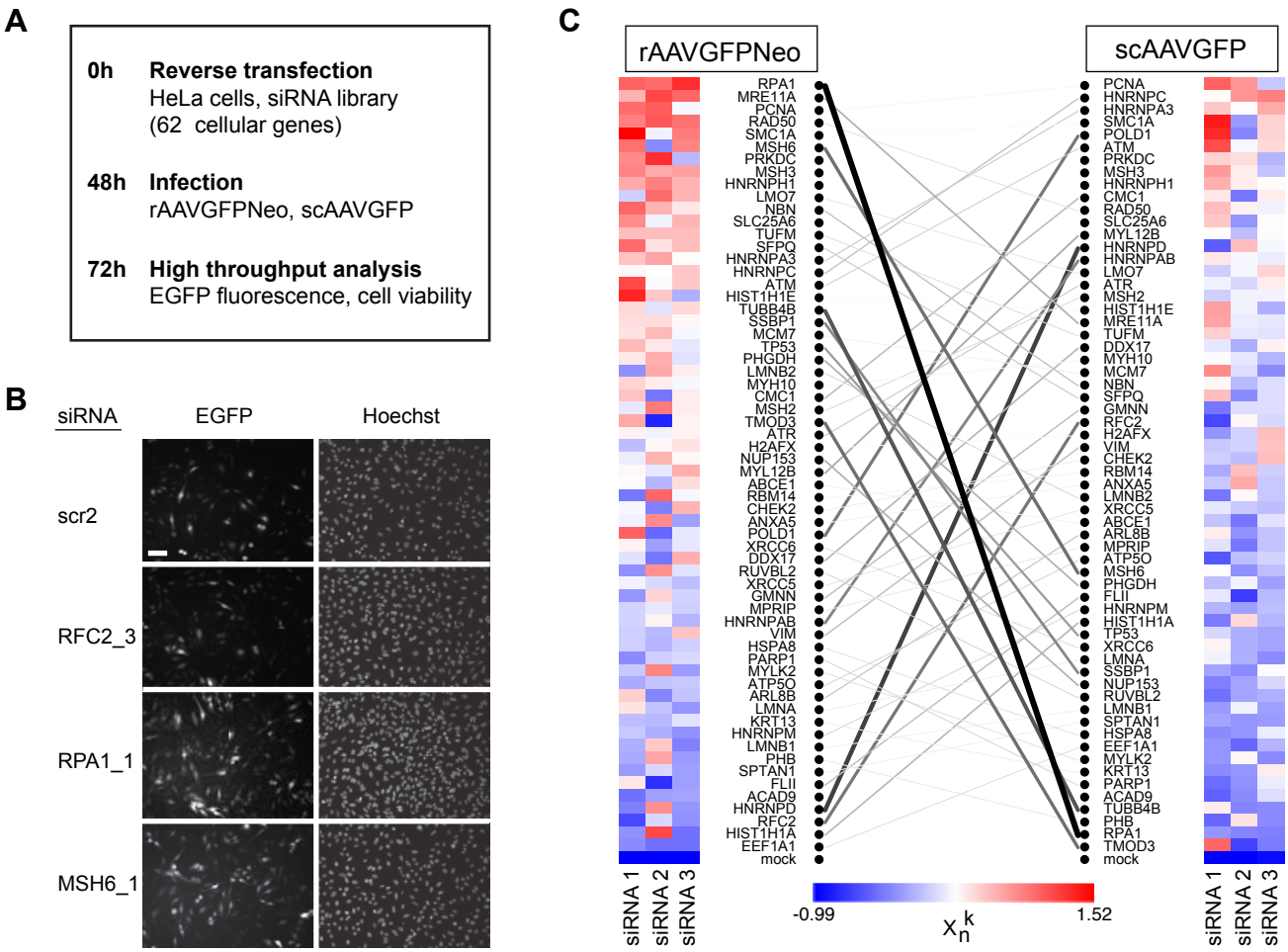

**Figure 2**

Click here to download Figure: Franzoso et al. Fig. 2.pdf

**Franzoso et al., Fig. 2**

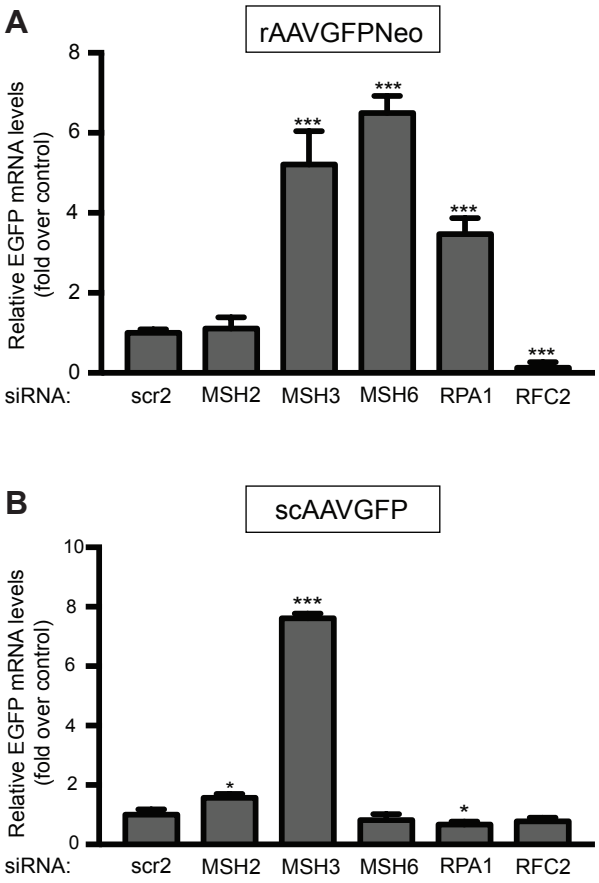

**Figure 3**

Click here to download Figure: Franzoso et al. Fig. 3.pdf

**Franzoso et al., Fig. 3**

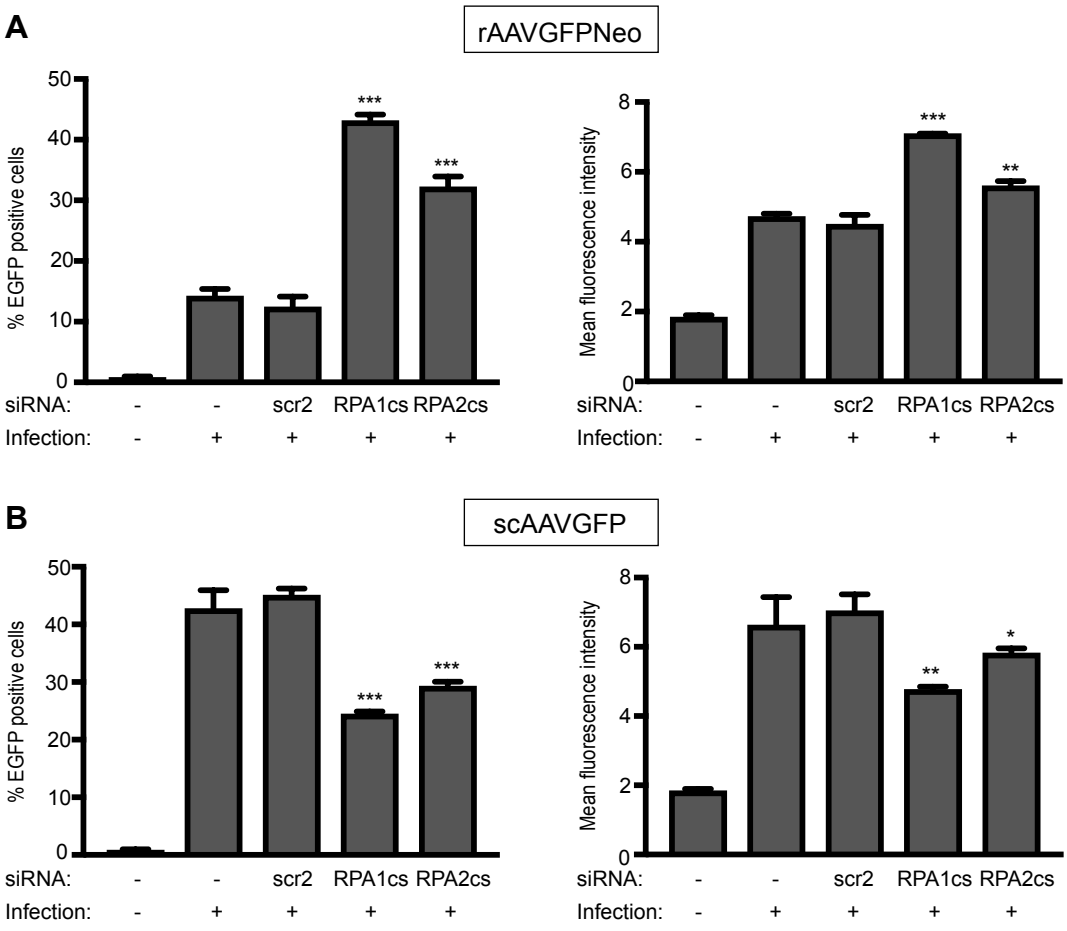

**Figure 4**

Click here to download Figure: Franzoso et al. Fig. 4.pdf

**Franzoso et al., Fig. 4**

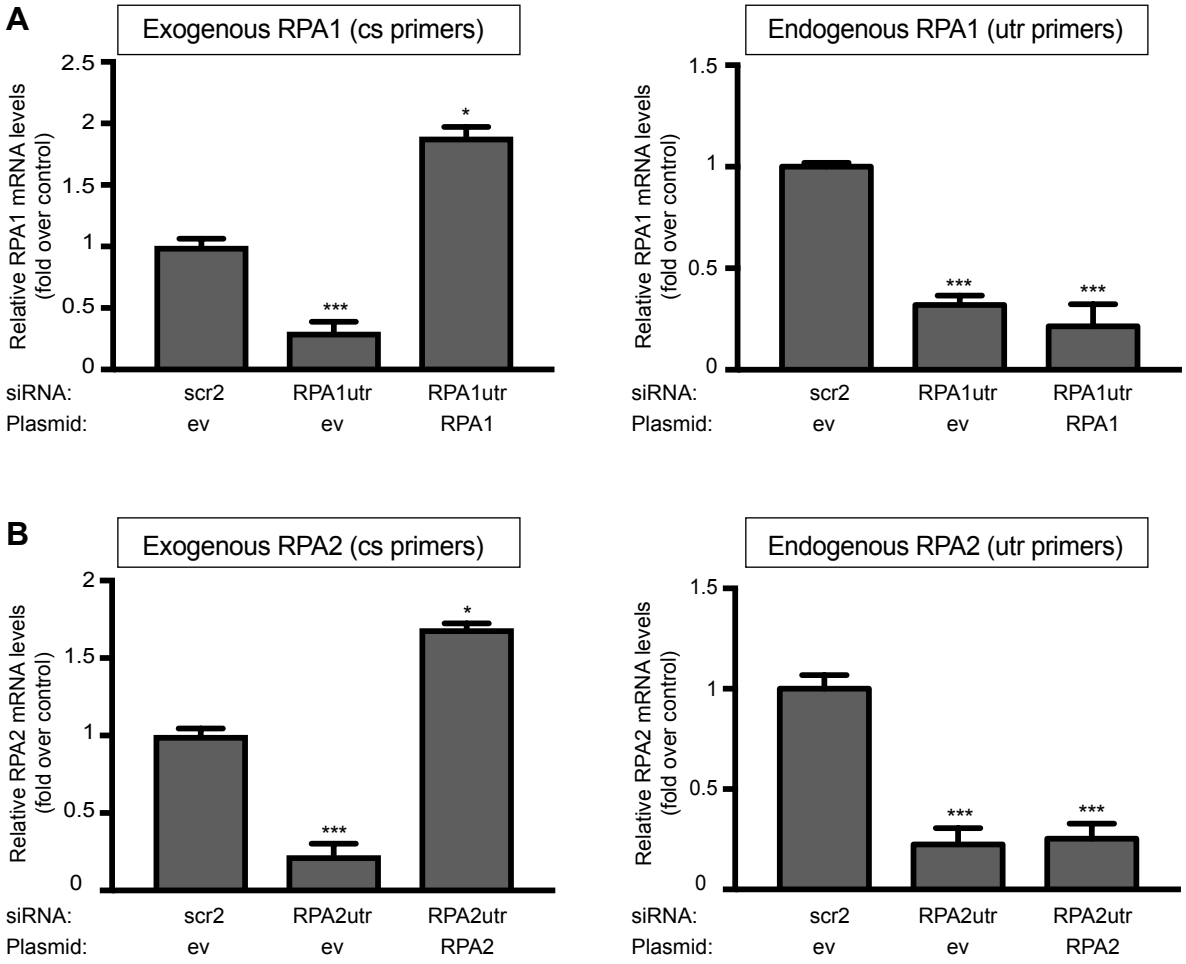

**Figure 5**

Click here to download Figure: Franzoso et al. Fig. 5.pdf

**Franzoso et al., Fig. 5**

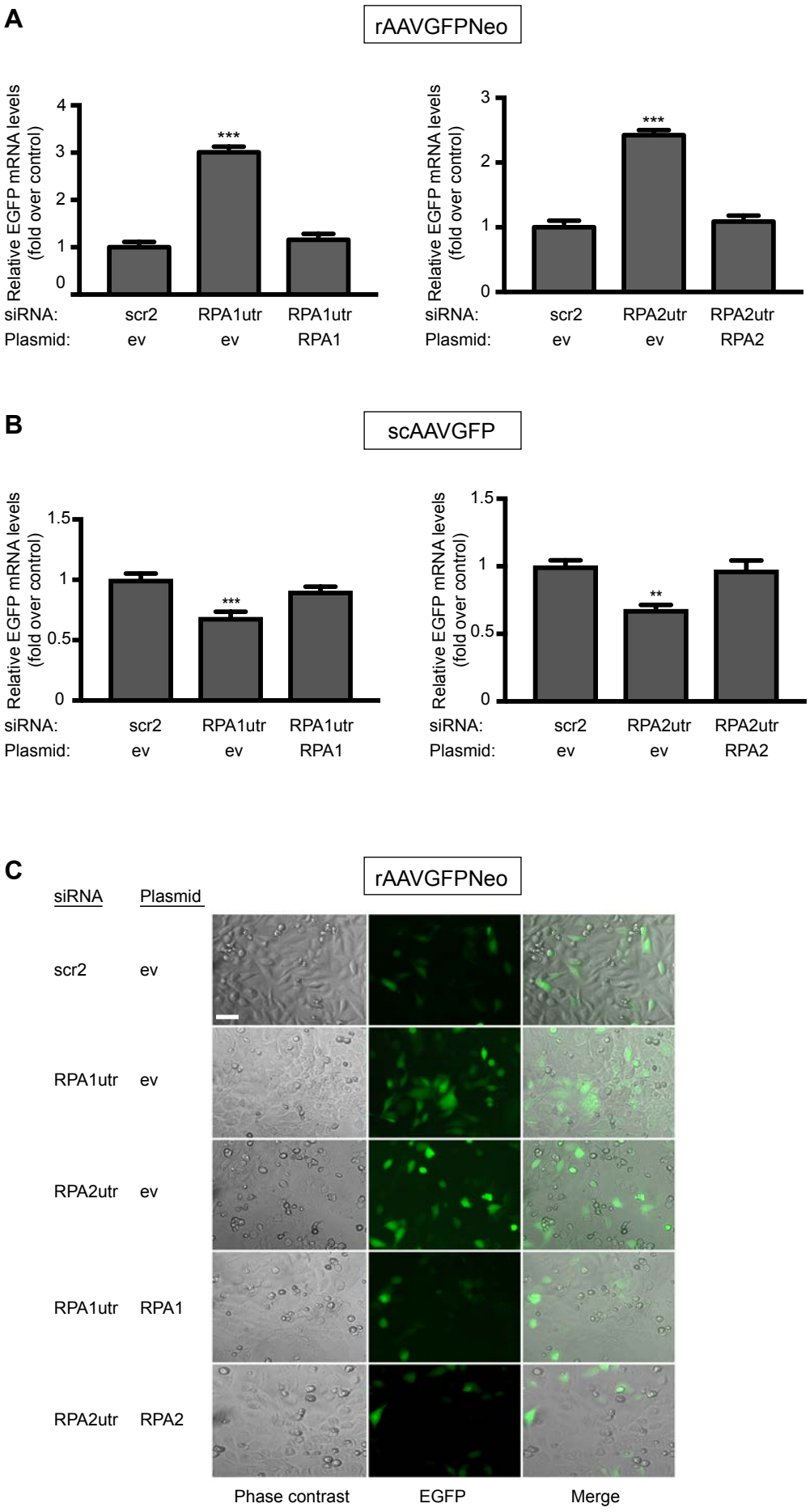

Figure 6

Click here to download Figure: Franzoso et al. Fig. 6.pdf

Franzoso et al., Fig. 6

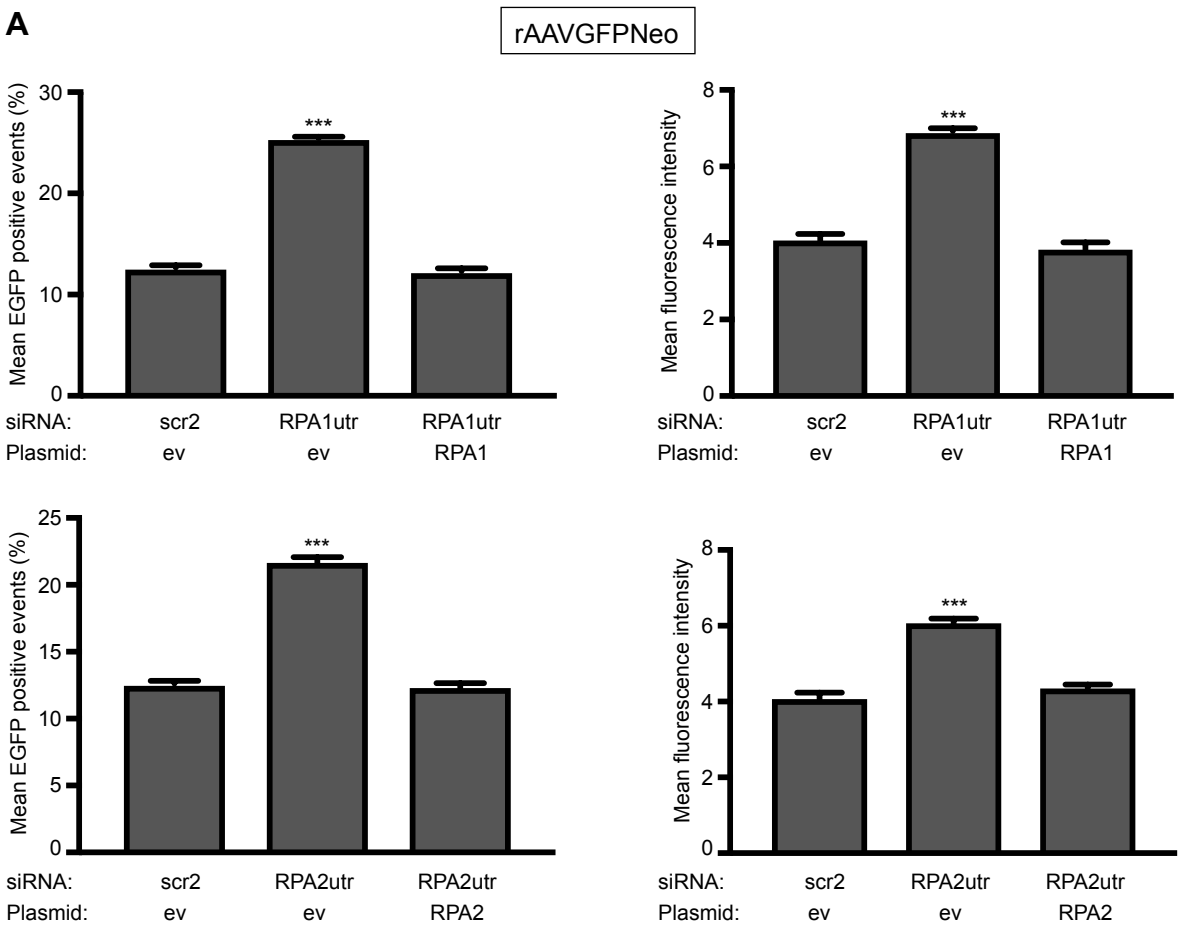


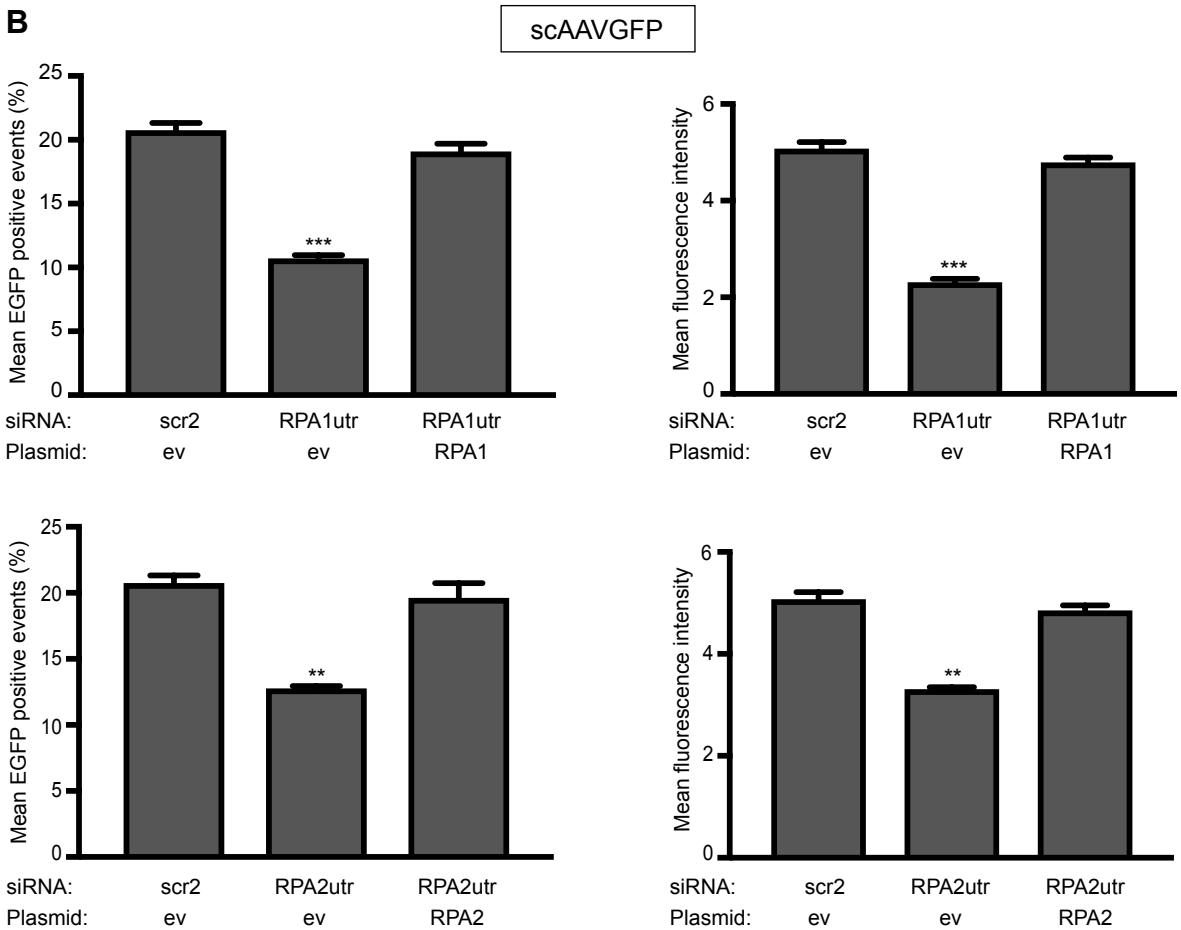

**Figure 7**

Click here to download Figure: Franzoso et al. Fig. 7.pdf

**Franzoso et al., Fig. 7**

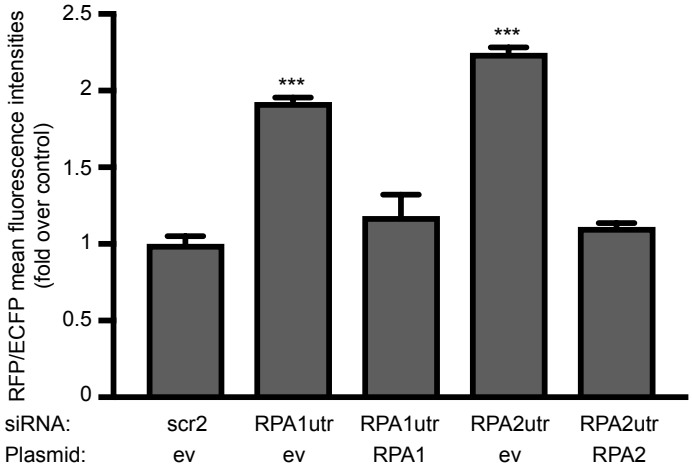

Figure 8

Click here to download Figure: Franzoso et al. Fig. 8.pdf

Franzoso et al., Fig. 8

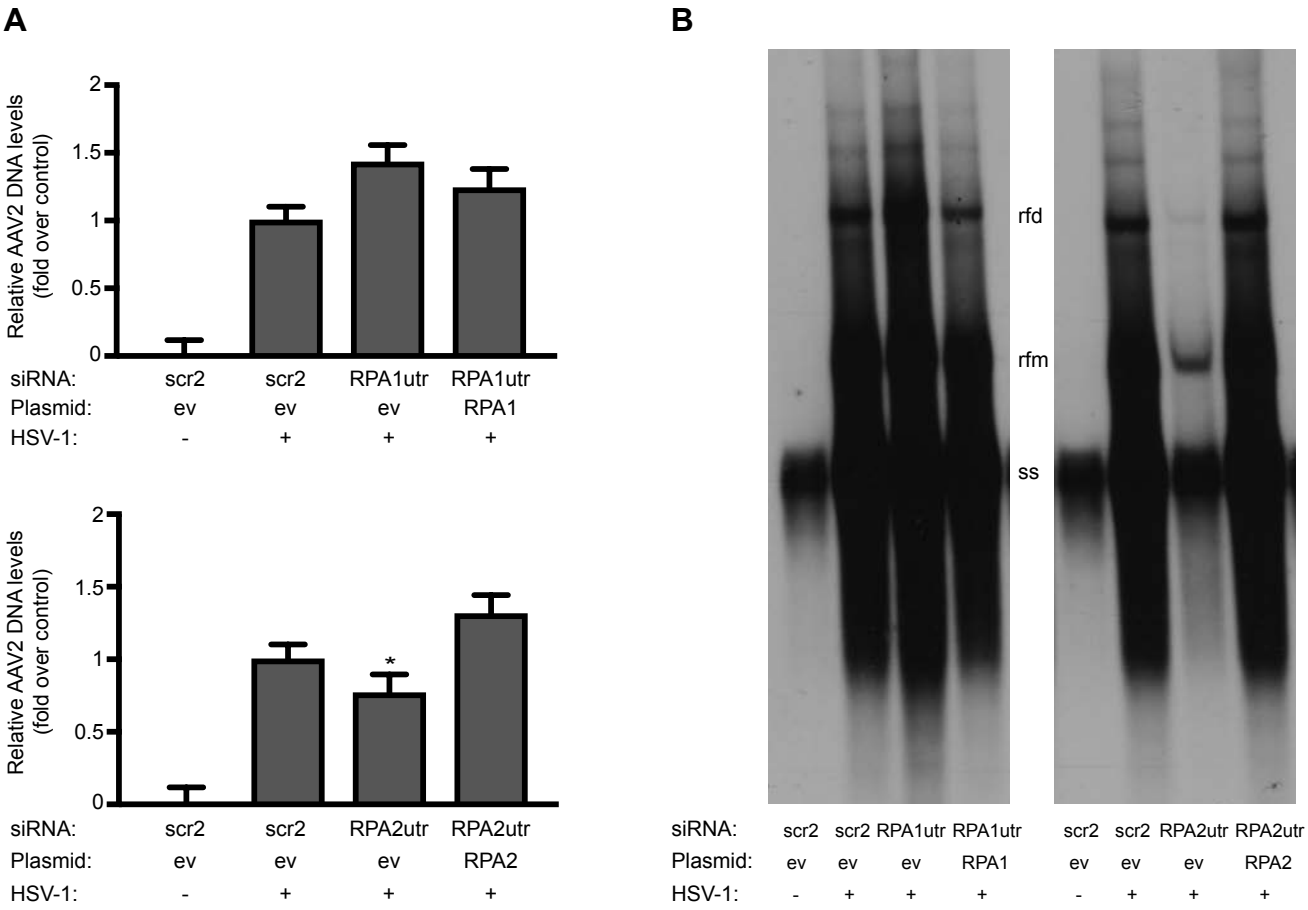

| GeneSymbol | Target sequence 1 | Target sequence 2 | Target sequence 3 | Supplier |
|---|---|---|---|---|
| ATM | UAACAAACAGGUGAUAUAU | UUGGUUUUAUGACAAUUGC | UUUUCAAACAGGUAACAGC | Ambion |
| ATR | UCAGUAUCCAUUUCUACAA | UUGACUUAAAAAAUCGGCUC | UAAAUUUUGCAUACUCAUC | Ambion |
| ABCE1 | AUCGGUCACAAAUUGUGGG | UUUCGUUCUUUUAGGUGGG | UUCGGUCCAAAAUAGAUCC | Ambion |
| ACAD9 | UGAUCCAUCAGAAUCAACG | UCUCUUUCUACUAUGAAUG | UCGCUUCUCAAGGAUCUGC | Ambion |
| ANXA5 | UCCUGAUAUAGUCAUGUAC | UUAGUUCUGAUUUCAGGUC | AACAGAUCAAUCUCACUCC | Ambion |
| ARL8B | UAUCUAGAAGAUUAUGUAG | UAUCUUCACUGAAUUGACC | AUAGCAUUGACUCCUCUGC | Ambion |
| ATP5O | UGUCAUUUAGGCUUUUCAC | AAUGGUCUGACCACAGAGG | UGACGGAUCAGUCUUAGCC | Ambion |
| CHEK2 | UAGGAUAAACUGACUGAUC | UUCUGUCGUAAAACGUGCC | UUCUGCUUAGUGACAGUGC | Ambion |
| CMC1 | UUAUAGUAAGCAGUUAGAC | UUACUACCAUAAGAACUCC | UUAGACAUUCUUUCAAUGC | Ambion |
| DDX17 | AUAGCUUGCAGAGUCUCUC | AUCGGUUUCACUACGAUCC | UAACCUAUCAUAUUGGUAG | Ambion |
| EEF1A1 | UUCACUCAAAGCUUCAUGG | AAUGUAAGUGCUGACUUCC | UUUCGACAGAUUUUACUUC | Ambion |
| FLII | UGAGGUCCAGGUAUAGUAG | UUUCGGGACAGGUUCAGAG | UCGUUGAUAACCUGCUUGC | Ambion |
| GMNN | UCUUGGGACAGAACUAUUC | AGAUGUUAAGUGGUCAUUC | UAAGAUCAAAUGACUCCUG | Ambion |
| H2AFX | UUACCAAGUGCUUCGUCCC | UGUGCUGGUAUCUAGGUGC | UUGGAUUGCCGAGUUGAGU | Ambion |
| HIST1H1E | UUAGUAAUGAGCUCGGACA | UUUGGUUUAGCCGCCUUGG | AGCUUUAGUAAUGAGCUCG | Ambion |
| HIST1H1A | UUAGAUGCACCCGUUGCCU | UUGGGUUUUACAGCCUUAG | UUGCCUUAGUUUUUGUAGC | Ambion |
| HNRNPA3 | UCUAUGGUUUCAAUCUUGC | UCAUCUGUAGUUUCAAAGC | UACACGCCCAUCAACCUUG | Ambion |
| HNRNPAB | UCUUUGAACAGGAUAAACC | UUUGUUCAACUUUGGAUCC | UUUCUUCACCGGGUCCUUC | Ambion |
| HNRNPC | UAUCAUAAUAGUCCCGUUG | UGACUUAUCAUUCUUCAUC | UUCUUGACCACAAGAGUGU | Ambion |
| HNRNPD | UAUCUACACUCUCCGAUUC | AAGGUAAUAAAGCAGAACC | UUAGGAUCAAUCACCUUCC | Ambion |
| HNRNPH1 | AUUUGGACCAGUAUGCUUC | UCUGCUUCACCAGUUACUC | AUCUAUCUGACCCAAAUCC | Ambion |
| HNRNPM | UGCUUUGCAAUGAUCUCUC | AAAGUAACAGUGCCUAUUC | UGGUCUAUCAAAUAGCAGC | Ambion |
| HSPA8 | UAUGCUUGCGCUUAAACUC | UUUUGUCUAAGCCGUAAGC | UCAUUCACCACCAUAAAGG | Ambion |
| KRT13 | UUAAGGCCUACGGACAUCA | UUGGUAGACACCUCCUUGU | UCCGUGAUCUCUGUCUUGC | Ambion |
| LMNA | UCCAGUUUGCGCUUUUUGG | UAUCAGGUCACCCUCCUUC | UCAGGGUGAACUUUGGUGG | Ambion |
| LMNB1 | UUUGCGAAACUCCAAGUCC | AAGGCUCUGACAACGAUUC | UUCUGGUCUCGUUAAUCUC | Ambion |
| LMNB2 | UCACGCAUCACCGAGGACU | AUCCUUGUCCGAGUUGUUC | UACUUGGGCGUGAACUUGU | Ambion |
| LMO7 | AACGUGAUAUCAGAGGAGC | UUUGUUGCCUCUCCAAUUC | UUCGAUACGACAUAUCAUC | Ambion |
| MCM7 | UCUUUAUUUACCACUUCCC | UUAUUUACCACUUCCCUCU | UUGGGUUUGACUUCAGAGA | Ambion |
| MPRIP | UUCUGAUUCUGCUUGUUGG | UACUCUGUGACAUCGUAAC | AAAGGAUGAAGAACCGUCG | Ambion |
| MRE11A | AACCGGACUAAUGUCUAUC | UUAGUAGUGACAUUUCGGG | UAUAGUCCACUCGCAGUCG | Ambion |
| MSH2 | UUACACGAAAGUAAUAUCC | UAAGAUCUGGGAAUCGACG | UAUCAUAUCCUUGCGAUUC | Ambion |
| MSH3 | UUCCGAUACAGCAUCAAGC | UGUAUUGUAAUUCUAGCGG | UCCGAUACAGCAUCAAGCC | Ambion |
| MSH6 | UCCAGUAUCGUUUACAGCC | UCUGUUACGUAAGUUGUGC | UUUCGAGCAACUUUGACAG | Ambion |
| MYH10 | ACAACGAACAAAGUUAGGG | UUGACGAACAGCACGAGAC | AACGGUACGAAACAUGCCC | Ambion |
| MYL12B | UAUGCAUCAGUGGGAUUCU | UACAUCAAAAAGAAGAGGC | AGUCUGAUUAUACAAGUGC | Ambion |
| MYLK2 | UGAUCUUCACCAAAUGCCC | UUGGUCAUAAUUCACCACC | UGUCUUAUCGGAGAUUUGG | Ambion |
| NBN | AAUAGGUCUAAGACCUUGC | UACCAUACUUAGAAUUAUC | UGACCAUAGUGAGUCUUCC | Ambion |
| NUP153 | AUCGGUAGAGAGAUUUUCG | AAUCUAUCUUCGGCGAUGC | UAUUUCGUAGUUUAGACUG | Ambion |
| PARP1 | UUUGUUGCUACCGAUCACC | UCAUAGUUGACAUCGAUGG | UCUUCGGUUAUGAAGCUGC | Ambion |
| PCNA | UGAGAUCUCGGCAUAUACG | UUGCAGAAAAUUUCACUCC | UUAGUGUAAUGAUAUCUUC | Ambion |
| PHB | AUUGGUUUCUGUACCCACG | UCAUAGUCCUCUCCGAUGC | UUGAGGAUCUCAGUUGUGA | Ambion |
| PHGDH | UAUUAGACGGUUAUUGCUG | UGAGCUCCAAGGUUAGAAG | UUUAUUAGACGGUUAUUGC | Ambion |
| POLD1 | UCCAUGAUACGGAUGAAGG | UUGGUUUUCUCGAUCAUCU | AAUGUUUGUACCUUGAGGG | Ambion |
| PRKDC | UGUUGUAGCACUCCAACGC | AGUUCACCCAGAAAAGCGC | AAGGCUAUAAAGUCGCUUG | Ambion |
| RAD50 | UUCACGAUGACAGUCUACC | UUCGAUCUAAGUCUAUUCC | UUCGUAACUGGACAACUGC | Ambion |
| RBM14 | AACUGUUUCAUGACGGCGC | UUCUUUGCCGUUGAGCUGC | UAUAGGAGCCCGAAUAGCG | Ambion |
| RFC2 | UGGUUUUAGAGUAGAUUUC | UUACAAGCAAGGGCGAAGC | UUCUCGAUAACAUUCAUCA | Ambion |
| RPA1 | UUCGCAAUGAUAGUGCUUG | UUUACUGACAGGAUCAUGC | UUUCGAGAAAUAAUACACC | Ambion |
| RUVBL2 | UGUUACAUCACGGAUCUCC | UGCUGGUCGAUCAAUCUGG | UUCUGUACCCUUGCGUUUC | Ambion |
| SFPQ | AGAUCUUCCACGAUCAUCC | UAUUCGUACUCAAACGUGC | UCCACUAUUACAACAGCCC | Ambion |
| SLC25A6 | UACGUGGUUCUCUUGGUUC | UAUUGUUUUGCAGCAGGAG | AAAGUACCUCCAGAACUGC | Ambion |
| SMC1A | AAACGAGGAAGUUACGAGC | UGUACUCAGAAGAACCUCC | UCGAAGGUCAGGACUUUGC | Ambion |
| SPTAN1 | UGUCCUUCAACCGUGACUC | UUAGCUUGGUUGCAAAUUC | UAAUCGCUUUGUCAAAGUC | Ambion |
| SSBP1 | UUUUUAUCCAUGUAUUCAC | UUAUCAGCUAUGAUUGUUG | UCAGCUAUGAUUGUUGUUG | Ambion |
| TP53 | UUCCGUCCCAGUAGAUUAC | UACUCCACACGCAAAUUUC | UUAGGUACUAAGGUUCACC | Ambion |
| TMOD3 | UGUCUUUAUGCUCCAAUGC | UCUUGGUCAACACCAUUAC | UAUUCGUUAUCAAAUUGUG | Ambion |
| TUBB4B | UUAUCAAUGCAGUAGGUCU | UUCGUUAUCAAUGCAGUAG | UGACCGAAAACGAAGUUGU | Ambion |
| TUFM | ACAUGAGCCGCAUUGAUGG | UAUUCUUAACAUAAUCUGC | UAACAUAAUCUGCAUGACC | Ambion |
| VIM | UUGCGUUCAAGGUCAAGAC | UUUUGAGUGGGUAUCAACC | AUCCAGAUUAGUUUCCCUC | Ambion |
| XRCC5 | UUCUAUACCAGGAAUGGAG | UUUGUUGUCACCUCAGCGG | UCCAUGCUCACGAUUAGUG | Ambion |
| XRCC6 | UGUCAACUCAUCUUCACUC | UUGAGCUUCAGCUUUAACC | UGUAGAACAAGGAUAUGUC | Ambion |
| KIF11 | CCAUCAACACUGGUAAGAA | | | Ambion |
| scr1 | UCGUAAGUAAGCGCAACCC | | | Ambion |
| scr2 | UAACGACGCGACGACGUAA | | | Ambion |
| | | | | |
| RPA1utr | GGAAUUAUGUCGUAAGUCAUU | | | Microsynth |
| RPA1cs | CAAGCACUAUCAUUGCGAA | | | Microsynth |
| RPA2utr | AACCUAGUUUCACAAUCUGUUUU | | | Microsynth |
| RPA2cs | GGAGAGCACCUAUCAGCAAUU | | | Microsynth |

**Supplementary Fig.**

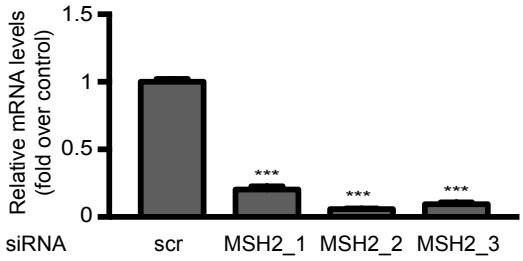


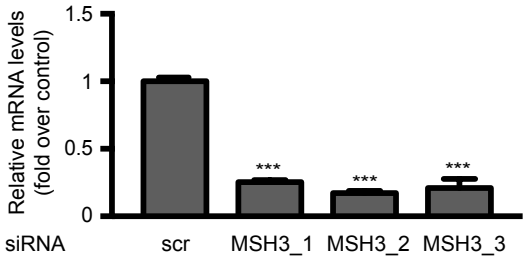


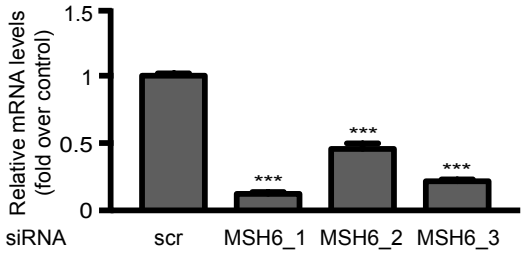


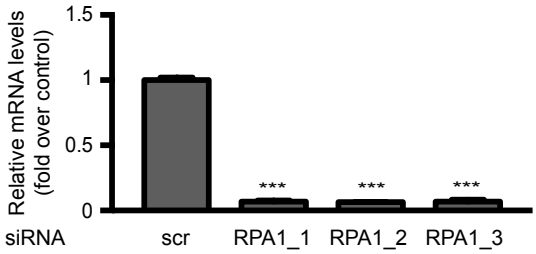


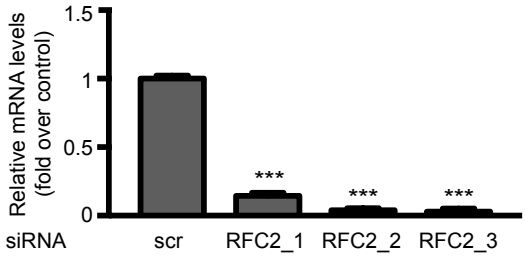


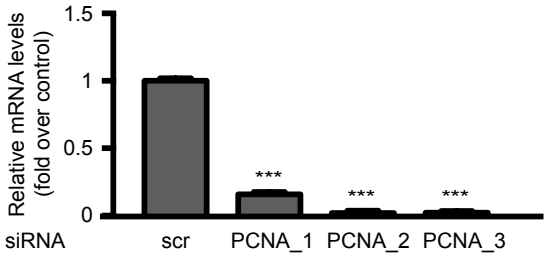

# 6. Discussion and Perspectives

The data on cell cycle dependent AAV2 gene expression/replication as well as effects of specific cellular proteins on the transduction efficiencies of AAV vectors are discussed in the respective manuscripts (chapters 5.1. and 5.2.). Here an overview of the recent strategies to overcome possible obstacles in order to create vectors with improved AAV-mediated gene delivery and the implications of this work for AAV2 research, AAV2 mediated gene therapy, and vector production is presented.

## 6.1. AAV vectors for therapeutic gene delivery

Increasing numbers of phase I-III clinical trials using AAV vectors with promising results appear to gradually remove the barriers for treating familial lipoprotein lipase LPL deficiency (first AAV1 vector encoding the gain-of-function LPL variant obtained market approval in EU in 2012) (93, 95), various monogenic disorders and chronic conditions such as Leber's congenital amaurosis type 2 (233), hemophilia B (89, 234, 235), nervous system, eye, muscle and heart diseases (91, 236, 237).

Persistent gene expression, one of the great advantages of using AAV vectors, was demonstrated *in vivo* with most AAV vectors. For example, beta-galactosidase was expressed for more than one year and half after intramuscular injection (238), erythropoietin for six months after systemic injection (239) or other genes showed long-term expression after injection into the eye, brain, spinal cord, muscle and liver (240–242). However, the ultimate goal would be treatment of genetic diseases with a single application of AAV vectors that would last for life.

One of the major rate-limiting steps for gene expression *in vivo* was demonstrated to be the second-strand synthesis (243). To overcome this limitation, McCarty et al (79, 244) created a ds vector termed self-complementary (sc) that has a greatly enhanced transduction efficiency. However, at the same time the transgene capacity is greatly reduced.

At the moment more than 13 different AAV serotypes with various in vivo tissue tropisms are used for packaging rAAV cassettes. Improvement of infectivity in the target cells was achieved either by capsid modifications (inserts of amino acids (245) or creating capsid libraries (246)) or changing specific promoters (247) or introducing

microRNA into the transgene cassette to inhibit gene expression in non-targeted organs (248). Other capsid engineering methods comprised also site-directed mutagenesis (249), creating capsid libraries, elaborating screening methods (250) or mutating tyrosine to phenylalanine to reduce risks of cytotoxic T lymphocyte immune responses (251). Empty AAV2 capsid particles with mutations targeting primary cell receptor binding showed also promising results (252).

Another interesting approach was to change the tropism to and for target cells, as the liver is often the target destination, by incorporation of high-affinity ligands which restrict or redirect viral tropism (253). Moreover, an AAV2/AAV8 chimera (AAV2i8) showed an altered transduction profile as it selectively transduced cardiac and skeletal muscle while losing the liver tropism (254).

## 6.2. Cellular factors and AAV vector transduction

Another important research strategy in AAV vectorology represents the investigation of possible pathways toward transgene expression and rAAV transduction mechanisms.

Ss DNA vector genomes are assumed to be uncoated within the nucleus and form discrete foci that directly correlate to the transduction efficiency (255).

It was demonstrated that Mre11, Nbs1, and ATM are required for efficient vector genome circularization in dividing cells, suggesting that recombination pathways occuring at the terminal repeats (TRs) are involved in AAV persistance (81). In nondividing skeletal muscle fibers, ATM and DNA-PKs were necessary for vector genome circularization, whereas Nbs1 was not required (194, 256).

rAAV transduction can elicit a DNA damage response that can greatly influence the transduction. Dividing cells deficient for ATM showed increased transduction due to enhancement of second-strand synthesis (85, 257). DNA synthesis inhibitors such as aphidicolin or hydroxyurea and topoisomerase inhibitors such as camptothecin or etoposide increased transduction in both dividing and nondividing fibroblast cultures (258) showing that treatments that affect DNA metabolism can influence AAV gene expression. Furthermore, when ATM defective cells were treated with a genotoxic agent the increase in AAV transduction efficiency was limited (85), supporting the concept that ATM inhibits transduction at the genome level. Ku86 and Rad52 are also involved in this effect as Ku86 can inhibit further maturation of AAV DNA while Rad52

leads to activation of AAV gene expression through activating the homologous recombination (HR) pathway (259). These findings further emphasize that a profound understanding of the role of host factors involved in recombination mechanisms would allow to characterize a potential rAAV gene therapy genotoxicity (29).

Interestingly, *in vivo* studies in mice demonstrated that downregulating of DNA repair proteins, in particular the MRN complex genes Mre11, Rad50, Nbs1 increased vector transduction (237, 261). The MRN complex has been shown to inhibit the transduction efficiency of ss and sc AAV vectors dependent on the physical interaction with the vector genome rather than the nuclease activity (86, 262).

Our high-throughput siRNA screening approach identified positive and negative effects on ss and sc AAV vector transduction . We found cellular proteins such as Mre11, Rad50, PCNA, PRKDC, MSH3 and SMC1A with a negative effect on the transduction efficiency of both ss and ds AAV vectors. EEF1A1 appears to enhance transduction of ss and sc AAV vectors, whereas the knockdown of RFC2 and HNRNPD augmented the transduction of ss AAV vectors. Cellular DNA damage responses appear to be a strong determinant of AAV transduction, as shown also on a genome-wide scale in Mano et al (263).

RPA1 showed the most differential effect on transduction of ss and ds and it was selected as our target gene. Similar results were obtained with RPA2. As RPA has an approximately 1000-fold higher affinity for ssDNA than for dsDNA (264), the differential effect was not surprising. However, the underlying molecular mechanism remains to be investigated. Two other RNAi screenings have been previously described aiming to identify cellular factors controlling AAV transduction. The screening of Wallen et al (24) in human aortic endothelial cells using the Druggable Genome Library of 5520 genes showed many off-target effects which makes difficult a solid comparison with our results. The genome-wide siRNA screening for 18120 gene targets reported by Giacca's laboratory (263) identifying positive and negative regulators in ssAAV2 and scAAV2 transduction showed similar results with our study for the DNA damage proteins like MRN complex but also discovering differential effects of new genes like SETD8, CASP8AP2 or TROAP in both *in vitro* and *in vivo* assays in the hepatic tissue.

Our study offers a new perspective when using RNAi strategy, with potential translational value and adds new knowledge that can further lead to possible tracking of new cellular pathways and improved AAV-based viral vectors for gene therapy.

## 6.3. Cell cycle and AAV vector transduction

The cell cycle appears to affect AAV vector transduction. Genotoxic stress that can provoke a cell cycle arrest resulted in increased transduction (265, 266). In absence of normal checkpoint functions, such as in p53-deficient cells or human embryonic stem cells, the AAV transduction results in cell death (168, 256). However, the mechanisms undelying these transduction effects are not well understood.

One report on AAV transduction and cell cycle by Russell and coworkers (198) showed that cells in S-phase are transduced up to 200-fold more efficiently compared to non S-phase cells. They concluded that, although S phase is preferentially transduced by AAV vectors, S phase is not absolutely required for transduction. At a mechanistic level, cellular DNA polymerases active in S phase could convert ss AAV vector genomes to transcriptionally active ds molecules (197, 198). Moreover, it was suggested that most transduction events were associated with vector integration and that integration is the rate-limiting step for transduction (198).

Importantly, AAV transduction induces a cell cycle arrest at G1 and G2/M checkpoints in wt diploid cells (168, 267). In cells defective for specific cell cycle checkpoints, the transduction is initially increased, probably due to a faster entry into S phase (256, 268).

In our first study we demonstrated that AAV2 transcription and replication was efficient in S/G2 and G1 cells when the template was a circular ds rather than a linear ss DNA, indicating that the S/G2 phase preference of ssAAV vectors is due to inefficient second-strand synthesis in that cell cycle phase. Indeed, as opposed to the ss AAV vectors, infection of cells with scAAV2 vectors resulted in a considerable proportion of AAV2 transgene-positive G1 cells in absence of the helper virus. However, our high-throughput multi-channel time-laps microscopy study showed that the majority of the scAAV2 transduced G1 cells originated from transduced S/G2 cells that progressed through mitosis. rAAV2 vectors can induce a cell cycle arrest more efficiently than scAAV2 vectors likely because of the ss versus ds nature of the genome. In presence of the helper virus, neither ss not ds vector transduced cells progressed through mitosis presumably because of an HSV-1 induced G2 arrest. These observations can be used in designing new vectors with a better transduction efficiency in slowly dividing cells, including hematopoietic stem cells or continuously repopulating epithelial cells from respiratory and intestinal tract.

AAV vectors preferentially transduce dividing cells. The fact that the transduction efficiency of ss and sc AAV vectors depends on cells in S/G2 phase (Franzoso et al., 2017 (269)) may explain their low transduction efficiency in post-mitotic cells. However, sc AAV vectors may be preferred over ss AAV vectors in mitotically active cells as in contrast to ss vectors, they allow cell cycle progression through mitosis (Franzoso et al., 2017 (269)).

Taken together, the findings presented in this thesis on cell cycle preference of AAV2 replication/gene expression and on the influence of cellular proteins on the transduction efficiencies of ss and sc AAV vectors furthers our knowledge on AAV biology and may help to design improved vectors for therapeutic gene delivery.

# 7. References


1. **Atchison RW**, **Casto BC**, **Hammon WM**. 1966. Electron microscopy of adenovirus-associated virus (AAV) in cell cultures. Virology **29**:353–357.
2. **Sun JY**, **Anand-Jawa V**, **Chatterjee S**, **Wong KK**. 2003. Immune responses to adeno-associated virus and its recombinant vectors. Gene Ther **10**:964–976.
3. **Daya S**, **Berns KI**. 2008. Gene therapy using adeno-associated virus vectors. Clin Microbiol Rev **21**:583–593.
4. **Wu Z**, **Asokan A**, **Samulski RJ**. 2006. Adeno-associated Virus Serotypes: Vector Toolkit for Human Gene Therapy. Mol Ther **14**:316–327.
5. **Zincarelli C**, **Soltys S**, **Rengo G**, **Rabinowitz JE**. 2008. Analysis of AAV serotypes 1-9 mediated gene expression and tropism in mice after systemic injection. Mol Ther **16**:1073–1080.
6. **Grimm D**, **Kay MA**. 2003. From virus evolution to vector revolution: use of naturally occurring serotypes of adeno-associated virus (AAV) as novel vectors for human gene therapy. Curr Gene Ther **3**:281–304.
7. **Gao G**, **Vandenberghe LH**, **Alvira MR**, **Lu Y**, **Calcedo R**, **Zhou X**, **Wilson JM**. 2004. Clades of Adeno-Associated Viruses Are Widely Disseminated in Human Tissues. J Virol **78**:6381–6388.
8. **Chen C-L**, **Jensen RL**, **Schnepp BC**, **Connell MJ**, **Shell R**, **Sferra TJ**, **Bartlett JS**, **Clark KR**, **Johnson PR**. 2005. Molecular characterization of adeno-associated viruses infecting children. J Virol **79**:14781–92.
9. **Samulski RJ**, **Berns KI**, **Tan M**, **Muzyczka N**. 1982. Cloning of adeno-associated virus into pBR322: rescue of intact virus from the recombinant plasmid in human cells. Proc Natl Acad Sci U S A **79**:2077–81.
10. **Tratschin J-D**, **West MHP**, **Sandbank T**, **Carter BJ**. 1984. A Human Parvovirus, Adeno-Associated Virus, as a Eucaryotic Vector: Transient Expression and Encapsidation of the Procaryotic Gene for Chloramphenicol Acetyltransferase. Mol Cell Biol **4**:2072–2081.
11. **Hauswirth WW**, **Berns KI**. 1977. Origin and termination of adeno-associated virus DNA replication. Virology **78**:488–99.
12. **Ni TH**, **McDonald WF**, **Zolotukhin I**, **Melendy T**, **Waga S**, **Stillman B**, **Muzyczka N**. 1998. Cellular proteins required for adeno-associated virus DNA replication in

the absence of adenovirus coinfection. J Virol **72**:2777–87.

13. **Wang X-S**, **Ponnazhagan S**, **Srivastava A**. 1995. Rescue and Replication Signals of the Adeno-associated Virus 2 Genome. J Mol Biol **250**:573–580.
14. **Chejanovsky N**, **Carter BJ**. 1989. Mutagenesis of an AUG codon in the adeno-associated virus rep gene: effects on viral DNA replication. Virology **173**:120–8.
15. **McCarty DM**, **Young SM**, **Samulski RJ**. 2004. Integration of adeno-associated virus (AAV) and recombinant AAV vectors. Annu Rev Genet **38**:819–45.
16. **Becerra SP**, **Rose JA**, **Hardy M**, **Baroudy BM**, **Anderson CW**. 1985. Direct mapping of adeno-associated virus capsid proteins B and C: a possible ACG initiation codon. Proc Natl Acad Sci U S A **82**:7919–23.
17. **Cassinotti P**, **Weitz M**, **Tratschin JD**. 1988. Organization of the adeno-associated virus (AAV) capsid gene: mapping of a minor spliced mRNA coding for virus capsid protein 1. Virology **167**:176–84.
18. **Sonntag F**, **Bleker S**, **Leuchs B**, **Fischer R**, **Kleinschmidt JA**. 2006. Adeno-associated virus type 2 capsids with externalized VP1/VP2 trafficking domains are generated prior to passage through the cytoplasm and are maintained until uncoating occurs in the nucleus. J Virol **80**:11040–54.
19. **Summerford C**, **Samulski RJ**. 1998. Membrane-associated heparan sulfate proteoglycan is a receptor for adeno-associated virus type 2 virions. J Virol **72**:1438–45.
20. **Srivastava A**, **Qing K**, **Mah C**, **Hansen J**, **Zhou S**, **Dwarki V**. 1999. Human fibroblast growth factor receptor 1 is a co-receptor for infectionby adeno-associated virus 2. Nat Med **5**:71–77.
21. **Kashiwakura Y**, **Tamayose K**, **Iwabuchi K**, **Hirai Y**, **Shimada T**, **Matsumoto K**, **Nakamura T**, **Watanabe M**, **Oshimi K**, **Daida H**. 2005. Hepatocyte growth factor receptor is a coreceptor for adeno-associated virus type 2 infection. J Virol **79**:609–14.
22. **Akache B**, **Grimm D**, **Pandey K**, **Yant SR**, **Xu H**, **Kay MA**. 2006. The 37/67-Kilodalton Laminin Receptor Is a Receptor for Adeno-Associated Virus Serotypes 8, 2, 3, and 9. J Virol **80**:9831–9836.
23. **Asokan A**, **Hamra JB**, **Govindasamy L**, **Agbandje-McKenna M**, **Samulski RJ**. 2006. Adeno-associated virus type 2 contains an integrin alpha5beta1 binding domain essential for viral cell entry. J Virol **80**:8961–9.
24. **Wallen AJ**, **Barker G a**, **Fein DE**, **Jing H**, **Diamond SL**. 2011. Enhancers of

adeno-associated virus AAV2 transduction via high throughput siRNA screening. Mol Ther **19**:1152–1160.

25. **Pillay S**, **Meyer NL**, **Puschnik AS**, **Davulcu O**, **Diep J**, **Jae LT**, **Wosen JE**, **Nagamine CM**, **Chapman MS**, **Carette JE**. 2016. An essential receptor for adeno-associated virus infection. Nature **530**.
26. **Bartlett JS**, **Wilcher R**, **Samulski RJ**. 2000. Infectious entry pathway of adeno-associated virus and adeno-associated virus vectors. J Virol **74**:2777–85.
27. **Duan D**, **Li Q**, **Kao AW**, **Yue Y**, **Pessin JE**, **Engelhardt JF**. 1999. Dynamin is required for recombinant adeno-associated virus type 2 infection. J Virol **73**:10371–6.
28. **Sanlioglu S**, **Benson PK**, **Yang J**, **Atkinson EM**, **Reynolds T**, **Engelhardt JF**. 2000. Endocytosis and nuclear trafficking of adeno-associated virus type 2 are controlled by rac1 and phosphatidylinositol-3 kinase activation. J Virol **74**:9184–96.
29. **Nonnenmacher M**, **Weber T**. 2011. Adeno-associated virus 2 infection requires endocytosis through the CLIC/GEEC pathway. Cell Host Microbe **10**:563–76.
30. **Di Pasquale G**, **Kaludov N**, **Agbandje-McKenna M**, **Chiorini JA**, **Nettesheim P**. 2010. BAAV Transcytosis Requires an Interaction with β-1-4 Linked-Glucosamine and gp96. PLoS One **5**:e9336.
31. **Di Pasquale G**, **Chiorini JA**, **Russell DW**, **Kotin RM**, **Kotin RM**, **Kachar B**. 2006. AAV transcytosis through barrier epithelia and endothelium. Mol Ther **13**:506–16.
32. **Douar AM**, **Poulard K**, **Stockholm D**, **Danos O**. 2001. Intracellular trafficking of adeno-associated virus vectors: routing to the late endosomal compartment and proteasome degradation. J Virol **75**:1824–33.
33. **Bantel-Schaal U**, **Hub B**, **Kartenbeck J**. 2002. Endocytosis of adeno-associated virus type 5 leads to accumulation of virus particles in the Golgi compartment. J Virol **76**:2340–9.
34. **Keiser NW**, **Yan Z**, **Zhang Y**, **Lei-Butters DCM**, **Engelhardt JF**. 2011. Unique characteristics of AAV1, 2, and 5 viral entry, intracellular trafficking, and nuclear import define transduction efficiency in HeLa cells. Hum Gene Ther **22**:1433–44.
35. **Nam H-J**, **Gurda BL**, **McKenna R**, **Potter M**, **Byrne B**, **Salganik M**, **Muzyczka N**, **Agbandje-McKenna M**. 2011. Structural studies of adeno-associated virus serotype 8 capsid transitions associated with endosomal trafficking. J Virol

**85**:11791–9.

36. **Johnson JS**, **Samulski RJ**. 2009. Enhancement of adeno-associated virus infection by mobilizing capsids into and out of the nucleolus. J Virol **83**:2632–2644.
37. **Johnson JS**, **Li C**, **DiPrimio N**, **Weinberg MS**, **McCown TJ**, **Samulski RJ**. 2010. Mutagenesis of adeno-associated virus type 2 capsid protein VP1 uncovers new roles for basic amino acids in trafficking and cell-specific transduction. J Virol **84**:8888–902.
38. **Johnson JS**, **Samulski RJ**. 2009. Enhancement of adeno-associated virus infection by mobilizing capsids into and out of the nucleolus. J Virol **83**:2632–44.
39. **Bevington JM**, **Needham PG**, **Verrill KC**, **Collaco RF**, **Basrur V**, **Trempe JP**. 2007. Adeno-associated virus interactions with B23/Nucleophosmin: identification of sub-nucleolar virion regions. Virology **357**:102–13.
40. **Qiu J**, **Brown KE**. 1999. A 110-kDa Nuclear Shuttle Protein, Nucleolin, Specifically Binds to Adeno-Associated Virus Type 2 (AAV-2) Capsid. Virology **257**:373–382.
41. **Sipo I**, **Fechner H**, **Pinkert S**, **Suckau L**, **Wang X**, **Weger S**, **Poller W**. 2007. Differential internalization and nuclear uncoating of self-complementary adeno-associated virus pseudotype vectors as determinants of cardiac cell transduction. Gene Ther **14**:1319–1329.
42. **Duan D**, **Yue Y**, **Yan Z**, **Yang J**, **Engelhardt JF**. 2000. Endosomal processing limits gene transfer to polarized airway epithelia by adeno-associated virus. J Clin Invest **105**:1573–87.
43. **Yan Z**, **Zak R**, **Luxton GWG**, **Ritchie TC**, **Bantel-Schaal U**, **Engelhardt JF**. 2002. Ubiquitination of both adeno-associated virus type 2 and 5 capsid proteins affects the transduction efficiency of recombinant vectors. J Virol **76**:2043–53.
44. **Buller RM**, **Janik JE**, **Sebring ED**, **Rose JA**. 1981. Herpes simplex virus types 1 and 2 completely help adenovirus-associated virus replication. J Virol **40**:241–7.
45. **Walz C**, **Deprez A**, **Dupressoir T**, **Du M**, **Rabreau le**, **Schlehofer rg R**. 1997. Printed in Great Britain Interaction of human papillomavirus type 16 and adeno-associated virus type 2 co-infecting human cervical epithelium. J Gen Virol **78**:1441–1452.
46. **Schnepp BC**, **Jensen RL**, **Chen C-L**, **Johnson PR**, **Clark KR**. 2005. Characterization of Adeno-Associated Virus Genomes Isolated from Human

Tissues. J Virol **79**:14793–14803.

47. **McPherson RA**, **Rosenthal LJ**, **Rose JA**. 1985. Human cytomegalovirus completely helps adeno-associated virus replication. Virology **147**:217–22.
48. **Thomson BJ**, **Weindler FW**, **Gray D**, **Schwaab V**, **Heilbronn R**. 1994. Human Herpesvirus 6 (HHV-6) Is a Helper Virus for Adeno-Associated Virus Type 2 (AAV-2) and the AAV-2 rep Gene Homologue in HHV-6 Can Mediate AAV-2 DNA Replication and Regulate Gene Expression. Virology **204**:304–311.
49. **Hong G**, **Ward P**, **Berns KI**. 1992. In vitro replication of adeno-associated virus DNA. Proc Natl Acad Sci U S A **89**:4673–7.
50. **Zkanyalkinoglu AÃ–**, **Heilbronn R**, **Bã¼rkle A**, **Schlehofer JR**, **Zur Hausen H**. 1988. DNA Amplification of Adeno-associated Virus as a Response to Cellular Genotoxic Stress1. CANCER Res **48**:3123–3129.
51. **Yakobson B**, **Hrynko TA**, **Peak MJ**, **Winocour E**. 1989. Replication of adeno-associated virus in cells irradiated with UV light at 254 nm. J Virol **63**:1023–30.
52. **Meyers C**, **Mane M**, **Kokorina N**, **Alam S**, **Hermonat PL**. 2000. Ubiquitous Human Adeno-Associated Virus Type 2 Autonomously Replicates in Differentiating Keratinocytes of a Normal Skin Model. Virology **272**:338–346.
53. **Richardson WD**, **Westphal H**. 1981. A Cascade of Adenovirus Early Functions Is Required for Expression of Adeno-Associated Virus. Cell **27**:133–41.
54. **Lehman IR**, **Boehmer PE**. 1999. Replication of herpes simplex virus DNA. J Biol Chem **274**:28059–62.
55. **Alazard-Dany N**, **Nicolas A**, **Ploquin A**, **Strasser R**, **Greco A**, **Epstein AL**, **Fraefel C**, **Salvetti A**. 2009. Definition of herpes simplex virus type 1 helper activities for adeno-associated virus early replication events. PLoS Pathog **5**:1–12.
56. **Stracker TH**, **Cassell GD**, **Ward P**, **Loo Y-M**, **Van Breukelen B**, **Carrington-Lawrence SD**, **Hamatake RK**, **Van Der Vliet PC**, **Weller SK**, **Melendy T**, **Weitzman MD**. 2004. The Rep Protein of Adeno-Associated Virus Type 2 Interacts with Single-Stranded DNA-Binding Proteins That Enhance Viral Replication. J Virol **78**:441–453.
57. **Fraefel C**, **Bittermann AG**, **Büeler H**, **Heid I**, **Bächi T**, **Ackermann M**. 2004. Spatial and temporal organization of adeno-associated virus DNA replication in live cells. J Virol **78**:389–98.
58. **Heilbronn R**, **Engstler M**, **Weger S**, **Krahn A**, **Schetter C**, **Boshart M**. 2003.

ssDNA-dependent colocalization of adeno-associated virus Rep and herpes simplex virus ICP8 in nuclear replication domains. Nucleic Acids Res **31**:6206–6213.

59. **Nash K**, **Chen W**, **Salganik M**, **Muzyczka N**. 2009. Identification of cellular proteins that interact with the adeno-associated virus rep protein. J Virol **83**:454–69.
60. **Nicolas A**, **Alazard-Dany N**, **Biollay C**, **Arata L**, **Jolinon N**, **Kuhn L**, **Ferro M**, **Weller SK**, **Epstein AL**, **Salvetti A**, **Greco A**. 2010. Identification of rep-associated factors in herpes simplex virus type 1-induced adeno-associated virus type 2 replication compartments. J Virol **84**:8871–87.
61. **Vogel R**, **Seyffert M**, **Pereira Bde A**, **Fraefel C**. 2013. Viral and Cellular Components of AAV2 Replication Compartments. Open Virol J **7**:98–120.
62. **Ni TH**, **McDonald WF**, **Zolotukhin I**, **Melendy T**, **Waga S**, **Stillman B**, **Muzyczka N**. 1998. Cellular proteins required for adeno-associated virus DNA replication in the absence of adenovirus coinfection. J Virol **72**:2777–2787.
63. **Janik JE**, **Huston MM**, **Rose JA**. 1981. Locations of adenovirus genes required for the replication of adenovirus-associated virus. Proc Natl Acad Sci U S A **78**:1925–9.
64. **Samulski RJ**, **Muzyczka N**. 2014. AAV-Mediated Gene Therapy for Research and Therapeutic Purposes. Annu Rev Virol **1**:427–451.
65. **Weindler FW**, **Heilbronn R**. 1991. A subset of herpes simplex virus replication genes provides helper functions for productive adeno-associated virus replication. J Virol **65**:2476–83.
66. **Slanina H**, **Weger S**, **Stow ND**, **Kuhrs A**, **Heilbronn R**. 2006. Role of the herpes simplex virus helicase-primase complex during adeno-associated virus DNA replication. J Virol **80**:5241–50.
67. **Hunter LA**, **Samulski RJ**. 1992. Colocalization of adeno-associated virus Rep and capsid proteins in the nuclei of infected cells. J Virol **66**:317–24.
68. **Ward P**, **Dean FB**, **O'Donnell ME**, **Berns KI**. 1998. Role of the adenovirus DNA-binding protein in in vitro adeno-associated virus DNA replication. J Virol **72**:420–7.
69. **Kotin ' RM**, **Linden2 RM**, **Berns2 KL**. 1992. Characterization of a preferred site on human chromosome 19q for integration of adeno-associated virus DNA by non-homologous recombination. EMBO J **1**:5071–5078.

70. **Kotin RM**, **Menninger JC**, **Ward DC**, **Berns KI**. 1991. Mapping and direct visualization of a region-specific viral DNA integration site on chromosome 19q13-qter. Genomics **10**:831–4.
71. **Kotin RM**, **Siniscalco M**, **Samulski RJ**, **Zhu XD**, **Hunter L**, **Laughlin CA**, **McLaughlin S**, **Muzyczka N**, **Rocchi M**, **Berns KI**. 1990. Site-specific integration by adeno-associated virus. Proc Natl Acad Sci U S A **87**:2211–5.
72. **Dutheil N**, **Shi F**, **Dupressoir T**, **Linden RM**. 2000. Adeno-associated virus site-specifically integrates into a muscle-specific DNA region. Proc Natl Acad Sci U S A **97**:4862–6.
73. **Tan I**, **Ng CH**, **Lim L**, **Leung T**. 2001. Phosphorylation of a novel myosin binding subunit of protein phosphatase 1 reveals a conserved mechanism in the regulation of actin cytoskeleton. J Biol Chem **276**:21209–16.
74. **Lamartina S**, **Sporeno E**, **Fattori E**, **Toniatti C**. 2000. Characteristics of the adeno-associated virus preintegration site in human chromosome 19: open chromatin conformation and transcription-competent environment. J Virol **74**:7671–7.
75. **Philpott NJ**, **Gomos J**, **Berns KI**, **Falck-Pedersen E**. 2002. A p5 integration efficiency element mediates Rep-dependent integration into AAVS1 at chromosome 19. Proc Natl Acad Sci U S A **99**:12381–5.
76. **Hendrie PC**, **Russell DW**. 2005. Gene Targeting with Viral Vectors. Mol Ther **12**:9–17.
77. **Burger C**, **Gorbatyuk OS**, **Velardo MJ**, **Peden CS**, **Williams P**, **Zolotukhin S**, **Reier PJ**, **Mandel RJ**, **Muzyczka N**. 2004. Recombinant AAV Viral Vectors Pseudotyped with Viral Capsids from Serotypes 1, 2, and 5 Display Differential Efficiency and Cell Tropism after Delivery to Different Regions of the Central Nervous System. Mol Ther **10**:302–317.
78. **McCarty DM**. 2008. Self-complementary AAV Vectors; Advances and Applications. Mol Ther **16**:1648–1656.
79. **McCarty DM**, **Monahan PE**, **Samulski RJ**. 2001. Self-complementary recombinant adeno-associated virus (scAAV) vectors promote efficient transduction independently of DNA synthesis. Gene Ther **8**:1248–1254.
80. **Choi VW**, **Samulski RJ**, **McCarty DM**. 2005. Effects of adeno-associated virus DNA hairpin structure on recombination. J Virol **79**:6801–6807.
81. **Choi VW**, **McCarty DM**, **Samulski RJ**. 2006. Host cell DNA repair pathways in

adeno-associated viral genome processing. J Virol **80**:10346–10356.

82. **Fragkos M**, **Breuleux M**, **Clément N**, **Beard P**. 2008. Recombinant adeno-associated viral vectors are deficient in provoking a DNA damage response. J Virol **82**:7379–87.
83. **Alexander IE**, **Russell DW**, **Miller AD**. 1994. DNA-damaging agents greatly increase the transduction of nondividing cells by adeno-associated virus vectors. J Virol **68**:8282–7.
84. **Russell DW**, **Alexander IE**, **Miller a D**. 1995. DNA synthesis and topoisomerase inhibitors increase transduction by adeno-associated virus vectors. Proc Natl Acad Sci U S A **92**:5719–5723.
85. **Zentilin L**, **Marcello A**, **Giacca M**. 2001. Involvement of cellular double-stranded DNA break binding proteins in processing of the recombinant adeno-associated virus genome. J Virol **75**:12279–87.
86. **Schwartz R a**, **Palacios JA**, **Cassell GD**, **Adam S**, **Giacca M**, **Weitzman MD**. 2007. The Mre11/Rad50/Nbs1 complex limits adeno-associated virus transduction and replication. J Virol **81**:12936–45.
87. **Cervelli T**, **Palacios JA**, **Zentilin L**, **Mano M**, **Schwartz RA**, **Weitzman MD**, **Giacca M**. 2008. Processing of recombinant AAV genomes occurs in specific nuclear structures that overlap with foci of DNA-damage-response proteins. J Cell Sci **121**.
88. **Carter B**, **Conrad C**, **Guggino W**, **Reynolds T**, **Rosenstein B**, **Taylor G**, **Walden S**, **Wetzel R**. 1996. Clinical Protocol A Phase I Study of an Adeno-Associated Virus-CFTR Gene Vector in Adult CF Patients with Mild Lung Disease. Hum Gene Ther **7**:1145–1159.
89. **High KA**, **Herzog RW**, **Yang EY**, **Couto LB**, **Hagstrom JN**, **Elwell D**, **Fields PA**, **Burton M**, **Bellinger DA**, **Read MS**, **Brinkhous KM**, **Podsakoff GM**, **Nichols TC**, **Kurtzman GJ**. 1999. Long-term correction of canine hemophilia B by gene transfer of bloodcoagulation factor IX mediated by adeno-associated viral vector. Nat Med **5**:56–63.
90. **Williams DA**. 2007. RAC Reviews Serious Adverse Event Associated with AAV Therapy Trial. Mol Ther **15**:2053–2054.
91. **Wells DJ**. 2017. Systemic AAV Gene Therapy Close to Clinical Trials for Several Neuromuscular Diseases. Mol Ther **25**:834–835.
92. **Feigin A**, **Kaplitt MG**, **Tang C**, **Lin T**, **Mattis P**, **Dhawan V**, **During MJ**,

**Eidelberg D**. 2007. Modulation of metabolic brain networks after subthalamic gene therapy for Parkinson's disease. Proc Natl Acad Sci U S A **104**:19559–64.

93. **Ferreira V**, **Petry H**, **Salmon F**. 2014. Immune Responses to AAV-Vectors, the Glybera Example from Bench to Bedside. Front Immunol **5**:82.
94. **Wierzbicki AS**, **Viljoen A**. 2013. Alipogene tiparvovec: gene therapy for lipoprotein lipase deficiency. Expert Opin Biol Ther **13**:7–10.
95. **Gaudet D**, **Méthot J**, **Déry S**, **Brisson D**, **Essiembre C**, **Tremblay G**, **Tremblay K**, **de Wal J**, **Twisk J**, **van den Bulk N**, **Sier-Ferreira V**, **van Deventer S**. 2013. Efficacy and long-term safety of alipogene tiparvovec (AAV1-LPLS447X) gene therapy for lipoprotein lipase deficiency: an open-label trial. Gene Ther **20**:361–369.
96. **Sawtell NM**. 1997. Comprehensive quantification of herpes simplex virus latency at the single-cell level. J Virol **71**:5423–31.
97. **Brown JC**, **C. J**. 2017. Herpes Simplex Virus Latency: The DNA Repair-Centered Pathway. Adv Virol **2017**:1–6.
98. **Roizman B**, **Zhou G**, **Du T**. 2011. Checkpoints in productive and latent infections with herpes simplex virus 1: conceptualization of the issues. J Neurovirol **17**:512–517.
99. **Eisenberg RJ**, **Atanasiu D**, **Cairns TM**, **Gallagher JR**, **Krummenacher C**, **Cohen GH**. 2012. Herpes virus fusion and entry: A story with many characters. Viruses **4**:800–832.
100. **Spear PG**, **Eisenberg RJ**, **Cohen GH**. 2000. Three Classes of Cell Surface Receptors for Alphaherpesvirus Entry. Virology **275**:1–8.
101. **Arvin A**, **Campadelli-Fiume G**, **Mocarski E**, **Moore PS**, **Roizman B**, **Whitley R**, **Yamanishi K**. 2007. Human HerpesvirusesHuman Herpesviruses: Biology, Therapy, and Immunoprophylaxis. Cambridge University Press.
102. **de Oliveira AP**, **Fraefel C**. 2010. Herpes simplex virus type 1/adeno-associated virus hybrid vectors. Open Virol J **4**:109–22.
103. **Akhtar J**, **Shukla D**. 2009. Viral entry mechanisms: cellular and viral mediators of herpes simplex virus entry. FEBS J **276**:7228–7236.
104. **Homa**, **Brown**. 1997. Capsid assembly and DNA packaging in herpes simplex virus. Rev Med Virol **7**:107–122.
105. **Sandri-Goldin RM**. 2003. Replication of the herpes simplex virus genome: does it really go around in circles? Proc Natl Acad Sci U S A **100**:7428–9.

106. **Dabrowski CE**, **Schaffer PA**. 1991. Herpes simplex virus type 1 origin-specific binding protein: oriS-binding properties and effects of cellular proteins. J Virol **65**:3140–50.
107. **Martin DW**, **Deb SP**, **Klauer JS**, **Deb S**. 1991. Analysis of the herpes simplex virus type 1 OriS sequence: mapping of functional domains. J Virol **65**:4359–69.
108. **Weller SK**, **Coen DM**. 2012. Herpes simplex viruses: mechanisms of DNA replication. Cold Spring Harb Perspect Biol **4**:a013011.
109. **Tong L**, **Stow ND**. 2010. Analysis of herpes simplex virus type 1 DNA packaging signal mutations in the context of the viral genome. J Virol **84**:321–9.
110. **Montgomery RI**, **Warner MS**. 1996. Herpes Simplex Virus-1 Entry into Cells Mediated by a Novel Member of the TNF/NGF Receptor Family. Cell **87**:427–436.
111. **Warner MS**, **Geraghty RJ**, **Martinez WM**, **Montgomery RI**, **Whitbeck JC**, **Xu R**, **Eisenberg RJ**, **Cohen GH**, **Spear PG**. 1998. A Cell Surface Protein with Herpesvirus Entry Activity (HveB) Confers Susceptibility to Infection by Mutants of Herpes Simplex Virus Type 1, Herpes Simplex Virus Type 2, and Pseudorabies Virus. Virology **246**:179–189.
112. **Cocchi F**, **Lopez M**, **Menotti L**, **Aoubala M**, **Dubreuil P**, **Campadelli-Fiume G**. 1998. The V domain of herpesvirus Ig-like receptor (HIgR) contains a major functional region in herpes simplex virus-1 entry into cells and interacts physically with the viral glycoprotein D. Proc Natl Acad Sci U S A **95**:15700–5.
113. **Geraghty RJ**, **Krummenacher C**, **Cohen GH**, **Eisenberg RJ**, **Spear PG**. 1998. Entry of Alphaherpesviruses Mediated by Poliovirus Receptor-Related Protein 1 and Poliovirus Receptor. Science (80- ) **280**.
114. **Gianni T**, **Campadelli-Fiume G**, **Menotti L**. 2004. Entry of Herpes Simplex Virus Mediated by Chimeric Forms of Nectin1 Retargeted to Endosomes or to Lipid Rafts Occurs through Acidic Endosomes. J Virol **78**:12268–12276.
115. **Clement C**, **Tiwari V**, **Scanlan PM**, **Valyi-Nagy T**, **Yue BYJT**, **Shukla D**. 2006. A novel role for phagocytosis-like uptake in herpes simplex virus entry. J Cell Biol **174**:1009–1021.
116. **Nicolas A**, **Alazard-dany N**, **Biollay C**, **Arata L**, **Jolinon N**, **Kuhn L**, **Weller SK**, **Epstein AL**, **Salvetti A**, **Greco A**, **Ferro M**. 2010. Identification of Rep-Associated Factors in Herpes Simplex Virus Type 1-Induced Adeno-Associated Virus Type 2 Replication Compartments Identification of Rep-Associated Factors in Herpes Simplex Virus Type 1-Induced Adeno-Associated Virus Type 2

Replicatio **84**:8871–8887.

117. **Nicola A V**, **Mcevoy AM**, **Straus SE**. 2003. Roles for Endocytosis and Low pH in Herpes Simplex Virus Entry into HeLa and Chinese Hamster Ovary Cells **77**:5324–5332.
118. **Navaratnarajah CK**, **Miest TS**, **Carfi A**, **Cattaneo R**. 2012. Targeted entry of enveloped viruses: measles and herpes simplex virus I. Curr Opin Virol **2**:43–9.
119. **Taylor TJ**, **Brockman MA**, **McNamee EE**, **Knipe DM**. 2002. Herpes simplex virus. Front Biosci **7**:d752-64.
120. **Roizman B**. 2011. The checkpoints of viral gene expression in productive and latent infection: the role of the HDAC/CoREST/LSD1/REST repressor complex. J Virol **85**:7474–82.
121. **MAUL GG**, **ISHOV AM**, **EVERETT RD**. 1996. Nuclear Domain 10 as Preexisting Potential Replication Start Sites of Herpes Simplex Virus Type-1. Virology **217**:67–75.
122. **Wysocka J**, **Herr W**. 2003. The herpes simplex virus VP16-induced complex: the makings of a regulatory switch. Trends Biochem Sci **28**:294–304.
123. **Smith CA**, **Bates P**, **Rivera-Gonzalez R**, **Gu B**, **DeLuca NA**. 1993. ICP4, the major transcriptional regulatory protein of herpes simplex virus type 1, forms a tripartite complex with TATA-binding protein and TFIIB. J Virol **67**:4676–87.
124. **Taylor TJ**, **Knipe DM**. 2004. Proteomics of herpes simplex virus replication compartments: association of cellular DNA replication, repair, recombination, and chromatin remodeling proteins with ICP8. J Virol **78**:5856–66.
125. **Knipe DM**, **Cliffe A**. 2008. Chromatin control of herpes simplex virus lytic and latent infection. Nat Rev Microbiol **6**:211–221.
126. **Ciufo DM**, **Mullen MA**, **Hayward GS**. 1994. Identification of a dimerization domain in the C-terminal segment of the IE110 transactivator protein from herpes simplex virus. J Virol **68**:3267–82.
127. **Everett R**, **O'Hare P**, **O'Rourke D**, **Barlow P**, **Orr A**. 1995. Point mutations in the herpes simplex virus type 1 Vmw110 RING finger helix affect activation of gene expression, viral growth, and interaction with PML-containing nuclear structures. J Virol **69**:7339–44.
128. **Everett RD**, **Maul GG**. 1994. HSV-1 IE protein Vmw110 causes redistribution of PML. EMBO J **13**:5062–9.
129. **Everett RD**, **Meredith M**, **Orr A**. 1999. The ability of herpes simplex virus type 1

immediate-early protein Vmw110 to bind to a ubiquitin-specific protease contributes to its roles in the activation of gene expression and stimulation of virus replication. J Virol **73**:417–26.

130. **Lehman IR**, **Boehmer PE**. 1999. Replication of herpes simplex virus DNA. J Biol Chem **274**:28059–62.
131. **McGeoch DJ**, **Dalrymple MA**, **Dolan A**, **McNab D**, **Perry LJ**, **Taylor P**, **Challberg MD**. 1988. Structures of herpes simplex virus type 1 genes required for replication of virus DNA. J Virol **62**:444–53.
132. **Challberg MD**. 1986. A method for identifying the viral genes required for herpesvirus DNA replication (plasmid transfection/transient assay/herpes simplex virus OrL and oris). Genetics **83**:9094–9098.
133. **Zhu LA**, **Weller SK**. 1992. The UL5 gene of herpes simplex virus type 1: isolation of a lacZ insertion mutant and association of the UL5 gene product with other members of the helicase-primase complex. J Virol **66**:458–68.
134. **Rabkin SD**, **Hanlon B**. 1990. Herpes simplex virus DNA synthesis at a preformed replication fork in vitro. J Virol **64**:4957–67.
135. **Mingo RM**, **Han J**, **Newcomb WW**, **Brown JC**. 2012. Replication of herpes simplex virus: egress of progeny virus at specialized cell membrane sites. J Virol **86**:7084–97.
136. **Johnson DC**, **Baines JD**. 2011. Herpesviruses remodel host membranes for virus egress. Nat Rev Microbiol **9**:382–394.
137. **Mettenleiter TC**, **Müller F**, **Granzow H**, **Klupp BG**. 2013. The way out: what we know and do not know about herpesvirus nuclear egress. Cell Microbiol **15**:170–178.
138. **Roller RJ**, **Bjerke SL**, **Haugo AC**, **Hanson S**. 2010. Analysis of a charge cluster mutation of herpes simplex virus type 1 UL34 and its extragenic suppressor suggests a novel interaction between pUL34 and pUL31 that is necessary for membrane curvature around capsids. J Virol **84**:3921–34.
139. **Hagen C**, **Dent KC**, **Zeev-ben-mordehai T**, **Mettenleiter TC**, **Gru K**, **Hagen C**, **Dent KC**, **Zeev-ben-mordehai T**, **Grange M**, **Bosse JB**, **Cheleski J**, **Werner S**, **Guttmann P**, **Rehbein S**, **Henzler K**, **Demmerle J**, **Adler B**. 2015. Article Structural Basis of Vesicle Formation at the Inner Nuclear Membrane 1692–1701.
140. **Klupp BG**, **Granzow H**, **Fuchs W**, **Keil GM**, **Finke S**, **Mettenleiter TC**. 2007. Vesicle formation from the nuclear membrane is induced by coexpression of two

conserved herpesvirus proteins. Proc Natl Acad Sci U S A **104**:7241–6.

141. **Bigalke JM**, **Heuser T**, **Nicastro D**, **Heldwein EE**. 2014. Membrane deformation and scission by the HSV-1 nuclear egress complex. Nat Commun **5**:4131.
142. **Morgan DO**. 1997. CYCLIN-DEPENDENT KINASES: Engines, Clocks, and Microprocessors. Annu Rev Cell Dev Biol **13**:261–291.
143. **Stark GR**, **Taylor WR**. 2006. Control of the G<sub>2</sub>/M Transition. Mol Biotechnol **32**:227–248.
144. **Bartek J**, **Lukas C**, **S?rensen CS**, **Kramer E**, **Santoni-Rugiu E**, **Lindeneg C**, **Peters J-M**, **Lukas J**. 1999. Accumulation of cyclin B1 requires E2F and cyclin-A-dependent rearrangement of the anaphase-promoting complex. Nature **401**:815–818.
145. **Taylor WR**, **Stark GR**. 2001. Regulation of the G2/M transition by p53. Oncogene **20**:1803–1815.
146. **Rhind N**, **Russell P**. 2012. Signaling pathways that regulate cell division. Cold Spring Harb Perspect Biol **4**.
147. **Maréchal A**, **Zou L**. 2013. DNA damage sensing by the ATM and ATR kinases. Cold Spring Harb Perspect Biol **5**.
148. **Branzei D**, **Foiani M**. 2008. Regulation of DNA repair throughout the cell cycle. Nat Rev Mol Cell Biol **9**:297–308.
149. **Lim S**, **Kaldis P**. 2013. Cdks, cyclins and CKIs: roles beyond cell cycle regulation. Development **140**.
150. **Hauck B**, **Zhao W**, **High K**, **Xiao W**. 2004. Intracellular viral processing, not single-stranded DNA accumulation, is crucial for recombinant adeno-associated virus transduction. J Virol **78**:13678–13686.
151. **Zhao RY**, **Elder RT**. 2005. Viral infections and cell cycle G2/M regulation. Cell Res **15**:143–149.
152. **Davy C**, **Doorbar J**. 2007. G2/M cell cycle arrest in the life cycle of viruses. Virology **368**:219–226.
153. **Chaurushiya MS**, **Weitzman MD**. 2009. Viral manipulation of DNA repair and cell cycle checkpoints. DNA Repair (Amst) **8**:1166–1176.
154. **Wilson R**, **Fehrmann F**, **Laimins LA**. 2005. Role of the E1?E4 Protein in the Differentiation-Dependent Life Cycle of Human Papillomavirus Type 31. J Virol **79**:6732–6740.
155. **Middleton K**, **Peh W**, **Southern S**, **Griffin H**, **Sotlar K**, **Nakahara T**, **El-Sherif A**,

**Morris L**, **Seth R**, **Hibma M**, **Jenkins D**, **Lambert P**, **Coleman N**, **Doorbar J**. 2003. Organization of human papillomavirus productive cycle during neoplastic progression provides a basis for selection of diagnostic markers. J Virol **77**:10186–201.

156. **Momoeda M**, **Wong S**, **Kawase M**, **Young NS**, **Kajigaya S**. 1994. A putative nucleoside triphosphate-binding domain in the nonstructural protein of B19 parvovirus is required for cytotoxicity. J Virol **68**:8443–6.
157. **Poole BD**, **Zhou J**, **Grote A**, **Schiffenbauer A**, **Naides SJ**. 2006. Apoptosis of Liver-Derived Cells Induced by Parvovirus B19 Nonstructural Protein. J Virol **80**:4114–4121.
158. **Davy CE**, **Jackson DJ**, **Wang Q**, **Raj K**, **Masterson PJ**, **Fenner NF**, **Southern S**, **Cuthill S**, **Millar JBA**, **Doorbar J**. 2002. Identification of a G(2) arrest domain in the E1 wedge E4 protein of human papillomavirus type 16. J Virol **76**:9806–18.
159. **Li H**, **Baskaran R**, **Krisky DM**, **Bein K**, **Grandi P**, **Cohen JB**, **Glorioso JC**. 2008. Chk2 is required for HSV-1 ICP0-mediated G2/M arrest and enhancement of virus growth. Virology **375**:13–23.
160. **Belyavskyi M**, **Braunagel SC**, **Summers MD**. 1998. The structural protein ODV-EC27 of Autographa californica nucleopolyhedrovirus is a multifunctional viral cyclin. Proc Natl Acad Sci U S A **95**:11205–10.
161. **Maruo S**, **Wu Y**, **Ishikawa S**, **Kanda T**, **Iwakiri D**, **Takada K**. 2006. Epstein-Barr virus nuclear protein EBNA3C is required for cell cycle progression and growth maintenance of lymphoblastoid cells. Proc Natl Acad Sci **103**:19500–19505.
162. **Choudhuri T**, **Verma SC**, **Lan K**, **Murakami M**, **Robertson ES**. 2007. The ATM/ATR signaling effector Chk2 is targeted by Epstein-Barr virus nuclear antigen 3C to release the G2/M cell cycle block. J Virol **81**:6718–30.
163. **Turner RL**, **Groitl P**, **Dobner T**, **Ornelles DA**. 2015. Adenovirus Replaces Mitotic Checkpoint Controls. J Virol **89**:5083–5096.
164. **Lai M**, **Zimmerman ES**, **Planelles V**, **Chen J**. 2005. Activation of the ATR Pathway by Human Immunodeficiency Virus Type 1 Vpr Involves Its Direct Binding to Chromatin In Vivo. J Virol **79**:15443–15451.
165. **Vassena L**, **Giuliani E**, **Matusali G**, **Cohen ÉA**, **Doria M**. 2013. The human immunodeficiency virus type 1 Vpr protein upregulates PVR via activation of the ATR-mediated DNA damage response pathway. J Gen Virol **94**:2664–9.
166. **DeHart JL**, **Zimmerman ES**, **Ardon O**, **Monteiro-Filho CM**, **Arga?araz ER**,

**Planelles V**. 2007. HIV-1 Vpr activates the G2 checkpoint through manipulation of the ubiquitin proteasome system. Virol J **4**:57.

167. **Yoshizuka N**, **Yoshizuka-Chadani Y**, **Krishnan V**, **Zeichner SL**. 2005. Human Immunodeficiency Virus Type 1 Vpr-Dependent Cell Cycle Arrest through a Mitogen-Activated Protein Kinase Signal Transduction Pathway. J Virol **79**:11366–11381.
168. **Raj K**, **Ogston P**, **Beard P**. 2001. Virus-mediated killing of cells that lack p53 activity. Nature **412**:914–917.
169. **Advani SJ**, **Weichselbaum RR**, **Roizman B**. 2003. Herpes simplex virus 1 activates cdc2 to recruit topoisomerase II alpha for post-DNA synthesis expression of late genes. Proc Natl Acad Sci U S A **100**:4825–30.
170. **Pyeon D**, **Pearce SM**, **Lank SM**, **Ahlquist P**, **Lambert PF**. 2009. Establishment of Human Papillomavirus Infection Requires Cell Cycle Progression. PLoS Pathog **5**:e1000318.
171. **Münger K**, **Baldwin A**, **Edwards KM**, **Hayakawa H**, **Nguyen CL**, **Owens M**, **Grace M**, **Huh K**. 2004. Mechanisms of human papillomavirus-induced oncogenesis. J Virol **78**:11451–60.
172. **Braunagel SC**, **Parr R**, **Belyavskyi M**, **Summers MD**. 1998. Autographa californicaNucleopolyhedrovirus Infection Results in Sf9 Cell Cycle Arrest at G2/M Phase. Virology **244**:195–211.
173. **Cannella D**, **Roberts JM**, **Fotedar R**. 1997. Association of cyclin A and cdk2 with SV40 DNA in replication initiation complexes is cell cycle dependent. Chromosoma **105**:349–59.
174. **Ludlow JW**. 1992. Selective ability of S-phase cell extracts to dephosphorylate SV40 large T antigen in vitro. Oncogene **7**:1011–4.
175. **Grand RJA**, **Ibrahim AP**, **Taylor AMR**, **Milner AE**, **Gregory CD**, **Gallimore PH**, **Turnell AS**. 1998. Human Cells Arrest in S Phase in Response to Adenovirus 12 E1A. Virology **244**:330–342.
176. **Singhal G**, **Leo E**, **Setty SKG**, **Pommier Y**, **Thimmapaya B**. 2013. Adenovirus E1A oncogene induces rereplication of cellular DNA and alters DNA replication dynamics. J Virol **87**:8767–78.
177. **Spitkovsky D**, **Jansen-Dürr P**, **Karsenti E**, **Hoffman I**. 1996. S-phase induction by adenovirus E1A requires activation of cdc25a tyrosine phosphatase. Oncogene **12**:2549–54.

178. **Song B**, **Liu JJ**, **Yeh K-C**, **Knipe DM**. 2000. Herpes Simplex Virus Infection Blocks Events in the G1 Phase of the Cell Cycle. Virology **267**:326–334.
179. **Jurvansuu J**, **Raj K**, **Stasiak A**, **Beard P**. 2005. Viral transport of DNA damage that mimics a stalled replication fork. J Virol **79**:569–580.
180. **Ehmann GL**, **McLean TI**, **Bachenheimer SL**. 2000. Herpes simplex virus type 1 infection imposes a G(1)/S block in asynchronously growing cells and prevents G(1) entry in quiescent cells. Virology **267**:335–349.
181. **Matsuda Y**, **Sanpei A**, **Wakai T**, **Kubota M**, **Osawa M**, **Hirose Y**, **Sakata J**, **Kobayashi T**, **Fujimaki S**, **Takamura M**, **Yamagiwa S**, **Yano M**, **Ohkoshi S**, **Aoyagi Y**. 2014. Hepatitis B virus X stimulates redox signaling through activation of ataxia telangiectasia mutated kinase. Int J Clin Exp Pathol **7**:2032–43.
182. **Studach L**, **Wang W-H**, **Weber G**, **Tang J**, **Hullinger RL**, **Malbrue R**, **Liu X**, **Andrisani O**. 2010. Polo-like kinase 1 activated by the hepatitis B virus X protein attenuates both the DNA damage checkpoint and DNA repair resulting in partial polyploidy. J Biol Chem **285**:30282–93.
183. **Wu X-Y**, **Qian J-J**, **Lin Y**, **Zheng M-H**. 2008. Hepatitis B virus X protein disrupts DNA interstrand crosslinking agent mitomycin C induced ATR dependent intra-S-phase checkpoint. Eur J Cancer **44**:1596–1602.
184. **Thomas M**, **Pim D**, **Banks L**. 1999. The role of the E6-p53 interaction in the molecular pathogenesis of HPV. Oncogene **18**:7690–7700.
185. **Nabel GJ**, **Friborg J**, **Kong W**, **Hottiger MO**. p53 inhibition by the LANA protein of KSHV protects against cell death. Nature **402**:889–894.
186. **Querido E**, **Blanchette P**, **Yan Q**, **Kamura T**, **Morrison M**, **Boivin D**, **Kaelin WG**, **Conaway RC**, **Conaway JW**, **Branton PE**. 2001. Degradation of p53 by adenovirus E4orf6 and E1B55K proteins occurs via a novel mechanism involving a Cullin-containing complex. Genes Dev **15**:3104–17.
187. **Lilyestrom W**, **Klein MG**, **Zhang R**, **Joachimiak A**, **Chen XS**. 2006. Crystal structure of SV40 large T-antigen bound to p53: interplay between a viral oncoprotein and a cellular tumor suppressor. Genes Dev **20**:2373–82.
188. **Truant R**, **Antunovic J**, **Greenblatt J**, **Prives C**, **Cromlish JA**. 1995. Direct interaction of the hepatitis B virus HBx protein with p53 leads to inhibition by HBx of p53 response element-directed transactivation. J Virol **69**:1851–9.
189. **O'Nions J**, **Allday MJ**. 2003. Epstein?Barr virus can inhibit genotoxin-induced G1 arrest downstream of p53 by preventing the inactivation of CDK2. Oncogene

**22**:7181–7191.

190. **Zhao F**, **Hou N-B**, **Song T**, **He X**, **Zheng Z-R**, **Ma Q-J**, **Li L**, **Zhang Y-H**, **Zhong H**. 2008. Cellular DNA repair cofactors affecting hepatitis B virus infection and replication. World J Gastroenterol **14**:5059–65.
191. **Gil-Ranedo J**, **Hernando E**, **Riolobos L**, **Domínguez C**, **Kann M**, **Almendral J éM**. 2015. The Mammalian Cell Cycle Regulates Parvovirus Nuclear Capsid Assembly. PLoS Pathog **11**:1–26.
192. **Moldovan G-L**, **Pfander B**, **Jentsch S**. 2007. PCNA, the Maestro of the Replication Fork. Cell **129**:665–679.
193. **Deleu L**, **Pujol A**, **Faisst S**, **Rommelaere J**. 1999. Activation of promoter P4 of the autonomous parvovirus minute virus of mice at early S phase is required for productive infection. J Virol **73**:3877–85.
194. **Raj K**, **Ogston P**, **Beard P**. 2001. Virus-mediated killing of cells that lack p53 activity. Nature **412**:914–917.
195. **Luo Y**, **Kleiboeker S**, **Deng X**, **Qiu J**. 2013. Human parvovirus B19 infection causes cell cycle arrest of human erythroid progenitors at late S phase that favors viral DNA replication. J Virol **87**:12766–75.
196. **Riolobos L**, **Valle N**, **Hernando E**, **Maroto B**, **Kann M**, **Almendral JM**. 2010. Viral oncolysis that targets Raf-1 signaling control of nuclear transport. J Virol **84**:2090–9.
197. **Saudan P**, **Vlach J**, **Beard P**. 2000. Inhibition of S-phase progression by adeno-associated virus Rep78 protein is mediated by hypophosphorylated pRb. EMBO J **19**:4351–4361.
198. **Russell DW**, **Miller AD**, **Alexander IE**. 1994. Adeno-associated virus vectors preferentially transduce cells in S phase. Proc Natl Acad Sci **91**:8915–8919.
199. **Hermanns J**, **Schulze A**, **Jansen-DBurr P**, **Kleinshmidt J**, **Schmidt R**, **zur Hausen H**. 1997. Infection of primary cells by adeno-associated virus type 2 results in a modulation of cell cycle-regulating proteins. J Virol **71**:6020–7.
200. **Wold MS**, **Weinberg DH**, **Virshup DM**, **Li JJ**, **Kelly TJ**. 1989. Identification of cellular proteins required for simian virus 40 DNA replication. J Biol Chem **264**:2801–9.
201. **Henricksen L a**, **Umbricht CB**, **Wold MS**. 1994. Recombinant replication protein A: expression, complex formation, and functional characterization. J Biol Chem **269**:11121–11132.

202. **Erdile LF**, **Wold MS**, **Kelly TJ**. 1990. The primary structure of the 32-kDa subunit of human replication protein A. J Biol Chem **265**:3177–82.
203. **Zou Y**, **Liu Y**, **Wu X**, **Shell SM**. 2006. Functions of human replication protein A (RPA): From DNA replication to DNA damage and stress responses. J Cell Physiol **208**:267–273.
204. **Kastan MB**. 2008. DNA damage responses: mechanisms and roles in human disease: 2007 G.H.A. Clowes Memorial Award Lecture. Mol Cancer Res **6**:517–524.
205. **Haring SJ**, **Humphreys TD**, **Wold MS**. 2010. A naturally occurring human RPA subunit homolog does not support DNA replication or cell-cycle progression. Nucleic Acids Res **38**:846–858.
206. **Mason AC**, **Haring SJ**, **Pryor JM**, **Staloch CA**, **Gan TF**, **Wold MS**. 2009. An alternative form of replication protein A prevents viral replication in vitro. J Biol Chem **284**:5324–5331.
207. **Bochkarev A**, **Bochkareva E**. 2004. From RPA to BRCA2: lessons from single-stranded DNA binding by the OB-fold. Curr Opin Struct Biol **14**:36–42.
208. **Bochkarev A**, **Pfuetzner RA**, **Edwards AM**, **Frappier L**. 1997. Structure of the single-stranded-DNA-binding domain of replication protein A bound to DNA. Nature **385**:176–181.
209. **Wold MS**. 1997. Replication protein A: A Heterotrimeric, Single-Stranded DNA-Binding Protein Required for Eukaryotic DNA Metabolism. Annu Rev Biochem **66**:61–92.
210. **Mer G**, **Bochkarev A**, **Gupta R**, **Bochkareva E**, **Frappier L**, **Ingles CJ**, **Edwards AM**, **Chazin WJ**. 2000. Structural basis for the recognition of DNA repair proteins UNG2, XPA, and RAD52 by replication factor RPA. Cell **103**:449–56.
211. **Aboussekhra A**, **Biggerstaff M**, **Shivji MKK**, **Vilpo JA**, **Moncollin V**, **Podust VN**, **Protid M**, **Hqbscher U**, **Egly J-M**, **Wood RD**. 1995. Mammalian DNA Nucleotide Excision Repair Reconstituted with Purified Protein Components. Cell **80**:859–868.
212. **Stauffer ME**, **Chazin WJ**. 2004. Physical interaction between replication protein A and Rad51 promotes exchange on single-stranded DNA. J Biol Chem **279**:25638–45.
213. **Van Komen S**, **Petukhova G**, **Sigurdsson S**, **Sung P**. 2002. Functional cross-talk among Rad51, Rad54, and replication protein A in heteroduplex DNA joint

formation. J Biol Chem **277**:43578–87.

214. **Lee J-H**, **Paull TT**. 2005. ATM Activation by DNA Double-Strand Breaks Through the Mre11-Rad50-Nbs1 Complex. Science (80- ) **308**:551–554.
215. **Bae SH**, **Bae KH**, **Kim JA**, **Seo YS**. 2001. RPA governs endonuclease switching during processing of Okazaki fragments in eukaryotes. Nature **412**:456–61.
216. **Din S**, **Brill SJ**, **Fairman MP**, **Stillman B**. 1990. Cell-cycle-regulated phosphorylation of DNA replication factor A from human and yeast cells. Genes Dev **4**:968–77.
217. **Oakley GG**, **Patrick SM**, **Yao J**, **Carty MP**, **Turchi JJ**, **Dixon K**. 2003. RPA Phosphorylation in Mitosis Alters DNA Binding and Protein?Protein Interactions ? Biochemistry **42**:3255–3264.
218. **Binz SK**, **Sheehan AM**, **Wold MS**. 2004. Replication Protein A phosphorylation and the cellular response to DNA damage. DNA Repair (Amst) **3**:1015–1024.
219. **Maréchal A**, **Zou L**. 2015. RPA-coated single-stranded DNA as a platform for post-translational modifications in the DNA damage response. Cell Res **25**:9–23.
220. **Vassin VM**, **Wold MS**, **Borowiec JA**. 2004. Replication protein A (RPA) phosphorylation prevents RPA association with replication centers. Mol Cell Biol **24**:1930–43.
221. **Dodson GE**, **Shi Y**, **Tibbetts RS**. 2004. DNA replication defects, spontaneous DNA damage, and ATM-dependent checkpoint activation in replication protein A-deficient cells. J Biol Chem **279**:34010–4.
222. **Araya R**, **Hirai I**, **Meyerkord CL**, **Wang H-G**. 2005. Loss of RPA1 induces Chk2 phosphorylation through a caffeine-sensitive pathway. FEBS Lett **579**:157–161.
223. **Haring SJ**, **Mason AC**, **Binz SK**, **Wold MS**. 2008. Cellular functions of human RPA1. Multiple roles of domains in replication, repair, and checkpoints. J Biol Chem **283**:19095–111.
224. **Wilkinson DE**, **Weller SK**. 2005. Inhibition of the herpes simplex virus type 1 DNA polymerase induces hyperphosphorylation of replication protein A and its accumulation at S-phase-specific sites of DNA damage during infection. J Virol **79**:7162–71.
225. **Mohni KN**, **Dee AR**, **Smith S**, **Schumacher AJ**, **Weller SK**. 2013. Efficient herpes simplex virus 1 replication requires cellular ATR pathway proteins. J Virol **87**:531–42.
226. **Loo Y-M**, **Melendy T**. 2004. Recruitment of replication protein A by the

papillomavirus E1 protein and modulation by single-stranded DNA. J Virol **78**:1605–15.

227. **Pan Z-Q**, **Amin AA**, **Gibbs E**, **Niu H**, **Hurwitz J**. 1994. Phosphorylation of the p34 subunit of human single-stranded-DNA- binding protein in cyclin A-activated G1 extracts is catalyzed by cdk-cyclin A complex and DNA-dependent protein kinase (DNA repctIon/cell cycle regulation/DNA transactions). Biochemistry **91**:8343–8347.
228. **Erdile LF**, **Heyer WD**, **Kolodner R**, **Kelly TJ**. 1991. Characterization of a cDNA encoding the 70-kDa single-stranded DNA-binding subunit of human replication protein A and the role of the protein in DNA replication. J Biol Chem **266**:12090–8.
229. **Umbricht CB**, **Erdile LF**, **Jabs EW**, **Kelly TJ**. 1993. Cloning, overexpression, and genomic mapping of the 14-kDa subunit of human replication protein A. J Biol Chem **268**:6131–6138.
230. **Stracker TH**, **Cassell GD**, **Ward P**, **Loo Y-M**, **van Breukelen B**, **Carrington-Lawrence SD**, **Hamatake RK**, **van der Vliet PC**, **Weller SK**, **Melendy T**, **Weitzman MD**. 2004. The Rep protein of adeno-associated virus type 2 interacts with single-stranded DNA-binding proteins that enhance viral replication. J Virol **78**:441–53.
231. **Weitzman MD**, **Fisher KJ**, **Wilson JM**. 1996. Recruitment of wild-type and recombinant adeno-associated virus into adenovirus replication centers. J Virol **70**:1845–54.
232. **Ward P**, **Dean FB**, **O'Donnell ME**, **Berns KI**. 1998. Role of the adenovirus DNA-binding protein in in vitro adeno-associated virus DNA replication. J Virol **72**:420–427.
233. **Maguire AM**, **Simonelli F**, **Pierce EA**, **Pugh EN**, **Mingozzi F**, **Bennicelli J**, **Banfi S**, **Marshall KA**, **Testa F**, **Surace EM**, **Rossi S**, **Lyubarsky A**, **Arruda VR**, **Konkle B**, **Stone E**, **Sun J**, **Jacobs J**, **Dell'Osso L**, **Hertle R**, **Ma J**, **Redmond TM**, **Zhu X**, **Hauck B**, **Zelenaia O**, **Shindler KS**, **Maguire MG**, **Wright JF**, **Volpe NJ**, **McDonnell JW**, **Auricchio A**, **High KA**, **Bennett J**. 2008. Safety and Efficacy of Gene Transfer for Leber's Congenital Amaurosis. N Engl J Med **358**:2240–2248.
234. **Nonnenmacher M**, **Weber T**. 2012. Intracellular transport of recombinant adeno-associated virus vectors. Gene Ther **19**:649–658.
235. **Kotterman MA**, **Schaffer D V**. 2014. Engineering adeno-associated viruses for

clinical gene therapy. Nat Rev Genet **15**:445–51.

236. **Zincarelli C**, **Soltys S**, **Rengo G**, **Rabinowitz JE**. 2008. Analysis of AAV Serotypes 1–9 Mediated Gene Expression and Tropism in Mice After Systemic Injection. Mol Ther **16**:1073–1080.
237. **Lovric J**, **Mano M**, **Zentilin L**, **Eulalio A**, **Zacchigna S**, **Giacca M**. 2012. Terminal differentiation of cardiac and skeletal myocytes induces permissivity to AAV transduction by relieving inhibition imposed by DNA damage response proteins. Mol Ther **20**:2087–97.
238. **Kaplitt MG**, **Leone P**, **Samulski RJ**, **Xiao X**, **Pfaff DW**, **O'Malley KL**, **During MJ**. 1994. Long-term gene expression and phenotypic correction using adeno-associated virus vectors in the mammalian brain. Nat Genet **8**:148–154.
239. **Kessler PD**, **Podsakoff GM**, **Chen X**, **McQuiston SA**, **Colosi PC**, **Matelis LA**, **Kurtzman GJ**, **Byrne BJ**. 1996. Gene delivery to skeletal muscle results in sustained expression and systemic delivery of a therapeutic protein. Proc Natl Acad Sci U S A **93**:14082–7.
240. **Flannery JG**, **Zolotukhin S**, **Vaquero MI**, **LaVail MM**, **Muzyczka N**, **Hauswirth WW**. 1997. Efficient photoreceptor-targeted gene expression in vivo by recombinant adeno-associated virus. Proc Natl Acad Sci U S A **94**:6916–21.
241. **Peel AL**, **Zolotukhin S**, **Schrimsher GW**, **Muzyczka N**, **Reier PJ**. 1997. Efficient transduction of green fluorescent protein in spinal cord neurons using adeno-associated virus vectors containing cell type-specific promoters. Gene Ther **4**:16–24.
242. **Acland GM**, **Aguirre GD**, **Bennett J**, **Aleman TS**, **Cideciyan A V.**, **Bennicelli J**, **Dejneka NS**, **Pearce-Kelling SE**, **Maguire AM**, **Palczewski K**, **Hauswirth WW**, **Jacobson SG**. 2005. Long-Term Restoration of Rod and Cone Vision by Single Dose rAAV-Mediated Gene Transfer to the Retina in a Canine Model of Childhood Blindness. Mol Ther **12**:1072–1082.
243. **Nakai H**, **Storm TA**, **Kay MA**. 2000. Recruitment of single-stranded recombinant adeno-associated virus vector genomes and intermolecular recombination are responsible for stable transduction of liver in vivo. J Virol **74**:9451–63.
244. **McCarty DM**. 2008. Self-complementary AAV Vectors; Advances and Applications. Mol Ther **16**:1648–1656.
245. **Hallek M**, **Girod A**, **Ried M**, **Wobus C**, **Lahm H**, **Leike K**, **Kleinschmidt J**, **Deléage G**. 1999. Genetic capsid modifications allow efficient re-targeting of

adeno-associated virus type 2. Nat Med **5**:1052–1056.

246. **Grimm D**, **Lee JS**, **Wang L**, **Desai T**, **Akache B**, **Storm TA**, **Kay MA**. 2008. In vitro and in vivo gene therapy vector evolution via multispecies interbreeding and retargeting of adeno-associated viruses. J Virol **82**:5887–911.
247. **Komáromy AM**, **Alexander JJ**, **Cooper AE**, **Chiodo VA**, **Glushakova LG**, **Acland GM**, **Hauswirth WW**, **Aguirre GD**. 2008. Targeting gene expression to cones with human cone opsin promoters in recombinant AAV. Gene Ther **15**:1049–55.
248. **Geisler A**, **Jungmann A**, **Kurreck J**, **Poller W**, **Katus HA**, **Vetter R**, **Fechner H**, **Müller OJ**. 2011. microRNA122-regulated transgene expression increases specificity of cardiac gene transfer upon intravenous delivery of AAV9 vectors. Gene Ther **18**:199–209.
249. **Shen S**, **Horowitz ED**, **Troupes AN**, **Brown SM**, **Pulicherla N**, **Samulski RJ**, **Agbandje-McKenna M**, **Asokan A**. 2013. Engraftment of a Galactose Receptor Footprint onto Adeno-associated Viral Capsids Improves Transduction Efficiency. J Biol Chem **288**:28814–28823.
250. **Perabo L**, **Endell J**, **King S**, **Lux K**, **Goldnau D**, **Hallek M**, **Büning H**. 2006. Combinatorial engineering of a gene therapy vector: directed evolution of adeno-associated virus. J Gene Med **8**:155–162.
251. **Maheshri N**, **Koerber JT**, **Kaspar BK**, **Schaffer D V**. 2006. Directed evolution of adeno-associated virus yields enhanced gene delivery vectors. Nat Biotechnol **24**:198–204.
252. **Mingozzi F**, **Anguela XM**, **Pavani G**, **Chen Y**, **Davidson RJ**, **Hui DJ**, **Yazicioglu M**, **Elkouby L**, **Hinderer CJ**, **Faella A**, **Howard C**, **Tai A**, **Podsakoff GM**, **Zhou S**, **Basner-Tschakarjan E**, **Wright JF**, **High KA**. 2013. Overcoming preexisting humoral immunity to AAV using capsid decoys. Sci Transl Med **5**:194ra92.
253. **Münch RC**, **Janicki H**, **Völker I**, **Rasbach A**, **Hallek M**, **Büning H**, **Buchholz CJ**. 2013. Displaying High-affinity Ligands on Adeno-associated Viral Vectors Enables Tumor Cell-specific and Safe Gene Transfer. Mol Ther **21**:109–118.
254. **Asokan A**, **Conway JC**, **Phillips JL**, **Li C**, **Hegge J**, **Sinnott R**, **Yadav S**, **DiPrimio N**, **Nam H-J**, **Agbandje-McKenna M**, **McPhee S**, **Wolff J**, **Samulski RJ**. 2010. Reengineering a receptor footprint of adeno-associated virus enables selective and systemic gene transfer to muscle. Nat Biotechnol **28**:79–82.
255. **Cervelli T**, **Palacios JA**, **Zentilin L**, **Mano M**, **Schwartz R a**, **Weitzman MD**,

**Giacca M**. 2008. Processing of recombinant AAV genomes occurs in specific nuclear structures that overlap with foci of DNA-damage-response proteins. J Cell Sci **121**:349–57.

256. **Hirsch ML**, **Fagan BM**, **Dumitru R**, **Bower JJ**, **Yadav S**, **Porteus MH**, **Pevny LH**, **Samulski RJ**. 2011. Viral Single-Strand DNA Induces p53-Dependent Apoptosis in Human Embryonic Stem Cells. PLoS One **6**:e27520.
257. **Sanlioglu S**, **Duan D**, **Engelhardt JF**. 1999. Two Independent Molecular Pathways for Recombinant Adeno-Associated Virus Genome Conversion Occur after UV-C and E4orf6 Augmentation of Transduction. Hum Gene Ther **10**:591–602.
258. **Russell DW**, **Alexander IE**, **Miller AD**. 1995. DNA synthesis and topoisomerase inhibitors increase transduction by adeno-associated virus vectors. Proc Natl Acad Sci U S A **92**:5719–23.
259. **Zentilin L**, **Marcello A**, **Giacca M**. 2001. Involvement of cellular double-stranded DNA break binding proteins in processing of the recombinant adeno-associated virus genome. J Virol **75**:12279–87.
260. **Inagaki K**, **Ma C**, **Storm TA**, **Kay MA**, **Nakai H**. 2007. The role of DNA-PKcs and artemis in opening viral DNA hairpin termini in various tissues in mice. J Virol **81**:11304–21.
261. **Nakai H**, **Wu X**, **Fuess S**, **Storm TA**, **Munroe D**, **Montini E**, **Burgess SM**, **Grompe M**, **Kay MA**. 2005. Large-Scale Molecular Characterization of Adeno-Associated Virus Vector Integration in Mouse Liver. J Virol **79**:3606–3614.
262. **Lentz TB**, **Samulski RJ**. 2015. Insight into the mechanism of inhibition of adeno-associated virus by the Mre11/Rad50/Nbs1 complex. J Virol **89**:181–94.
263. **Mano M**, **Ippodrino R**, **Zentilin L**, **Zacchigna S**, **Giacca M**. 2015. Genome-wide RNAi screening identifies host restriction factors critical for in vivo AAV transduction. Proc Natl Acad Sci U S A **112**:11276–81.
264. **Kim C**, **Paulus BF**, **Wold MS**. 1994. Interactions of Human Replication Protein A with Oligonucleotides'. Biochemistry **33**:14197–14206.
265. **Rahman SH**, **Bobis-Wozowicz S**, **Chatterjee D**, **Gellhaus K**, **Pars K**, **Heilbronn R**, **Jacobs R**, **Cathomen T**. 2013. The Nontoxic Cell Cycle Modulator Indirubin Augments Transduction of Adeno-Associated Viral Vectors and Zinc-Finger Nuclease-Mediated Gene Targeting. Hum Gene Ther **24**:67–77.
266. **Mitchell AM**, **Nicolson SC**, **Warischalk JK**, **Samulski RJ**. 2010. AAV's

anatomy: roadmap for optimizing vectors for translational success. Curr Gene Ther **10**:319–40.

267. **Winocour E**, **Callaham MF**, **Huberman E**. 1988. Perturbation of the cell cycle by adeno-associated virus. Virology **167**:393–9.
268. **McCarty DM**, **Fu H**, **Monahan PE**, **Toulson CE**, **Naik P**, **Samulski RJ**. 2003. Adeno-associated virus terminal repeat (TR) mutant generates self-complementary vectors to overcome the rate-limiting step to transduction in vivo. Gene Ther **10**:2112–2118.
269. **Franzoso FD**, **Seyffert M**, **Vogel R**, **Yakimovich A**, **de Andrade Pereira B**, **Meier AF**, **Sutter SO**, **Tobler K**, **Vogt B**, **Greber UF**, **Büning H**, **Ackermann M**, **Fraefel C**. 2017. Cell cycle-dependent expression of AAV2 Rep in HSV-1 co-infections gives rise to a mosaic of cells replicating either AAV2 or HSV-1. J Virol JVI.00357-17.

## 7. Acknowledgements

This PhD thesis was not possible without the valuable contribution of many people who inspired me and advised me, who shared with me joyful moments when discovering research paths, encouraging me and supporting my work all this time. The words are very limited to express my entire gratitude to all of you.

Firstly, I would like to express my sincere gratitude to my thesis supervisor, Prof. Dr. Cornel Fraefel for giving me this great opportunity, for guiding me through this research work and for his continuous help, understanding, patience, immense scientific knowledge and precious support during my PhD study. I am deeply grateful to his mentorship and advices as well as for introducing me to the fascinating AAV research world, for inspiring me through his great passion for science and for encouraging me to participate to many national and international conferences to present my work.

My sincere thanks to my thesis committee members, Prof. Dr. Urs Greber and Prof. Dr. Michael Linden for their great support, critical discussions and thoughtful suggestions.

Prof. Dr. Mathias Ackermann, for this great opportunity and his valued support through my PhD thesis, as the Director of the Virology Institute.

Dr. Kurt Tobler for all his great input, valued contribution, helpful discussions and excellent bioinformatical support.

Dr. Artur Yakimovich, for all his best and invaluable advice, kindest help and outstanding experimental support in assay building and troubleshooting.

Bernd Vogt for his excellent technical support, great help and helpful discussions.

And, of course, many thanks to all the Cornel Fraefel's lab team and Institute's members for their never-ending support and priceless help all this time and for sharing with me great moments that I will never forget. Rebecca Vogel, Michael Seyffert (Michi), Sereina Sutter, Anita Meier, Sophie Ramsauer, Cedric Vogt, Andrea Leimbacher, Adrian Man and Neeta Shresta for all help, friendship, wonderful discussions, and for making my PhD time so enjoyable (tiptop)!

My personal thanks go to my dearest friend and partner, Giampaolo, for all his superb support and magnificent help all this time. My deepest thanks go to my family for their unconditional help and for continuously motivating me.

For all the people who contributed to this work as sources of scientific and moral advice, to all of you, my very special thanks.

Dr.med.vet. FRANCESCA DANIELA FRANZOSO, Dipl. ECVP

Seenerstrasse 221
8405 Winterthur
077/463 63 9
francesca.franzoso@uzh.ch

## AUSBILDUNG & PROFESSIONELLE ERFAHRUNG

| | |
|---|---|
| 11/2016 | Dozentin (Ass. Prof.)<br>**Universität Nantes**, Veterinärmedizinische Fakultät, Frankreich<br>Institut Veterinärpathologie |
| 2013-2016 | PhD Studium Mikrobiologie & Immunologie<br>**Universität Zürich**, Matematisch-Naturwiseschaftliche Fakultät & VetSuiss<br>Fakultät ; Life Science Graduate School Zürich<br>- Doktorarbeit: Host factors and cell cycle progression modulation i<br>adeno-associated virus infected cells<br>- Lehraufgaben, und Betreuung von Studenten |
| 2012-2013 | Wissenschaftliche Mitarbeiterin<br>**Universität Zürich**, **Kinderspital Zürich**<br>- Forschungsprojektleitung Klinische Forschung Kardiologie |
| 2008-2012 | Universitätsassistentin<br>**Universität Bern**, Institut Tierpathologie, VetSuisse Fakultät<br>- Forschungsprojekt: Pathogenese von *Clostridium perfringens typ C*<br>Enteritis Menschen und Schwein<br>- Lehraufgaben, Betreuung von Studenten, Masters, Laborante<br>Organisation Kurse, Seminaren, Workshops |
| 2007-2008 | Postdoktorandin<br>**Universität Wien**, Konrad Lorentz Institut, Österreich<br>Forschungsprojekt: Stresshormonen und evolution - Cyclid Fisch Modell |
| 2004-2007 | Doktoratstudium (Dr.med.vet.)<br>**Veterinärmedizinische Universität Wien**, Forschungsinstitut für Wildtierkunde, Österreich<br>Projekt: Physiologie Vedauungstrakt und Fettsäuren Biologie - *Laepu*<br>*europaeus* |

## KURSE & WEITERBILDUNG

| | |
|---|---|
| 05/2017 | Project management for advanced researchers, Kurs, ETH Zürich & UZH Zürich, EU Relations |
| 06/2015 | Animal models for human disease, Workshop, Institute Pasteur Paris, France |
| 2013/2016 | Zellulär Biologie für Postgraduierten, Universität Zürich |

| | |
|---|---|
| 09-12/2014 | Translational medicine: Infection and Immunity, Universitätspital Zürich |
| 11/2013 | Lehre Kurs für Universität Assistenten (Pädagogie), Universität Zürich |
| 10/2013 | Leadership Kompetenzen für Doktoranden, Kurs, Universität Zürich |
| 09/2013 | CIMST Summer School Biomedical Imaging in Research, ETH Zürich |
| 10/2012 | Good Clinical Practice Kurs für Klinische Forschung, UniversitätSpital Zürich |
| 05/2011 | Descriptive Course in Anatomic Veterinary Pathology, Charles Louis Davis DVM Foundation, University of Dublin, Ireland |
| 07/2011 | ECVP Summer School in Veterinary Anatomic Pathology, Universität Bern |
| 07/2010 | ECVP Summer School in Veterinary Anatomic Pathology, Universität Zürich |
| 04/2009 | European Course on the Anatomic Pathology of Laboratory Animals (EuroPOLA), Institute Pasteur, Paris, France |

## SPRACHEN

| | |
|---|---|
| Deutsch | gut, schriftlich und mündlich |
| Englisch | sehr gut, schriftlich und mündlich |
| Französisch | sehr gut, schriftlich und mündlich |
| Italienisch | sehr gut, schriftlich und mündlich |

## PUBLIKATIONEN (short list)

**F.D. Franzoso**, A. Yakimovich, K. Tobler, R. Vogel, H. Büning, U. Greber, C. Fraefel. Targeted image-based RNAi screen identifies host cell proteins with differential effects on the transduction efficiency of single-stranded and self-complementary AAV vectors. Manuscript submitted June 2017.

M. Crameri, R. Walker, **F.D. Franzoso**, C. Gujer, N. Caduff, M. Bauer, F. Steiner, T. Kucera, A. Zbinden, U. Greber, C. Münz, C. Fraefel, J. Pavlovic. MxB is an interferon-induced restriction factor for human herpesviruses. Manuscript under revision and consideration, Manuscript submitted April 2017.

**F.D. Franzoso,** R. Vogel, M. Seyffert, B. Pereira, M. Avila, B. Vogt, H. Büning, M. Ackerman, C. Fraefel. Cell cycle-dependent expression of AAV2 Rep in HSV-1 co-infections gives rise to a mosaic of cells replicating either AAV2 or HSV-1. Manuscript accepted, *Journal of Virology,* 2017, DOI: 10.1128/JVI.00357-17

**F.D. Franzoso,** Wohlmuth C, Greutman M, Kellenberger CK, Oxenius A, Voser EM, Valsangiacomo Buechel ER. Atrial Function after the atrial switch operation for transposition of the great arteries: comparison with arterial switch and normals by cardiovascular magnetic resonance. *Congenital Heart Disease,* 2015*,* 11(5):426-436*,* doi: 10.1111/chd.12323

N. Borel, CF. Frey, B. Gottstein, M. Hilbe, A. Pospschil, **F.D. Franzoso,** A. Waldvogel. Laboratory diagnosis of ruminant abortion in Europe – REVIEW - *The Veterinary Journal,* 2014, 200(2):218-29

Organ Clearing and Biphotonic Microscopy - an Innovative Complementary Technological Approach to Investigate the Central Nervous System
L. Dubreil, R. Fleurisson, J. Deniaud, **F.D. Franzoso**, M.A. Colle
Medical imaging, Brain imaging, FOM, Bordeaux, 09-12 April 2017, France (**Poster** Presentation)

The interferon-induced MxB protein is a Herpes Simplex virus Type I restriction factor
Crameri M, Walker R, **Franzoso FD**, Fraefel C, Pavlovic C
Cytokines International Congress 4th Annual Meeting of International Cytokine and Interferon Society, San Francisco, CA, 16-19 October 2016, USA (**Oral** Presentation)

Effects of host cell factors on transduction by adeno-associated virus 2 (AAV2) vectors
**Franzoso FD**, Yakimovich A, Tobler K, Man A, Vogel R, Greber U, Ackermann M, Fraefel C.
ESVP/ECVP Annual Meeting, Bologna, 07-10 September 2016, Italy (**Oral** Presentation)

Restricted siRNA screen reveals differential effects of cellular proteins in gene expression from single-stranded and double-stranded AAV2 vectors
Franzoso FD, Yakimovich A, Tobler K, Man A, Vogel R, Greber U, Ackermann M, Fraefel C.
16th International Parvovirus Workshop, Ajaccio, 20-23 June 2016, Corsica (**Oral** Presentation)

Differential transduction efficiency of AAV2 vectors
**Franzoso FD**, Yakimovich A, Tobler K, Man A, Vogel R, Greber U, Ackermann M, Fraefel C.
Swiss Society for Microbiology, Bern, 13-15 June 2016, Switzerland (**Oral** Presentation)

Can the subsystemic right ventricle remodel and contract like a left ventricle after atrial switch repair for transposition of the great arteries? Pathologic and magnetic resonance features
Burkhardt B.E.U, Kellenberger C.J, Weber R, Oxenius A, Geiger J, **Franzoso FD**, Valsangiacomo Buechel E.R
9th Annual Meeting of the Association for European Paediatric and Congenital Cardiology (AEPC), Prague, 20 – 23 May 2015, Czech Republic (**Poster** Presentation)

Cellular factors involved in HSV-1-supported AAV2 replication
**Franzoso FD**, Yakimovich A, Vogel R, Greber U, Vogt B, Ackermann M, Fraefel C.
Swiss Virology Meeting, Thun, 03-04 September 2014, Switzerland (**Poster** Presentation)

Replication of HSV-1 and AAV2 in co-infected cells depends on the cell cycle
Vogel R, Seyffert M, Bräm A, Vogt B, **Franzoso FD,** Pereira B, Büning H, Ackermann M, and Fraefel C.
15th International Parvovirus Workshop, Bordeaux, 03-06 September 2014, France (**Oral** Presentation)

Atrial versus arterial switch repair for transposition of great arteries. CMR and pathologic evaluation of atrial function – a comparative study
**Franzoso FD**, Wohlmuth C, Kellenberger CK, Valsangiacomo Buechel ER.
European-Echo Imaging Congress, Istanbul, 11-14 December, Turkey (**Poster** Presentation)

Of man and pigs: New insights into the pathogenesis of Clostridium perfringens type C enteritis.
ESVP/ECVP Annual Meeting, Belgrade, 08-11 September 2010, Serbia (**Oral** Presentation)

Identification of natural target cells of Clostridium perfringens beta-toxin

Expression of recombinant Clostridium perfringens beta-toxin for cell toxicity assays – Gurtner C, **FD** Clostpath International Conference, Clostridia: the impact of genomics on disease control, Istituto Superiore di Sanità, ROME**,** 08-11 September 2010, Italy (Two **posters** Presentations)